

UPLIFT BEHAVIOUR OF HORIZONTAL ANCHOR PLATES IN SANDS

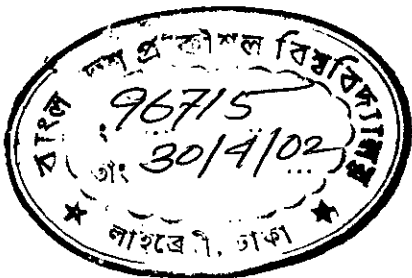
A PROJECT REPORT SUBMITTED TO THE DEPARTMENT OF CIVIL
ENGINEERING, BANGLADESH UNIVERSITY OF ENGINEERING AND
TECHNOLOGY (BUET), DHAKA IN PARTIAL FULFILMENT OF THE
REQUIREMENTS FOR THE DEGREE

Of

MASTER OF ENGINEERING IN CIVIL ENGINEERING

BY

SYED RAJAB ALI



DEPARTMENT OF CIVIL ENGINEERING
BANGLADESH UNIVERSITY OF ENGINEERING AND TECHNOLOGY
DHAKA, BANGLADESH

DECEMBER, 2001



UPLIFT BEHAVIOUR OF HORIZONTAL ANCHOR PLATES IN SANDS

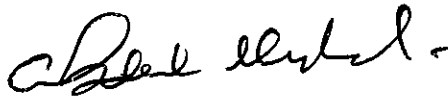
A PROJECT REPORT

BY

SYED RAJAB ALI

ROLL 9304205P

Approved as to style and content by:



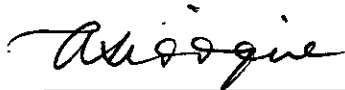
Dr. Md. Abdul Muqtadir
Professor
Department of Civil Engineering
BUET, Dhaka-1000

Chairman
(Supervisor)



Dr. Syed Fakhrul Ameen
Professor
Department of Civil Engineering
BUET, Dhaka-1000

Member



Dr. Abu Siddique
Professor
Department of Civil Engineering
BUET, Dhaka-1000

Member

December, 2001

Dedication:


To

My parents

DECLARATION

Declared that except where specific references are made to other investigators, the work embodied in this thesis is the result of the investigation carried out by the author under the supervision of Professor Dr. Md. Abdul Muqtadir, Department of Civil Engineering, Bangladesh University of Engineering & Technology (BUET), Dhaka, Bangladesh. Neither this thesis nor any part of it has been submitted or is being concurrently submitted elsewhere for any other purpose (except for publication).

December 07, 2001



(Syed Rajab Ali)

ACKNOWLEDGMENT

The author wishes to express his deepest gratitude to his supervisor Dr. Md. Abdul Muqtadir, Professor, Department of Civil Engineering, Bangladesh University of Civil Engineering & Technology (BUET), for his constant guidance, invaluable suggestions, ardent encouragement, generous help and unfailing enthusiasm at all the stages of this research work. His active interests in this topic and valuable advice were the source of the author's inspiration.

Grateful appreciation are due Dr. A. M. M. Safiullah, Professor; Dr. Md. Zoynul Abdein, Professor; Dr. Syed Fakhrul Ameen, Professor and Dr. Abu Siddique, Professor, Department of Civil Engineering, BUET, for their constructive and valuable suggestions.

The author owes his thanks to the members of the Board of Post Graduate Studies (BPGS) of the Department of Civil Engineering, Bangladesh University of Civil Engineering & Technology (BUET), and also to the members of the Committee of Advanced Studies and Research (CASR) for kind approval of the research proposal and financing the experimental work which are reported in this thesis.

The author is also thankful to Md. Habibur Rahman and Mr. Alimuddin of Geotechnical Engineering laboratory for their continuous assistance during laboratory testing. Help of Mr. Rafiqul Islam, Mr. Md. Abdul Malek and Mr. Md. Sharafat Ali of Civil Engineering Department also appreciated.

Finally, the author wishes to thank his family, relatives, colleagues and friends who helped him with necessary advice and information during the course of the study.

ABSTRACT

In this research a series of anchor pull out test are performed in the laboratory. These tests are done using various types of sand at different density. In this project work, three types of sands have been collected locally. These soils have been characterised in the laboratory. Anchor shape and size as well as depth of embedment of anchor are also varied during carrying out the model test. Pullout load is applied on the horizontal anchor plate by an incremental manner. The load is transmitted through a smooth wire attached to the anchor plates. Vertical movements of the anchor plate after each load increment is measured. Loads are applied in incremental manner till failures are observed. The load-displacement behaviour of anchor plates, variation of displacement with embedment ratio, variation of breakout factor with embedment ratio and anchor size and shapes have also been studied. The results of model tests are compared with various theoretical analyses. From the test results, it has been observed that the load-displacement behaviour of anchor plates is consistent with most of the similar investigations (Dickin,1988; Kulhawy et al. 1987; Rowe and Davies 1982). Failure modes of the anchors observed are fully consistent with almost all the available similar tests (Dickin,1988; Rowe and Davies 1982; Kulhawy et al. 1987; Ghaly and Hanna, 1994). Variations of breakout factor and displacement with embedment ratio also qualitatively satisfy most of the theoretical observations (Ghaly and Hanna, 1994; Clemence et al, 1977) and similar test results.

NOTATIONS

<u>Notations</u>	<u>Brief Explanation</u>
D	= Embedment depth of anchor.
B	= Anchor dia /least dimension.
D/B	= Embedment ratio.
N_{qu}	= Breakout factor. = $Q_u / \gamma AD$
Q_u	= Ultimate uplift load.
Z	= Displacement of anchor.
Z_f	= Displacement of anchor at ultimate uplift load.
ϕ	= Angle of internal friction of soil.
C	= Cohesion of soil.
γ	= Unit weight of soil.
Z_f/D	= Relative displacement at failure.
K	= Coefficient of earth pressure.
A	= Area of anchor plate.
C_u	= Uniformity coefficient, (D_{60}/D_{10}) .
C_z	= Coefficient of curvature, $(D_{30}^2 / D_{10} D_{60})$.

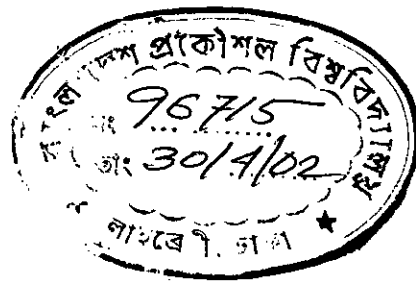
CONTENTS

ACKNOWLEDGEMENT	i
ABSTRACT	ii
NOTATIONS	iii
CHAPTER 1 INTRODUCTION	1
1.1 GENERAL	1
1.2 BACKGROUND	2
1.3 SCOPES AND OBJECTIVES	2
1.4 METHODOLOGY	3
CHAPTER 2 LITERATURE REVIEW	5
2.1 GENERAL	5
2.2. THEORETICAL ANALYSIS OF UPLIFT BEHAVIOUR OF ANCHOR PLATES IN SAND	5
2.3 THEORETICAL ANALYSIS OF ANCHOR PLATE BEHAVIOUR IN CLAY	28
2.4 BEHAVIOUR OF HORIZONTAL ANCHOR PLATE IN SAND	31
2.4.1 Nature of load displacement curve	31
2.4.2 Failure mode of anchor plate	33
2.4.3 Variation of breakout factor with embedment ratio	35
2.4.4 Variation of failure displacement with embedment ratio	35
2.4.5 Variation of shape factor with embedment ratio	37
2.4.6 Effect of overconsolidation on uplift capacity	38
2.4.7 Effect of angle of internal friction of sand on uplift capacity	39
2.4.8 Effect of backfill compaction on uplift capacity of backfilled anchor	40
2.4.9 Effect of native soil density on uplift capacity of backfilled anchor	40
2.4.10 Effect of aspect ratio on uplift capacity	40
2.5 BEHAVIOUR OF HORIZONTAL ANCHOR PLATES IN LAYERED SOIL	43
2.5.1 Effect of layering on the uplift capacity of anchors in clay	43
2.5.2 Effect of layering on the uplift capacity of anchors in sand	46
2.6 BEHAVIOUR OF HORIZONTAL ANCHOR PLATES UNDER CYCLIC LOADING	48
2.7 SUMMARY OF LITERATURE REVIEW	50

CHAPTER 3 EXPERIMENTAL SET UP, TEST PROCEDURE AND RESULTS	53
3.1 GENERAL	53
3.2 CHARACTERIZATION OF SAND SAMPLES	53
3.3 THE TEST SET UP	54
3.3.1 The test tank	54
3.3.2 The anchor plate	55
3.3.3 Other equipment	55
3.4 THE TEST PROCEDURE	55
3.4.1 Preparation of sand bed	55
3.4.2 Pullout of anchor plate	56
3.5 DESCRIPTION OF PULLOUT TESTS	59
3.6 THE TEST RESULTS	60
3.7 LIMITATIONS OF THE MODEL TESTS	62
CHAPTER 4 ANALYSIS AND INTERPRETATION OF TEST RESULTS	64
4.1 GENERAL	64
4.2 INTERPRETATION OF TEST RESULTS	64
4.2.1 Load-Displacement Behaviour	64
4.2.2 Variation of breakout factor with embedment ratio	75
4.2.3 Variation in relative displacement with embedment ratio	75
4.2.4 Variation of breakout capacity with anchor area	75
4.2.5 Variation of breakout capacity with anchor area	83
4.2.6 Variation of the pattern of failure surface	83
4.2.7 Variation of load with embedment ratio in different plate size at Sylhet sand	85
4.2.8 Variation of breakout capacity with relative density	87
4.2.9 Variation of breakout capacity with angle of friction	87
4.3 COMPARISON OF MODEL TEST RESULTS WITH SIMILAR TESTS AND THEORETICAL ANALYSES BY DIFFERENT RESEARCHERS	87
CHAPTER 5 CONCLUSIONS AND RECOMMENDATIONS	92
5.1 CONCLUSIONS	92
5.2 RECOMMENDATIONS FOR FUTURE STUDY	93
REFERENCES	95

CHAPTER 1

INTRODUCTION



1.1 GENERAL

Anchors are foundation systems that are designed primarily to resist uplift (tensile) loads. Anchor usage was started in early 1930's and with a boom after the Second World War and today, anchoring is a well-established branch of Geotechnical engineering. Now-a-days a good number of engineers are considering ground anchoring as an interesting solution to problems where uplift loading or overturning loading predominates. Different types of anchors and anchoring systems are being used widely all over the world and engineers are showing more enthusiasm on anchor usage techniques, their behaviour and design.

Anchor plate is a variation of anchor system with a wide usage in transmission tower foundations and in offshore engineering. It consists of a spread portion with a rod or cable to transmit the load to the superstructure from the ground. This type of anchor has a huge potential especially in foundations of transmission towers. About half of the existing transmission towers in the United States have this kind of foundations and a good portion of them planned for the future are going to have the same (Trauthmann et al, 1988). For offshore structures, plate anchor types of foundations are the most preferred due to their convenient installation procedure. Structures like cable-supported bridges also have this kind of support.

In Bangladesh, anchor foundations are of limited use, primarily due to lack of proper installation technology and practice of designers not to accept new technology. Here tension piles while small ones by gravity blocks support larger transmission towers. Introduction of tension members like anchor plate can reduce cost of foundation of such structures significantly. Moreover, earth reinforcement by anchor structures can reduce demand of land for construction of river and coastal embankments, which is effective for densely populated countries like Bangladesh. Therefore, anchor foundations have good potential in Bangladesh.

1.2 BACKGROUND

Despite of its wide usage in different fields, anchor foundations have not got that much importance by researches in comparison with conventional type of foundations (compressive type). However, so far, researchers all over the world has stressed the following fields in analysing anchor plate behaviour both theoretically and experimentally.

- The load-displacement behaviour of anchor plate under different kinds of loading and embedment,
- The variation of breakout capacity of anchor plate at different embedment ratio,
- The variation of uplift capacity under different loading conditions.
- The variation of uplift capacity with angle of internal friction of sand.
- The variation of uplift capacity at different backfill densities.
- The variation of displacement at different embedment ratio.
- Effect of over consolidation ratio on uplift capacity.
- Effect of aspect ratio on uplift capacity.
- The failure mode of anchor plate at different depths.
- Uplift behaviour of anchor plates in layered sand and clay.
- Group behaviour of anchor plates under different loading conditions.
- Critical depth ratio at different loading conditions.
- Effect of suction below anchor plate (especially for anchor plates in clay).
- Shape of the failure surface.

1.3 SCOPES AND OBJECTIVES

In recent years, several researchers (Majer,1955; Murray and Geddes, 1987; Clemence and Veeseart, 1977; Vermeer and Sutjiadi, 1985; Dana, 1961; Meyerhof and Adams, 1968; Tang, 1959; Mariopol'skii, 1965; Vesic, 1977; Das and Seely, 1975; Ovesen, 1981; Rowe and Davies, 1982; Rao and Kumar, 1994 & Ghaly and Hanna, 1994) have

performed some theoretical analysis of uplift behaviour of anchor plate and laboratory experiments. The present research has a summarisation of those. Moreover the researchers have done some laboratory model tests. In brief, the present research has the following objectives:

- a) To prepare a summary of the available anchor plate theories and previous laboratory investigations,
- b) To perform a series of laboratory model tests with a view to observe uplift behaviour of anchor plates embedded in Sylhet sand, Local (Gazaria) sand and Fills (Vethi sand) sand, and
- c) To study the load deformation behaviour of horizontal anchor plates and also to compare the experimental results with theoretical analyses.

1.4 METHODOLOGY

An attempt was taken to make a summarisation of the existing theories and laboratory investigations; the researchers had studied several research papers on the topic published in different journals and conference proceedings. Some available textbooks were also consulted. A list of the research papers and textbooks is attached with the back of this project as reference.

Three types of sands, such as Fills (vethi sand), Local (Gazaria) and Sylhet were collected locally. These soils were characterised in the laboratory. This characterisation included determination of specific gravity, grain size distribution, relative density and strength parameters. An experimental set up was made in the laboratory to carry out anchor-pull out test. A series of test were carried out on various size and shapes of anchor plates embedded at different depths. Loads were applied in incremental manner till failure is observed. The displacement of anchor plates was recorded using a dial gauge.

Model tests were performed at the Geotechnical Laboratory of the Department of Civil Engineering of BUET. Model test procedure was based on available research papers describing similar tests.

A #4 sieve was used to deposit the sand in layer. Pullout load was applied on the horizontal anchor plate by placing weights of different magnitudes in the loading hanger. Loads were applied in incremental manner till failures were observed.

CHAPTER 2

LITERATURE REVIEW

2.1 GENERAL

In this chapter, a brief review of the existing theoretical analyses regarding anchor plate behaviour in sand and clay is presented. Various experimental investigations performed by several researchers are also summarised here.

2.2. THEORETICAL ANALYSIS OF UPLIFT BEHAVIOUR OF ANCHOR PLATES IN SAND

Theoretical analyses of uplift behaviour of sand have been performed by various investigators all over the world in last 45 years. Below a summarisation of those theories is presented.

2.2.1 Theory of Majer (1955)

Majer (1955) was the first to formulate the behaviour of anchor plate. He assumed the simplest approach (vertical slip surface approach) (Fig. 2.1a). The uplift capacity Q_u for a long plate anchor of area A and thickness t at shallow depth D may be expressed in dimensionless form as the breakout factor $N_{qu} = T_u / \gamma AH$, in which γ = the soil density; and L = the anchor in length. Neglecting the shearing resistance at the ends, N_{qu} is given by

$$N_{qu} = \left(1 - \frac{t}{H} + K \tan \phi_{ps} \right) \dots (2.1)$$

Weight of soil
above anchor

Weight of soil
displaced by anchor

Shearing resistance
on slip surfaces

ϕ_{ps} = the angle of friction in plane strain and K = the coefficient of lateral stress in the soil. For loose sand K can be assumed as K_o , earth pressure coefficient at rest.

2.2.2 Murray and Geddes (1987)

This theory is based on the limit -analysis approach. They assumed an inverted cone slip surface (Fig. 2.1 b) having the cone angle equal to internal angle of friction of soil.

According to the theory of Murray and Geddes (1987)

$$N_{qu} = 1 + \left(\frac{D}{B}\right) \tan \phi \left[2 + \frac{\pi}{3} \left(\frac{D}{B}\right) \tan \phi \right] \quad \dots (2.2)$$

We are now discussing two most recent theories in detail concerning uplift behaviour of horizontal anchor plate in sand.

2.2.3 Theory of Clemence and Veeseart (1977)

According to this theory, the failure surface in soil is assumed to be a truncated cone (for shallow anchor) (Fig. 2.1c). The net ultimate capacity of a circular anchor in sand can be expressed as

$$Q_0 = \gamma V_s + \pi \gamma K_0 \tan \phi \cos^2(\phi/2) \left[\frac{BD^2}{2} + \frac{D^3 \tan(\phi/2)}{3} \right] \quad \dots (2.3)$$

Where V_s = Volume of the truncated cone. K_0 = coefficient of lateral earth pressure. The value of K_0 varies from the 0.7 to 1.5, with an average of about 1.0. The lower limit of K_0 is for the case in which sand is poured by the raining technique and the upper limit is for the case where sand is compacted around after the placement of the anchor. It can easily be seen that

$$V_s = \frac{\pi}{4} [B + D \tan(\pi/2)]^2 D \gamma \quad \dots (2.3)$$

Substituting this into Equation (2.2) and rearranging

$$N_{qu} = \frac{Q_0}{\left(\frac{\pi}{4}\right) B^2 \gamma D} = \frac{Q_0}{A \gamma D} = \left[1 + \left(\frac{D}{B}\right) \tan(\phi/2) \right]^2 + 4K_0 \tan \phi \cos^2(\phi/2) \left[\frac{1}{2} \left(\frac{D}{B}\right) + \left(\frac{D}{B}\right)^2 \frac{\tan(\phi/2)}{3} \right] \dots (2.4)$$

Using the average value of $K_o = 1$, the breakout factor variation with ϕ and D/B has been calculated and is shown in Fig. 2.2. In this figure, the embedment ratio at which deep anchor behaviour starts have been taken to be the same as defined by Meyerhof and Adams (1968) and Clemence and Veersart (1977).

2.2.4 Theory of Vermeer and Sutjiadi (1985)

Their analyses involving straight rupture surfaces at an inclination to the vertical equal to the dilatancy angle ϕ (Fig. 2.1d). The analysis yielded the following simple relation.

$$N_{qu} = 1 + \left(\frac{D}{B}\right) \tan \phi_{ps} \cos \phi_{cv} \quad \dots \quad (2.5)$$

2.2.5 Theory of Dana (1961)

Balla (1961) was the first to adopt a systematic analysis. He tried to satisfy Kotter's equation for a prefixed tangential-curve slip surface (Fig. 2.1e) extending from the vertical component of shear stress over the surface but neglected to include the effects of normal stresses on the failure surface.

According to Balla's theory

$$N_{qu} = (F_1 + F_2) \left(\frac{4}{\pi}\right) \left(\frac{D}{B}\right)^2 \quad \dots \quad (2.6)$$

Where, F_1 and F_2 are factors dependent on ϕ and γ'

2.2.6 Theory of Meyerhof and Adams (1968)

Meyerhof and Adams (1968) shallow anchor theory was based on earth-pressure coefficient of Caquot and Kerisel (1948) over a curved rupture surface coupled with an assumption of mobilized friction angle on the cylinder surface.

According to this theory, the ultimate uplift capacity of a shallow circular anchor can be given as

$$Q_o = \left(\frac{\pi}{2}\right) S \gamma B D^2 K' \tan \phi + W \quad \dots (2.7)$$

$$\text{Where } S = \text{Shape factor} = 1 + m'(D/B) \quad \dots (2.8)$$

K' = Nominal uplift earth pressure coefficient.

W = Weight of soil immediately above the anchor.

m' = Shape factor co-efficient = $f(\phi)$.

For circular anchors,

$$W = \left(\frac{\pi B^2}{4}\right) \gamma D \quad \dots (2.9)$$

The variation of K' and m' (which are functions of ϕ) are shown in Fig. 2.3.

Substitutions of Equations (2.9) and (2.8) into equation (2.7) yields

$$Q_o = \left(\frac{\pi}{2}\right) S \gamma B D^2 K_u \tan \phi + \left(\frac{\pi B^2}{4}\right) \gamma D$$

or

$$\frac{Q_o}{\gamma \left(\frac{\pi B^2}{4}\right) D} = \frac{Q_o}{\gamma A D} = N_{qu} = 2[1 + m'(D/B)](D/B) K_u \tan \phi + 1 \quad \dots (2.10)$$

By using equation (2.10) and with the values of K_u and m' given in Fig. 2.3, the variation of the breakout factor (N_{qu}) with embedment ratio for shallow circular anchors in sand has been calculated and is given in Fig. 2.4

For deep anchors, Meyerhof and Adams modified the assumption of Majer's vertical slip surface, as it was not consistent with field observations, especially in case of dense sand. The more realistic pyramidal-shaped rupture surface (Fig. 2.1f) was assumed by them. Their analysis resulted in the omission of the second term and insertion of a value of $K =$

0.95 in Majer's equation. At greater depths, Meyerhof and Adams proposed the following equation,

$$N_{qu} = 1 + \left(\frac{2D}{B} - \frac{D_c}{B} \right) \left(\frac{D_c}{D} \right) 0.95 \tan \phi_{ps} \quad \dots(2.11)$$

In which D_c is the vertical extent of the failure surface and is dependent upon B and ϕ_{ps} .

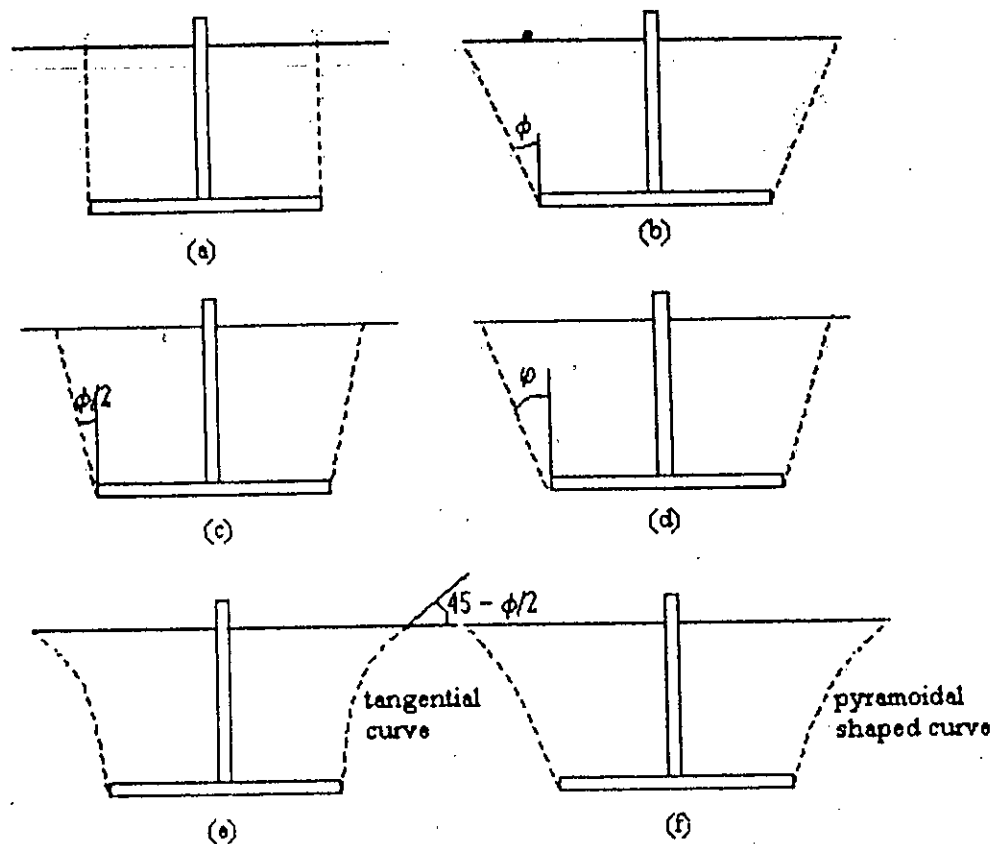


Fig. 2.1 Failure surface assumed by different researchers

- a) Majer, 1955
- b) Murray and Geddes, 1987
- c) Clemence and Veeseart, 1977
- d) Vermeer and Sutjiadi, 1985
- e) Balla, 1961
- f) Meyerhof and Adams, 1968

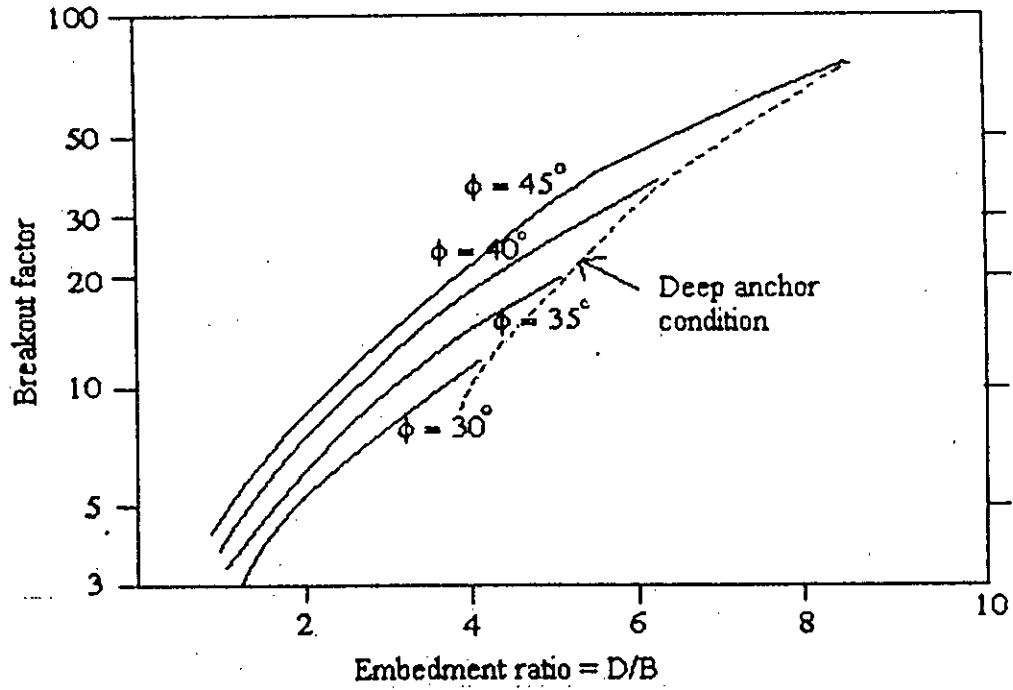


Fig. 2.2 Variation of breakout factor with embedment ratio (after Clemence, 1977)

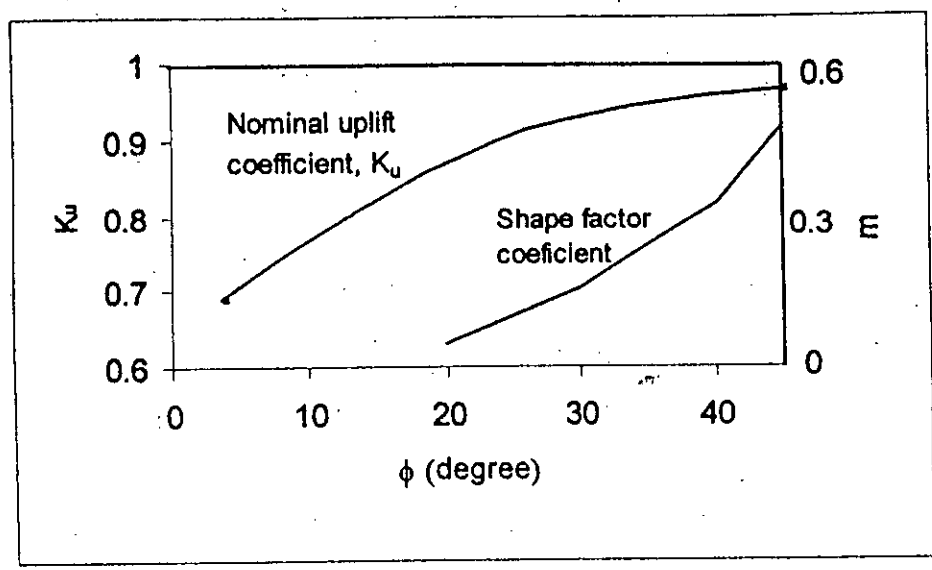


Fig. 2.3 Shape factor variation with friction angle (after Meyerhof, 1968)

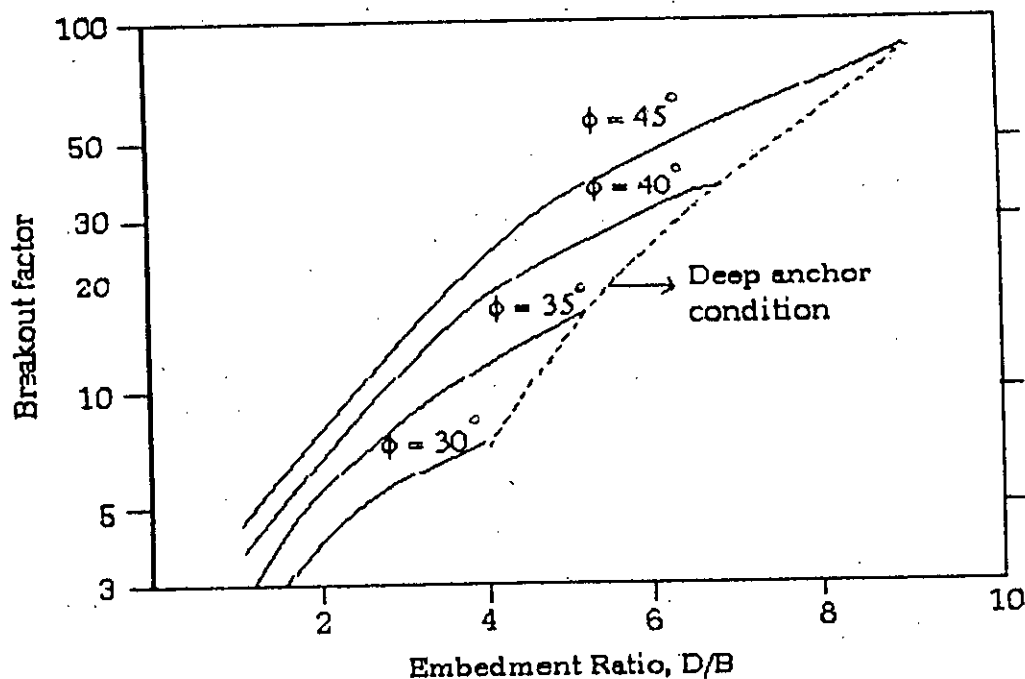


Fig. 2.4 Variation of breakout factor with embedment ratio (after Meyerhof, 1968)

2.2.7 Theory of Tang (1959)

For shallow anchor, according to Tang's theory (1969), total uplift resistance of the anchor plate is taken as the weight of the prism of the soil contained within an arbitrarily determined failure surface generated above the anchor by the uplift force. For deep anchor, failure is assumed to occur along a cylindrical surface equal in diameter of the anchor, the resistance to uplift being provided by the weight of the soil cylinder and the shear resistance mobilised by earth pressure acting on the cylinder.

2.2.8 Theory of Mariopol'skii (1965)

In analysing shallow anchor behaviour, Mariopol'skii (1965) assumed a curved slip surface with a presumption that failure occurs not by shearing but in tension, a wedge of soil lifting away from the soil mass below at the limiting value of shear stress of the soil. For deep anchor, he presented a solution based on the assumption that the work done by

the anchor during vertical displacement should equal the work needed to expand a vertical cavity to the radius of the anchor.

2.2.9 Theory of Vesic (1971)

For shallow anchors Vesic's (1971) theory is based on the concept of cavity expansion. Vesic assumed a circular slip failure surface. Uplift shearing resistance is the resultant of shearing and normal forces on the slip failure surface. He presented the variation of the breakout factor (N_{qu}) with embedment ratio (D/B) and the soil friction angle (ϕ) for shallow circular anchors embedded in sand. These values are shown in Fig. 2.5.

For deep anchors, Vesic used the analogy of the expanding cavity in an infinite mass to limiting cavity pressure that caused a change in volume equal to the volume of soil displaced by the anchor.

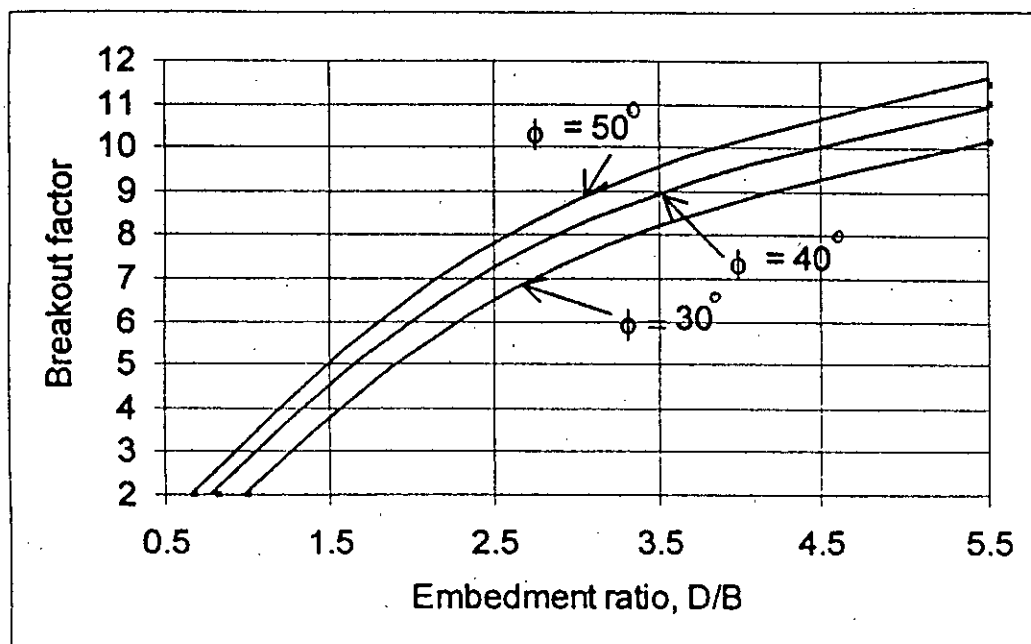


Fig. 2.5 Variation of breakout factor with embedment ratio (after Vesic, 1971)

2.2.10 Semi-empirical relation by Das and Seely (1975)

Das and Seely (1975) developed the following semi-empirical relation for strip anchor originally proposed by Meyerhof and Adams (1968).

$$N_{qu} = \frac{D}{B} K' \tan \phi_{ps} \left[\left(2m \frac{D}{B} + 1 \right) \frac{B}{L} + 1 \right] + 1 \quad \dots \quad (2.12)$$

In which m = a function of friction angle. K' = Uplift coefficient of earth pressure,
 L = Length of the anchor.

2.2.11 Empirical equation by Ovesen (1981)

Ovesen proposed the following empirical formula based on his centrifugal tests.

$$N_{qu} = 1 + (4.32 \tan \phi_i - 1.58) \left(\frac{D}{B} \right)^{3/2} \quad \dots \quad (2.13)$$

Where ϕ_i = Angle of internal friction based on triaxial test. This equation is valid for $I < D/B < 3.5$ in a sand with $29^\circ < \phi_i < 42^\circ$.

2.2.12 Theory of Rowe and Davies (1982)

Rowe and Davies used the finite element approach in obtaining the uplift capacity. According to their theory, the average applied pressure to cause failure of an anchor plate in a cohesionless soil with angle of friction ϕ may be expressed in the form

$$Q_u = \gamma D F'_{\gamma} \quad \dots \quad (2.14)$$

F'_{γ} is an anchor capacity factor which is a function of orientation, embedment ratio, angle of friction, dilatancy, initial stress state and anchor roughness.

$$N_{qu} = F_\gamma \cdot R_\phi \cdot R_R \cdot R_K \quad \dots \quad (2.15)$$

In which F_γ is the basic anchor capacity for a smooth anchor in a non-dilatant soil with $K_o = 1$, and R_ϕ , R_R , R_K are correction factors for soil dilatancy, anchor roughness and initial stress state, respectively. For horizontal anchors, both R_R and R_K have little influences on N_{qu} and can be taken as unity, while dilatancy correction factor R_ϕ varies linearly with embedment D/B and increases nonlinearly with σ'_v for associated materials, R_ϕ for non associated materials may be determined by linear interpolation. Appropriate values of dilatancy angle ϕ , may be determined for particular values of ϕ_{ps} and ϕ_{cv} , from the stress-dilatancy relation proposed by Rowe (1978).

$$\tan\left(\frac{45 + \phi}{2}\right) = \frac{\tan\left(\frac{45 + \phi_{ps}}{2}\right)}{\tan\left(\frac{45 + \phi_{cv}}{2}\right)} \quad \dots \quad (2.16)$$

Where ϕ_{ps} is the angle of friction in plain strain, ϕ_{cv} is the critical state friction angle in plane strain.

Two-dimensional design approaches require modification by suitable shape factors when applied to isolated anchors. These shape factors are defined as

$$S_u = \frac{N_{qu} \text{ of isolated anchor}}{N_{qu} \text{ of continuous anchor}}$$

The values of shape factors can be determined experimentally.

2.2.13 Theory of Rao and Kumar (1994)

Consider a strip horizontal anchor of width B subjected to vertical uplift as shown in Fig. 2.6. By assuming the anchor to be smooth, the vertically upward direction along the

anchor plate becomes the direction of major principle stress. For a horizontal ground surface and uniform surcharge pressure, The Rankine passive zones form near the ground at failure of the anchor. Experiments have shown that close to the centerline AG, the soil is either in a semi-active or rest state.

Neither the limit equilibrium approach nor the method of characteristics can be straightaway applied to determine the uplift capacity, since boundary stresses along the edges of the anchor plate at anchor level are unknown and since the region close to centerline AG is not in a plastic state. Again the limit-equilibrium approach also becomes difficult since there are two unknowns, anchor uplift capacity and lateral force along the centerline.

To overcome these difficulties, a combination approach is taken. To avoid the intersection of the central semi-active zone with the field of characteristics, it is assumed that the failure surface from the edge of the anchor plate is an arc of a log-spiral meeting tangentially the Rankine passive zone at E. It is then possible to start from the known stress conditions at E and move towards O, thus determining the state of stress along OKE (Fig. 2.7). The base pressure distribution on the anchor plate can then also be determined. From the vertical-equilibrium conditions of soil mass ABEOG, the uplift capacity of the anchor is established along with the critical failure surface and the pressure distribution on the anchor.

The following assumptions were made:

1. The anchor plate is perfectly smooth
2. The anchor tie rod has no influence on the failure load or on the pattern of failure.
3. The soil at failure follows a Mohr-Coulomb failure criterion.

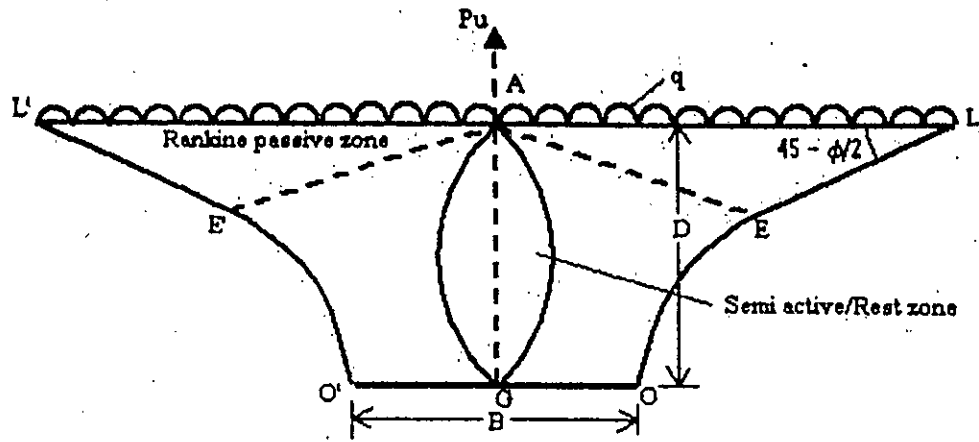


Fig. 2.6 Failure mechanism during uplift (after Rao et al. 1994)

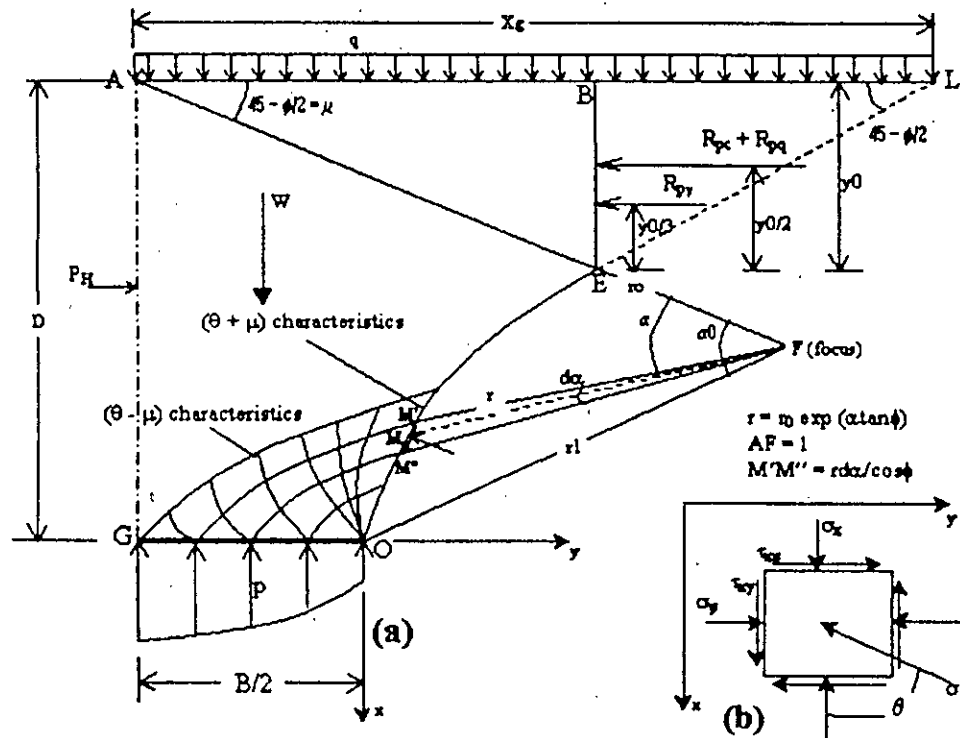


Fig. 2.7 Failure pattern and system of forces (after Rao et al. 1994)

4. The failure surface is a log-spiral arc from the edge of the anchor in the curved rupture zone and a straight line thereafter in the Rankine passive zone.
5. The suction force under the base of the anchor can be neglected.
6. The problem is a two-dimensional, plane strain problem.

For any chosen value of the distance l between the A and the focus F of the log-spiral (Fig. 2.7), the failure surface OEL is drawn such that it meets the edge of the anchor plate at o . The distances r_0 , r_1 and y_0 are then established. Taking o , the edge of the anchor plate anchor plate, as the origin, and orienting the x -axis and y -axis as shown in Fig. 2.7, the co-ordinates of any point $M(x, y)$ on the log-spiral portion of the failure surface become

$$x = -[D - l \sin \mu - r \sin(\alpha - \mu)] \quad \dots (2.17)$$

$$y = r_1 \cos(\alpha_0 - \mu) - r \cos(\alpha - \mu) \quad \dots (2.18)$$

Where r_1 = distance OF; D = depth of anchor plate from the ground level; α_0 = central angle BFO; $\mu = \frac{\pi}{4} - \frac{\phi}{2}$ and α = angle BFM.

The radial distance r between F and M is given by

$$r = r_0 e^{\alpha \tan \phi} \quad \dots (2.19)$$

For a given value of α at point M , the angle θ between the major principal stress σ_1 and the x -axis becomes

$$\theta = -[\phi - \alpha + 2\mu] \quad \dots (2.20)$$

The counterclockwise direction of σ_1 from the x -axis is taken as positive (Fig. 2.7). Because $\theta = -\pi/2$ in the Rankine passive zone, the log-spiral failure OME becomes the $\alpha(\theta + \mu)$ field of characteristics. Starting from the known state of stress at any point B , the state of stress at any point over OB is established by applying the standard equations to the characteristics. Again, starting from the edge O of the anchor plate, which is a

singular point, and making use of the condition that the shear stress along OG is zero, and base pressure distribution on the anchor plate is obtained.

The described analysis can be carried out for a number of failure surfaces by varying the distance l (Fig. 2.7). By taking into the account the symmetry of the problem about the centerline AG, the overall vertical equilibrium of the soil mass ABBOG is used to establish the correct failure surface. For all except the correct failure surface, the vertical equilibrium condition is not satisfied. For the correct failure surface

$$P_u = 2 \int_0^{B/2} p dy = 2(Q + W + V) \quad \dots(2.21)$$

Where P_u = total ultimate vertical uplift load; p = uplift pressure at any point on anchor plate; W = weight of the soil mass ABEOG; $Q = (q \cdot X_g)/2$; q = surcharge pressure; X_g = extent of the failure surface at ground level from the centerline of the anchor plate; and V = total vertical downward component of resultant force on the failure surface EMO.

The total vertical downward component of the resultant force on

$$V = \int_0^{\alpha_0} \Delta V \cdot d\alpha \quad \dots (2.22)$$

the failure surface EMO is given by

Where ΔV is the vertical component of resultant force for an element $M'M''$, (Fig. 2.8).

$$\Delta V = \Delta T \cos(\phi - \alpha + \mu) - \Delta N \sin(\phi - \alpha + \mu) \quad \dots (2.23)$$

Here ΔT and ΔN are shear and normal forces on the element $M'M''$;

$$\Delta T = \tau \cdot r d\alpha / \cos \phi \quad \dots(2.24)$$

and

$$\Delta N = \sigma_n \cdot r d\alpha / \cos \phi \quad \dots (2.25)$$

Shear stress τ and normal stress σ_n are given by

$$\tau = -\sigma \sin \phi \sin 2(\theta + \phi - \alpha + \mu) \quad \dots (2.26)$$

$$\sigma_n = \sigma[1 - \sin \phi \cos 2(\theta + \phi - \alpha + \mu)] - H \quad \dots (2.27)$$

$$H = c \cot \phi \quad \dots (2.28)$$

Where c = cohesion value of the soil; and σ = distance between the center of the Mohr circle and the point where Coulomb's failure envelope intersects the σ -axis.

The ultimate pullout load P_u per unit length of strip anchor is written as

$$P_u - W_R = c.F_c.B + q.F_q.B + 0.5\gamma B^2 F_\lambda \quad \dots (2.29)$$

In which B = width of the anchor plate; W_R = weight rectangular portion of the soil mass over the anchor plate (γBD); γ = unit weight of rectangular portion of the soil mass; and F_c , F_q and F_r are the uplift- capacity factors corresponding to cohesion, surcharge and unit weight respectively.

Expressing the net uplift capacity as $P_{u.net} = (P_u - W_R)/B$, the anchor uplift capacity is written in the form

$$P_{u.net} = c F_c + q F_q + 0.5 \gamma B F_r \quad \dots (2.30)$$

For an anchor with a shape other than that of a strip, appropriate shape factors may be introduced for calculating the uplift capacity. Such shape factors can be established by experiments.

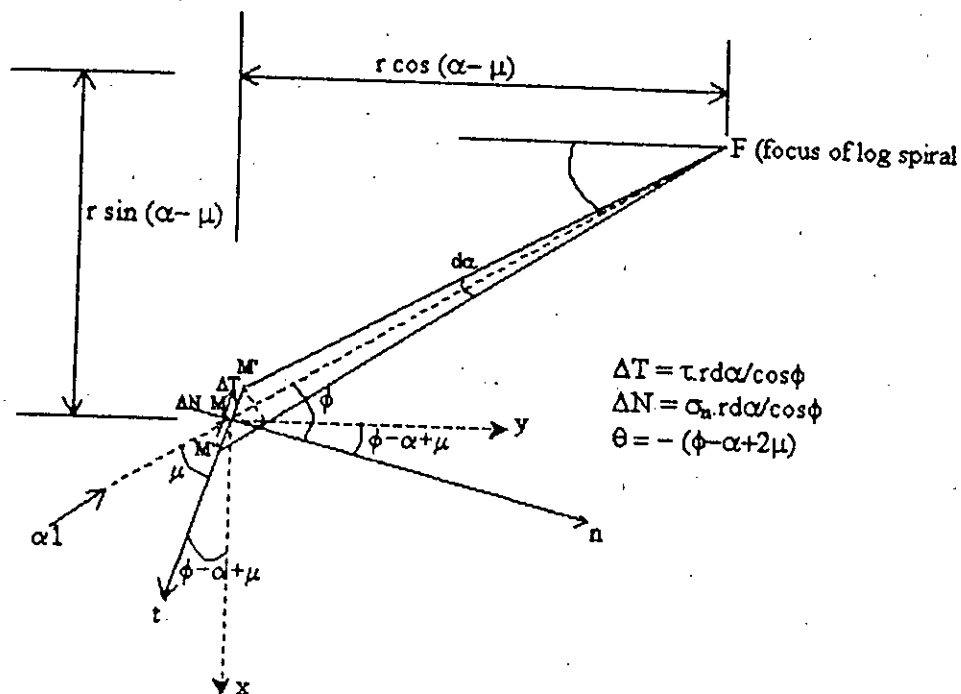


Fig. 2.8 Forces acting over the element on curved failure surfaces (after Rao et al. 1994)

2.2.14 Theory of Ghaly and Hanna (1994)

In this theory, the observed log-spiral rupture surface (Ghaly and Hanna, 1994) was employed, together with the limit equilibrium method of analysis, to develop a theoretical model to predict the uplift capacity of plate anchors in sand deposits. The geometrical properties of the segment of the log-spiral are shown in Fig. 2.9. The equation representing a log-spiral curve is as follows:

$$r_w = r_0 e^{\omega \tan \phi} \quad \dots (2.31)$$

Where r_w is radius of log-spiral at an angle ω , r_0 is initial radius of the log-spiral at ω equal to zero, ω is angle of revolution and ϕ is angle of shearing resistance of the sand.

For shallow single anchors, the uplift resistance is of three components, namely the self-weight of the anchor, the dead weight of the soil mass confined within the rupture surface, and the vertical component of the shearing resistance mobilised along the rupture surface. There is little or no frictional resistance between the anchor plate and shaft and

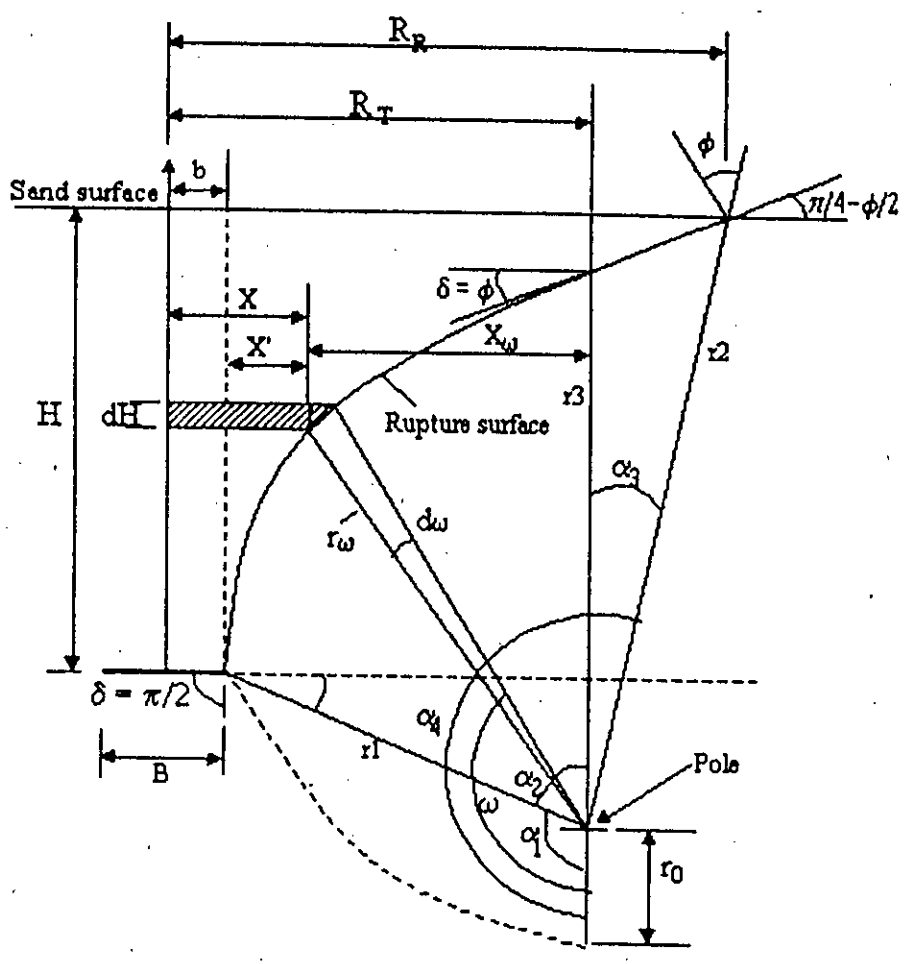


Fig: 2.9 Geometric properties of the log-spiral (after Ghaly and Hanna, 1994)

the surrounding sand because the anchor was given a smooth finish to minimize the torque required for installation. The self-weight of the anchor can be disregarded, as it constitutes a very small fraction when compared with the other two components. The volume (V) of the breaking-out sand mass can be calculated by integrating an elemental circular area of radius of revolution (X) on the total height (H) of the log-spiral (Fig. 2.10):

$$V_{ss} = \int_0^H \pi X^2 dH \quad \dots (2.32)$$

$$X = b + \left[r_1 \cos \phi - r_w \cos \left(\omega - \frac{\pi}{2} \right) \right] \quad \dots (2.33a)$$

$$dH = \left[r_0 e^{\omega \tan \phi} d\omega \frac{\sin(\omega - \phi)}{\cos \phi} \right] \quad \dots (2.33b)$$

Where V_{ss} is volume of breaking-out sand mass of a shallow single anchor, X is radius of revolution of elemental circular area, and b is the radius of the anchor plate.

Put

$$H = r_2 \cos \alpha_3 - r_1 \sin \phi \quad \dots (2.34)$$

$$r_2 = r_0 e^{\alpha_4 \tan \phi} \quad \dots (2.35a)$$

$$r_1 = r_0 e^{\alpha_1 \tan \phi} \quad \dots (2.35b)$$

And

$$e^{\alpha_1 \tan \phi} = \alpha \quad \dots (2.36a)$$

$$e^{\alpha_4 \tan \phi} = \beta \quad \dots (2.36b)$$

Where a is a constant $\alpha_{1,2,3,4}$ are angles of revolution and β is a constant.

$$r_0 = \frac{H}{\beta \cos \alpha_3 - \alpha \sin \phi} \quad \dots (2.37)$$

Where

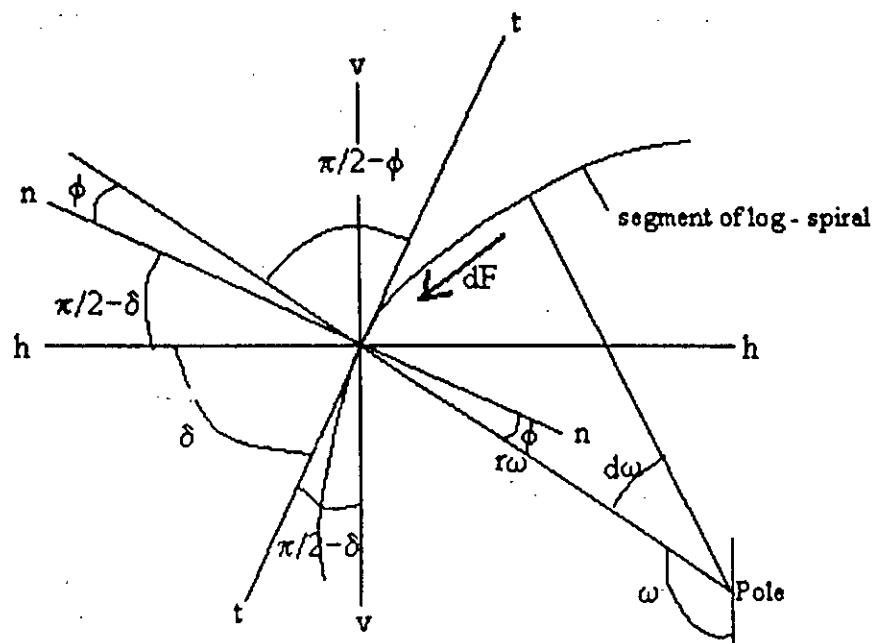


Fig. 2.10 Schematic representation of shearing forces acting on rupture surface of shallow anchor (a) Plan View (after Ghaly and Hanna, 1994)

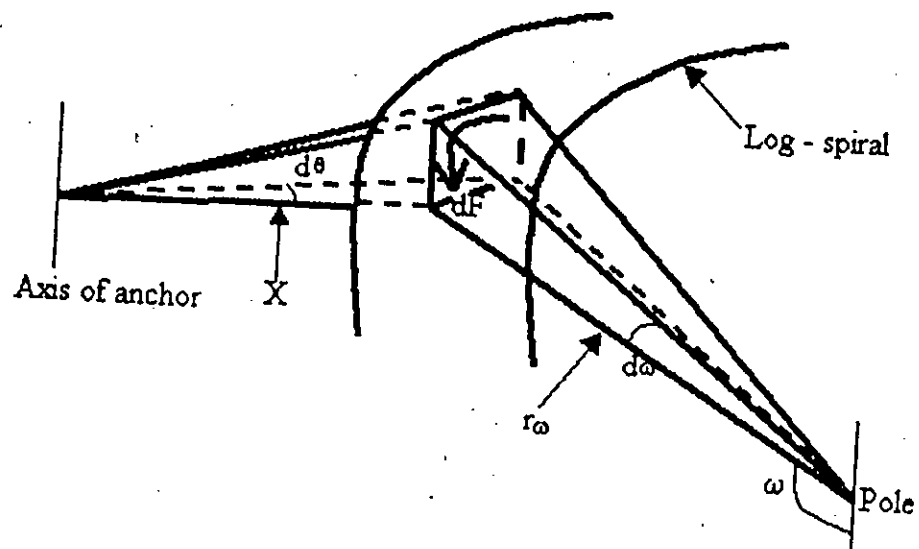


Fig. 2.10 Schematic representation of shearing forces acting on rupture surface of shallow anchors (b) Three-D view (after Ghaly and Hanna, 1994)

$$\alpha_1 = \frac{\pi}{2} + \phi \quad \dots (2.38a)$$

$$\alpha_2 = \frac{\pi}{2} - \phi \quad \dots (2.38b)$$

$$\alpha_3 = \frac{3\phi}{2} - \frac{\pi}{4} \quad \dots (2.38c)$$

$$\alpha_4 = \frac{3\pi}{4} + \frac{3\phi}{2} \quad \dots (2.38d)$$

The integration in (2.32) yields the following equation:

$$V_{ss} = \pi \int_{\alpha_1}^{\alpha_4} (r_0^2 \alpha^2 \cos^2 \phi + r_0^2 e^{2\omega \tan \phi} \sin^2 \phi - 2\alpha r_0^2 \cos \phi e^{\omega \tan \phi} \sin \omega + b^2 + 2br_0 \alpha \cos \alpha - 2br_0 e^{\omega \tan \phi} \sin \omega) (r_0 e^{\omega \tan \phi} \sin \omega - r_0 \tan \phi e^{\omega \tan \phi} \cos \omega) d\omega \quad \dots (2.39)$$

Where α_1 and α_4 are angles of revolution at the beginning and at the end of the log-spiral segment, respectively. The weight (W_{ss}) of the breaking out sand mass of a shallow anchor plate is

$$W_{ss} = \gamma V_{ss} \quad \dots (2.40)$$

Where γ is unit weight of the sand.

Expressing r_0 in terms of height (H) of sand over the anchor and substituting in the result of the integration given by (2.39)

$$W_{ss} = \gamma H^3 FW_{ss} \quad \dots (2.41)$$

Where FW_{ss} is a weight factor for shallow single anchors; its value is dependent on the angle (ϕ) of shearing resistance of the sand and the relative depth ratio (H/B). The determination of the shearing force contributing to the uplift capacity requires the

evaluation of the shear stresses acting on the observed log-spiral rupture surface. The variation of shear stress along the rupture surface can be determined by using Kotter's differential equation. This equation expresses the relationship between the resultant stress acting on the observed rupture surface at the critical state of limit equilibrium and the radius of curvature of this surface. The following simplifying assumptions have been made {Kazdi 1964, Jumikis 1969}.

1. The sand is at the state of limit-equilibrium, i.e. Mohr-Coulomb failure criterion is satisfied ($\tau = \sigma_n \tan \phi$). Where τ and σ_n are shear and normal stresses, respectively.
2. Stresses acting on a plane passing through the anchor's axis are considered. These stresses act on the outer side of the rupture surface and depend on two co-ordinates in a semi-infinite mass, namely depth and distance from the anchor's axis.
3. As the problem of anchor pullout is a three-dimensional axisymmetrical problem in physical reality, a full solution can be obtained by integrating the resulting stress from the plane considered in the above assumption around the axis of the anchor.

Kotter's differential equation in the case of uplift load involving passive resistance from lateral earth pressure has the following form (Kazdi, 1964 ; Jumikis, 1969):

$$\frac{d\tau}{d\delta} + 2(\tan \phi)\tau = \gamma \sin \phi \sin(\delta + \phi)\rho \quad \dots(2.42)$$

Where τ is shear stress along the rupture surface, δ is angle between the horizontal and the rupture surface, and ρ is radius of curvature of the rupture surface.

For a log-spiral rupture surface, the radius of curvature (ρ) is given by the following expression:

$$\rho = r_0 e^{\omega \tan \phi} \left(\sqrt{1 + \tan^2 \phi} \right) = \left(\frac{r_\omega}{\cos \phi} \right) \quad \dots (2.43)$$

Equation (2.42) can be written in the following form:

$$\frac{d\tau}{d\omega} - 2(\tan \phi)\tau = -[r_w \tan \phi \sin(\omega - 2\phi)] \quad \dots (2.44)$$

Where r_w is as given by (2.32), the solution of (2.44) is

$$\tau = c_1 e^{\omega \tan \phi} \cos(\omega - 3\phi) - (c_1 c_2 e^{2\omega \tan \phi}) \quad \dots (2.45)$$

Where c_1 and c_2 are constants given by

$$c_1 = r_0 \sin \phi \quad \dots (2.46a)$$

$$c_2 = \frac{1}{\beta} \cos\left(\frac{3\pi}{4} - \frac{3\phi}{2}\right) \quad \dots (2.46b)$$

The vertical component of the shearing resistance of shallow single anchor (F_{ss}) acting on the rupture surface can be calculated by considering the shearing resistance acting on an elemental area on the surface of the log-spiral (Fig. 2.10):

$$dF_{ss} = \tau \sec \phi (r_w d\omega) (Xd\theta) \sin \delta \quad \dots (2.47)$$

Substituting the values of τ , X , and δ in 2.47, the shearing resistance of a vertically pulled single shallow plate anchor is given by the following equation:

$$F_{ss} = \int_0^{2\pi\alpha_4} \int_{\alpha_1} dF_{ss} d\omega d\theta \quad \dots (2.48)$$

This integration yields the following equation:

$$F_{ss} = \gamma H^3 FF_{ss} \quad \dots (2.49)$$

Where FF_{ss} is a shear factor for shallow single anchors; its value is dependent on the angle of shearing resistance of the sand (ϕ) and the depth to diameter ratio (H/B) of the anchor. Ultimate pullout load of single shallow anchor (QU_{ss}) is given by the following equation:

$$QU_{ss} = W_{ss} + F_{ss} \quad \dots (2.50)$$

2.3 THEORETICAL ANALYSIS OF ANCHOR PLATE BEHAVIOUR IN CLAY

Several theories concerning uplift behaviour of horizontal plate anchor in clay are available in the literature. Below, some prominent theories name are given below.

Shallow anchor theories

- a. Theory of Tang (1962)
- b. Theory of Dana (1961)
- c. Theory of Mariupol'skii's (1965)
- d. Theory of Vesic (1971)
- e. Theory of Matsuo (1967)
- f. Theory of Meyerhof and Adams (1968)

Deep anchor theories

- a. Theory of Mariupol'skii (1965)
- b. Theory of Vesic (1971)
- c. Ali's modification of Vesic's theory (1968)
- d. Theory of Meyerhof and Adams (1968)

2.3.1 Comparison of theories for purely cohesive soils

The shallow anchor theories are based on ultimate shear failure alone and do not consider the influence of the elastic and tensile properties of the soil on uplift resistance. Fig: 2.11 plots F_u [$F_u = (P_u - \gamma gD)/c$] vs. D/B for theories of Balla(1961), Mariupol'skii (1965), Vesic(1971), Matsuo (1967) and Meyerhof and Adams (1968). The theories of Mariupol'skii, Vesic and Meyerhof and Adams lead to a unique curve. In theories of Balla and Matsuo, F_u is function of $c/(\gamma gB)$ as well as of D/B and curves are plotted for two $c/(\gamma gB)$ values covering the range of 0.5 and 4.0. With the exception of Balla, the predictions from the shallow anchor theories are in relatively good agreement, the

influence of $c/(\gamma gB)$ being comparatively small with the theory of Matsuo. Balla's solution contains numerical values of uplift factors that appear to be incorrect.

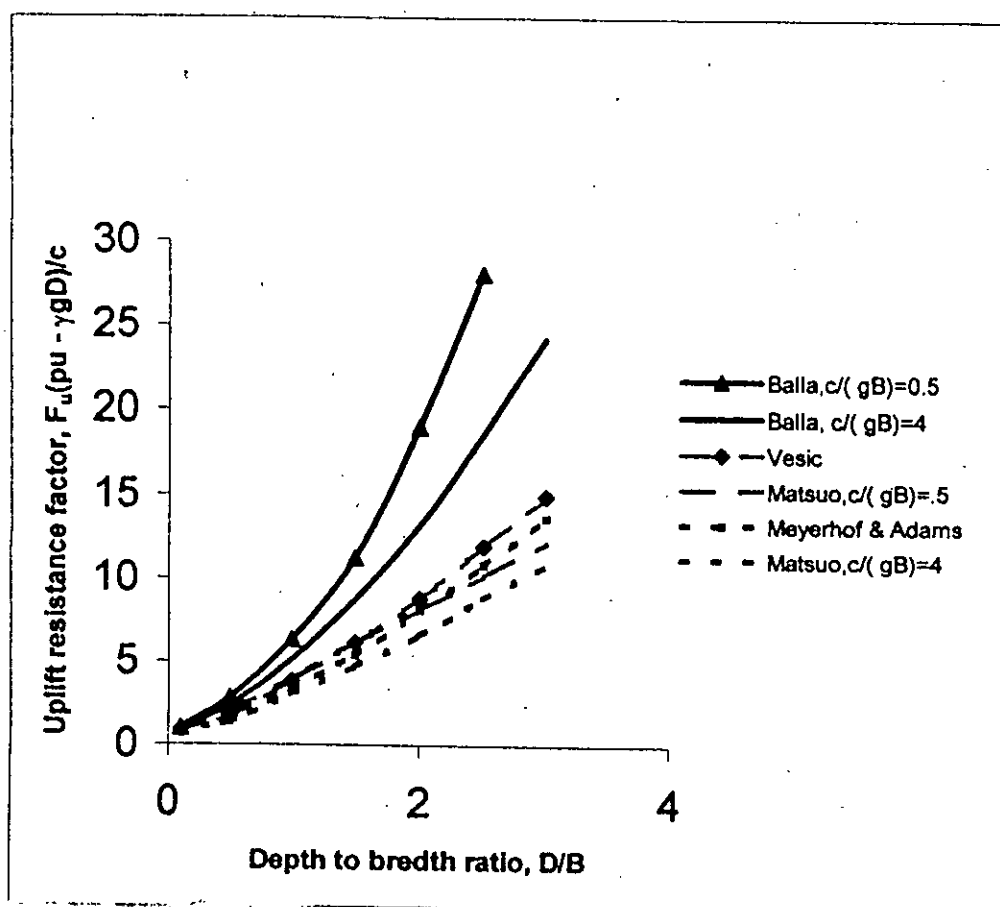


Fig. 2.11 Comparison of shallow anchor plate theories (after Davie et al, 1977)

For deep anchors theories different theories contain different parameters in their solutions. These are as follows:

Theory of Mariupol'skii: ω (compressibility of soil, ω is a function of the reciprocal of the coefficient of volume compressibility.)

Vesic 's theory: I_r and Δ matter in soil compressibility. I_r is the rigidity index and Δ is a measure of average volume strain in the plastic zone. $I_r = G/c$. G is the shear modulus of the soil.

Theory of Meyerhof and Adam: Assumption is $N_c = F_u$. In case of rigid incompressible material, $N_c = 9.34$, but if compressibility is taken into account, N_c could be reduced to 7. Comparison of different anchor theories are summarised in Table 2.1

Table 2.1 Comparison of difference deep anchor plate theories (Davie et al, 1977)

Type	Theory	Uplift resistance factor, F_u	Values of parameters included in the solution
Rigid, incompressible	Mariupol'skii (1965)	7.00	$\omega=200$
Rigid, incompressible	Vesic (1971)	9.94	$I_r=300, \Delta=0$
Rigid, incompressible	Meyerhof and Adams (1968)	9.34	
Non-rigid, compressible	Mariupol'skii (1965)	4.6	$\omega=25$
Non-rigid, compressible	Vesic (1971)	5.15	$I_r=10, \Delta=0.02$

2.4 BEHAVIOUR OF HORIZONTAL ANCHOR PLATE IN SAND

Different features of behaviour of horizontal anchor plate in sandy soil are described according to experiments performed by researchers in past years. Following topics are covered here.

1. The load -displacement behaviour
2. Failure mode of anchor plates
3. Variation of breakout factor with embedment ratio
4. Variation of failure displacement with embedment ratio
5. Variation of shape factor with embedment ratio
6. Effect of over consolidation on uplift capacity
7. Effect of angle of internal friction on uplift capacity
8. Effect of backfill compaction on uplift capacity of backfilled anchors
9. Effect of native soil density on uplift capacity of backfilled anchors
10. Effect of aspect ratio on uplift capacity

2.4.1 Nature of load displacement curve

According to tests performed by Dickin (1988), uplift resistance increased linearly with anchor displacement in the initial stages of each test, and it eventually reduced, exhibiting a well-defined peak resistance for anchors of all geometries at shallow embedment ratios up to three. This was not always the case for embedment ratios greater than five. With the exception of the anchor with aspect ratio of eight, for which a brittle failure was observed, anchor resistance exhibited oscillatory behaviour at large displacements. The anchor load/displacement relationship at an embedment depth of seven meters in dense sand in Fig. 2.12 typifies the behaviour. These oscillations were attributable to the collapse of sand into the gap below the anchor as breakaway occurred.

Experiments performed by Kulhawy et al., 1987, showed that the anchor response to load become increasingly dilatant as the soil density increases. Another important finding of

their experiment was that as the peak resistance increased (with increase of density and depth), there is a tendency for increased stiffness in the load-displacement response (slope of load-displacement curve steeper). As the limiting factor for plate anchors is displacement rather than peak resistance, this observation was important. According to experiments performed by Rowe and Davis (1982), load-displacement of all anchors (from $D/B = 1.0$ to $D/B = 8.0$, $V/B = 8.75$) clearly showed distinct peaks, in general there was little or no evidence of anchor failure at the soil surface. The collapse of shallow anchors ($D/B \sim 3$) occurred at displacements less than 3 mm (anchor size = 51 mm). The displacement before collapse increased with the embedment ratio and at larger displacements (greater than 8 mm). The load displacement curve oscillated. The cause of oscillation is mentioned earlier.

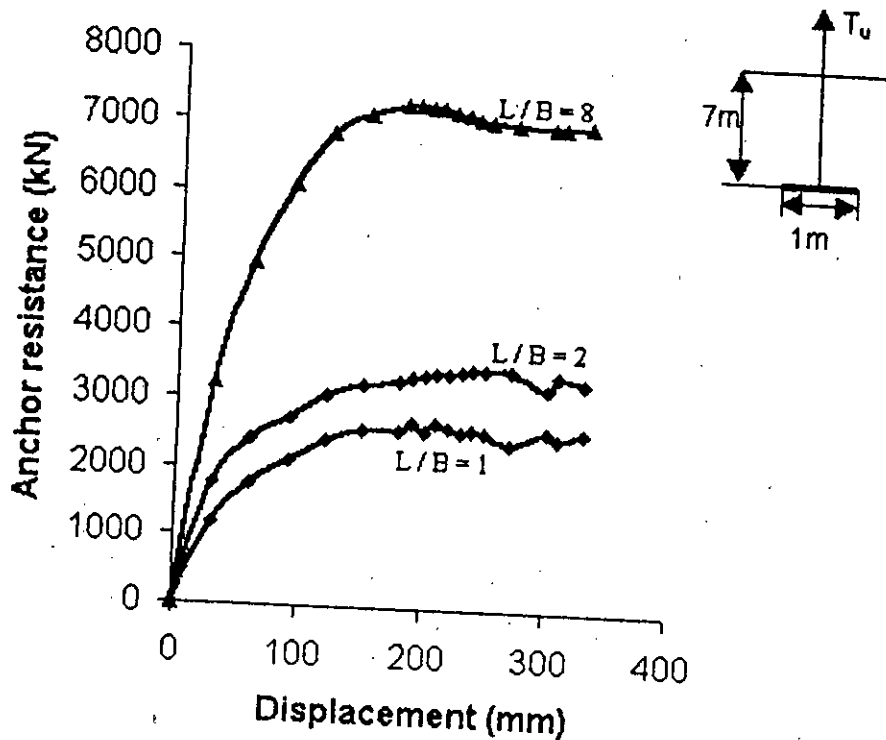


Fig. 2.12 Load-displacement behaviour of anchor plates (after Dickin, 1988)

2.4.2 Failure mode of anchor plate

According to Sutherland et al (1982), the shallowest embedment ratio at which no surface heave occurs can be called as critical depth ratio.

According to the experiments performed by Dickin (1988), evidence of anchor failure at the soil surface was observed after centrifugal tests on shallow anchors at embedment ratios up to three. Only a slight bulge of the soil surface occurred at $D/B=5$, the zone of the heave was larger than for shallower cases. Surface heave was not evident after the centrifuge tests on anchors at embedment ratios of seven and eight.

Ghaly and Hanna (1991), (experiments were performed with single screw anchor) found similar results. According to their experiment, critical depth ratios were 14, 10 and 8, respectively for dense, medium and loose sand. Shallow mode of behaviour (general shear failure) terminated at 11, 9 and 7, respectively. Between shallow and deep behaviour, transition mode took place.

Kulhawy et al. (1987), observed three kinds of failure modes in their experiments with backfilled anchors. Those were shear along vertical surfaces extending from the edges of the anchor, wedge or combined wedge and side shear failure, and punching failure. Most of the tests exhibited failure by shear along vertical surfaces, as illustrated in Fig 2.13. Wedge or combined shear failure occurred, in general, for anchors with D/B less than two in medium to dense native soil, where the backfill was at least 85% as dense as the native soil. This failure mode is illustrated in Fig: 2.14. Punching failure occurred only at D/B equal to three where the backfill was less dense than the native soil. Punching failure produced essentially no disturbance at the soil surface as the soil near the anchor flowed down around the edges of the anchor model. For anchors having D/B ratio more than three also showed punching shear failures (Esquivel-Diaz, 1967).

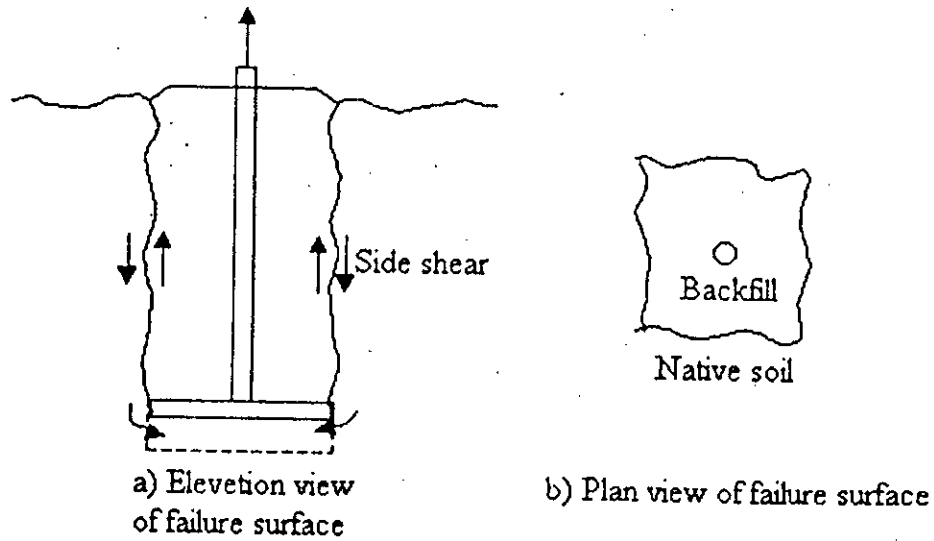


Fig. 2.13 Failure mode of anchor plate along vertical shear surface(after Kulhawy, 1987)

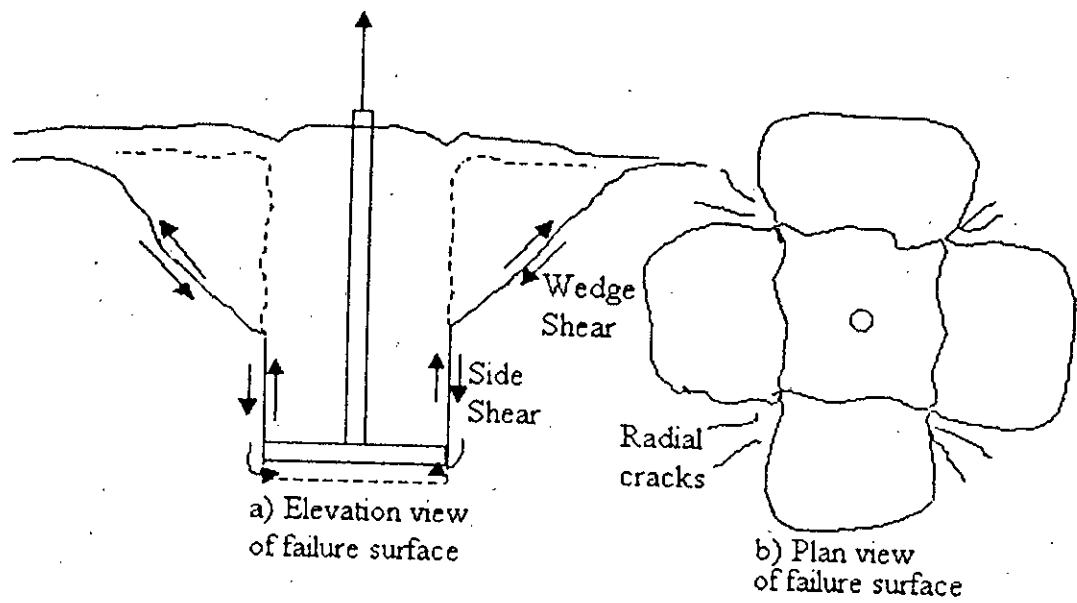


Fig. 2.14 Combine shear failure of anchor plate, (after Kulhawy, 1987)

2.4.3 Variation of breakout factor with embedment ratio

According to experiments performed by Dickin (1988), all geometries of one-meter anchors in dense sand exhibited a substantial increase in N_{qu} with embedment ratio as shown in Fig. 2.15, although an increase in aspect ratio led to a reduction in N_{qu} at all embedment. A more modest increase in breakout factors in loose sand is shown in Fig. 2.16, which compares both loose and dense test data. A maximum value of N_{qu} occurred at $D/B \sim 6$ for both anchor geometries in loose sand. This limiting value provided Das's definition of critical depth $(D/B)_{cr}$, beyond which anchors may be considered deep. Das (1980), provided an empirical equation relating critical embedment with relative density.

$$(D/B)_{cr} = 4 + 0.0332D_r \quad \dots (2.51)$$

Experiments performed by Harvey et al (1981), showed that N_{qu} increases with depth at shallow depths and tend to approximate constant values. For shallow depths the ultimate uplift capacity increased at a rate greater than in proportion of D^2 . But as the depth of embedment increases and failure becomes more localised there is not the same dependence on depth as for the shallow anchor, and the ultimate load- relative depth relationships tend to become linear.

For backfilled anchors, the experiment performed by Kulhawy et al. (1987), showed that if the embedment ratio is increased from 1 to 3, breakout factor of anchor increases by 75% to 500%, respectively for loose and dense backfill.

2.4.4 Variation of failure displacement with embedment ratio

Failure displacement q can be conveniently expressed in dimensionless form as relative failure displacements $Z_f/B\%$. According to tests performed by Dickin (1988), a general increase in $Z_f/B\%$ with D/B occurs. Failure displacements for continuous anchors are always smaller than for square ones, as might be expected since the soil around the former experiences plane-strain conditions, whereas that around the latter is subjected conditions closer to triaxial compression. It is well established that deformation in plain

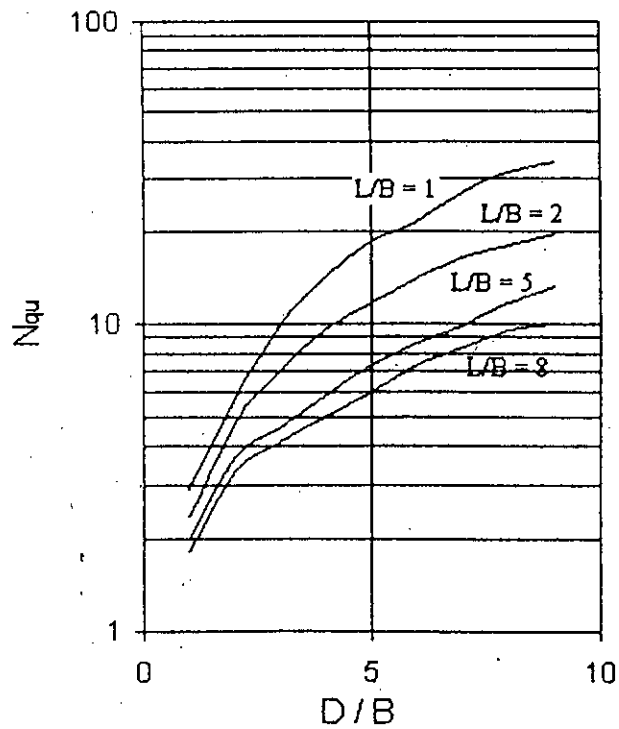


Fig. 2.15 Variation of breakout factor in dense sand (after Dickin, 1988)

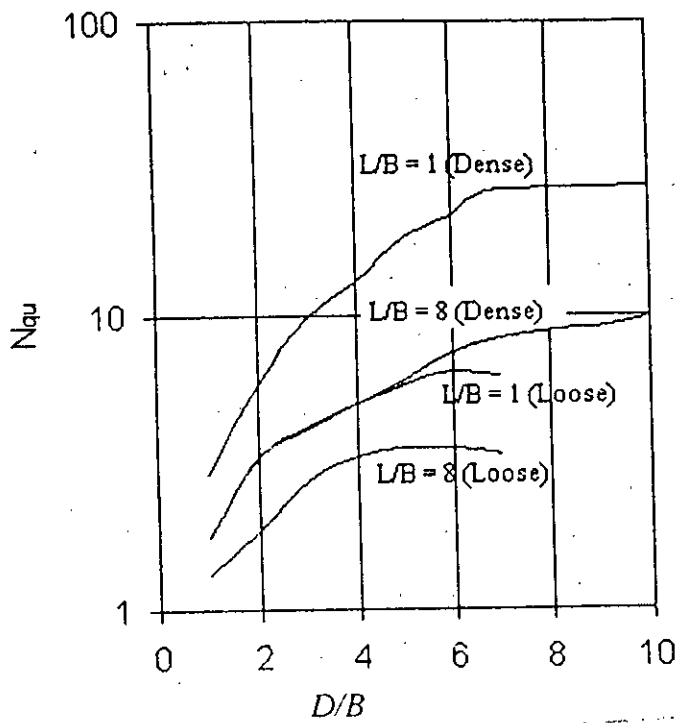


Fig. 2.16 Variation of breakout factor in both loose and dense sand (after Dickin, 1988)

strain is smaller than in triaxial compression. This shape effect is less pronounced for tests on anchors in loose sand, which also exhibited a limiting failure displacement at embedment ratios close to $(D/B)_{cr}$ (Fig. 2.17).

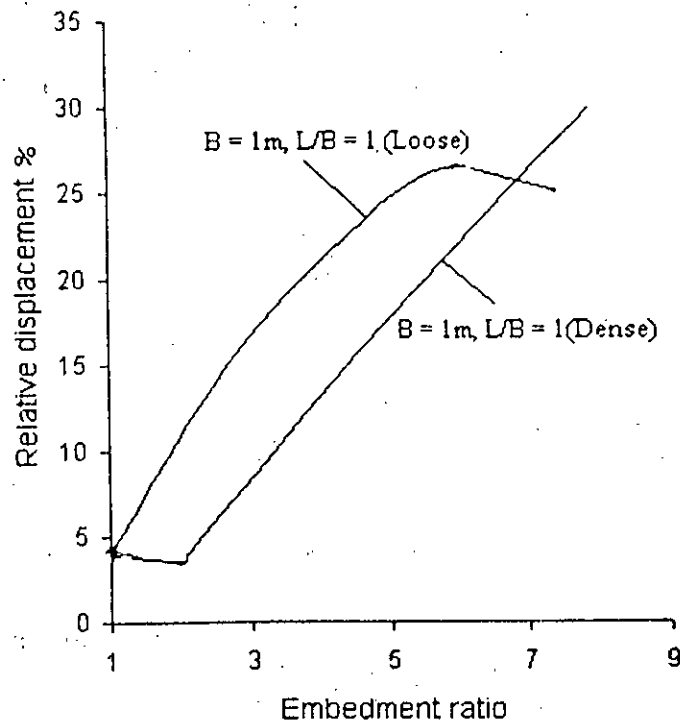


Fig. 2.17 Variation of breakout factor in both loose and dense sand (after Dickin, 1988)

2.4.5 Variation of shape factor with embedment ratio

Shape factor, S_u = (Breakout factor of an isolated anchor / Breakout factor of a continuous anchor with the same width). Anchor having L/B ratio of 8 can be considered as a continuous anchor. The experiments performed by Dickin (1988), showed a non-linear increase in S_u with embedment and a reduction with increased aspect ratio for one-meter anchors in dense sand. Shape factors are strongly influenced by density, S_u values for square anchors in loose sand being approximately half those in dense sand (Fig. 2.18).

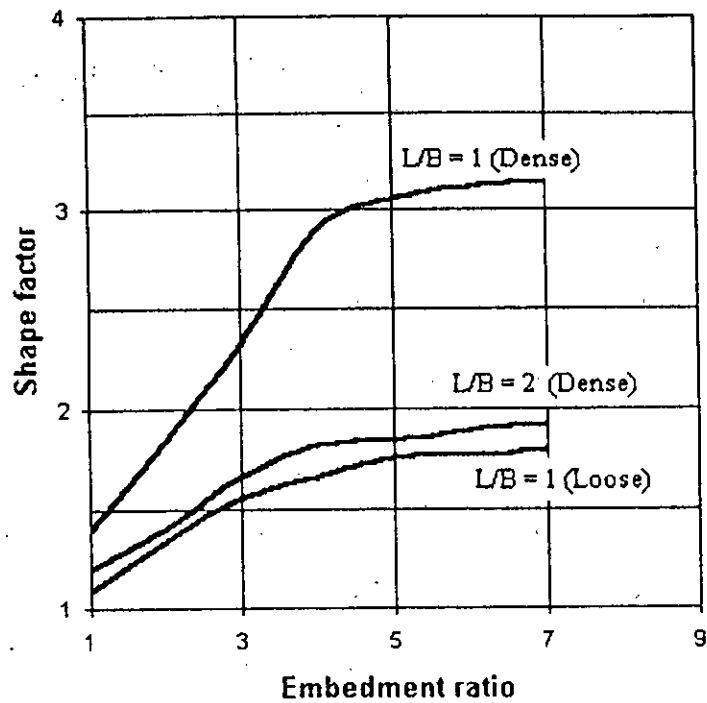


Fig. 2.18 Variation of shape factor in dense sand (after Dickin, 1988)

2.4.6 Effect of overconsolidation on uplift capacity

Hanna and Carr (1971), and Hanna et al. (1971), demonstrated that the stress history built into a sand stratum controls the uplift load that an anchor can sustain in that stratum. They conducted tests in NC sand and OC sand (with OCR upto 14) and found that the increase in the OCR significantly varies the uplift capacity of the anchor plate. As mentioned earlier, the total uplift capacity comprises of two components, (I) the dead weight of the breaking out sand mass and (II) vertical component of shearing resistance. Fig. 2.19 shows the variation of the total uplift capacity and vertical component of shearing resistance with different values of OCR. Ghaly and Hanna (1992), to predict vertical component of shearing resistance at a given OCR propose the following mathematical relation.

$$VS_{(OC)} = VSR_{(NC)} \sqrt{(OCR)}$$

$VS_{(OC)}$ = Vertical component of shearing resistance for overconsolidated soil.

$VSR_{(NC)}$ = Vertical component of shearing resistance for normally consolidated soil.

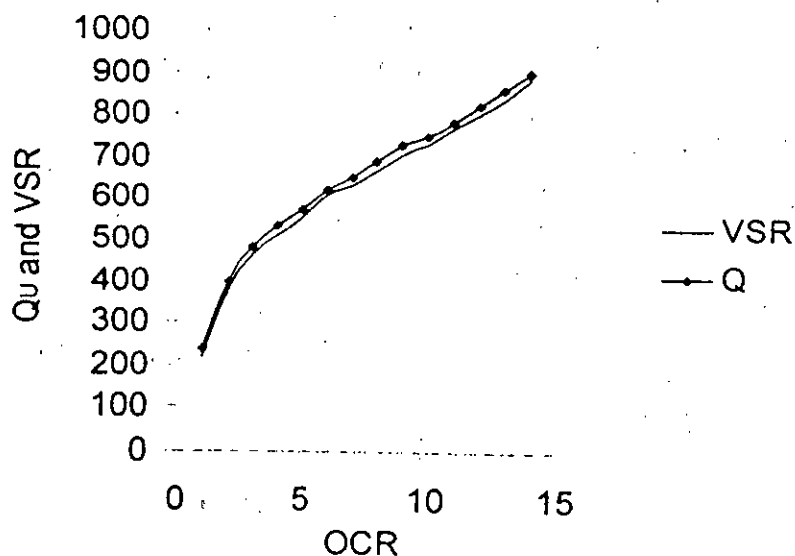


Fig. 2.19 Variation of Q_u and VSR with OCR. (after Hanna, 1992)

2.4.7 Effect of angle of internal friction of sand on uplift capacity

Wang et al. (1990), performed tests varying angle internal friction of sand. The results are shown in Fig. 2.20. According to the test results, anchor capacity increases with increasing internal friction angle; the effect is more prominent at greater embedment-breadth ratios. Some theoretical results are also given for Comparison.

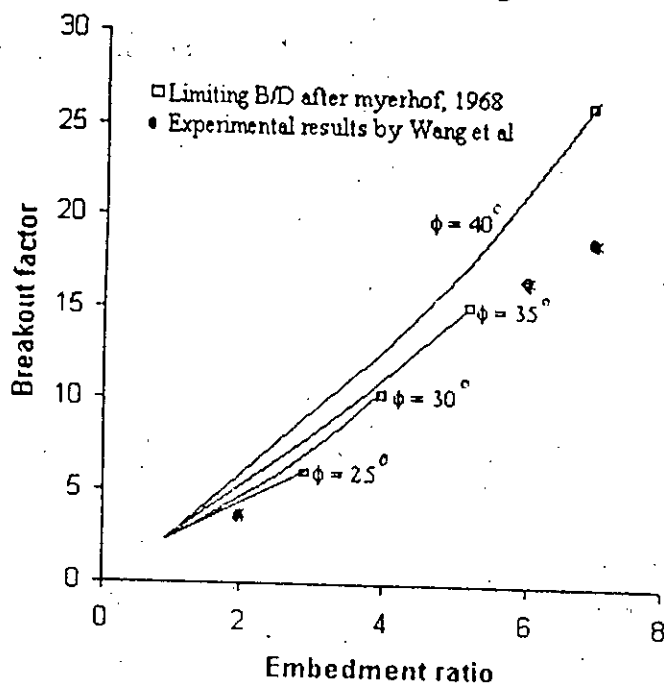


Fig. 2.20 Variation of breakout factor with angle of internal friction (after Wang et al, 1990)

2.4.8 Effect of backfill compaction on uplift capacity of backfilled anchor

According to the experiments done by Hekkala and Laine (1964), substantial increase of uplift capacity occurs due to increase in backfill compaction. But in case of compacted backfill, the load -displacement curve shows a sharp fall after reaching the peak load.

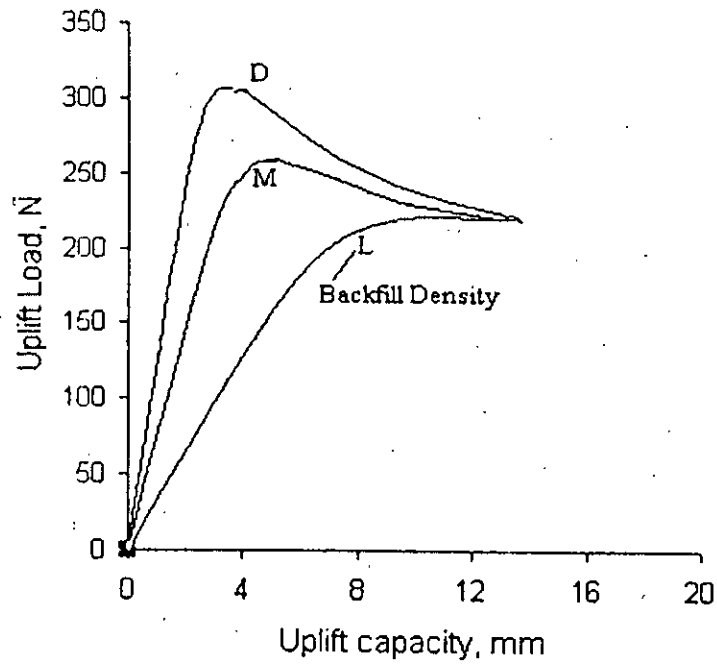
Similar results were also found by Kulhawy et al. (1987). They experimented on backfilled anchors with $D/B = 3.0$ and found that densification of backfill increased the uplift capacity by 40% and 110% respectively for loose and dense native soil. Respectively for loose and dense native soil, displacement at 50% of peak load reduced by 75% and 35% for densification (Fig. 2.21).

2.4.9 Effect of native soil density on uplift capacity of backfilled anchor

According to experiments performed by Kulhawy et al. (1987), native soil density has a marked influence on uplift capacity of backfilled anchors, with the effects more pronounced at greater depths and where the backfill was well compacted. This behaviour is illustrated in Fig. 2.22, which shows the load-displacement response for square model anchors with loose and dense backfill. The capacity increased about 190% as the native soil density increased from loose to dense with loose backfill. For densely compacted backfill, the increase was about 365%.

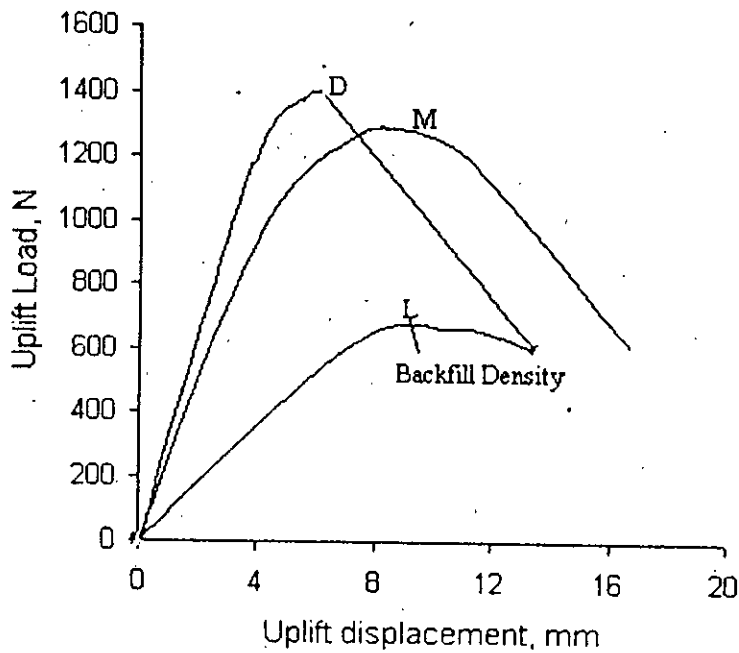
2.4.10 Effect of aspect ratio on uplift capacity

Experiments conducted by Rowe and Davis (1982), showed that decreasing aspect ratio leads to increase in anchor capacity (Fig. 2.23). For anchors having L/B ratios of 5, 3, 2 and 1, uplift capacities were respectively 10%, 25%, 35% and 120% higher from that of anchor having $L/B = 8.75$ (with same B).



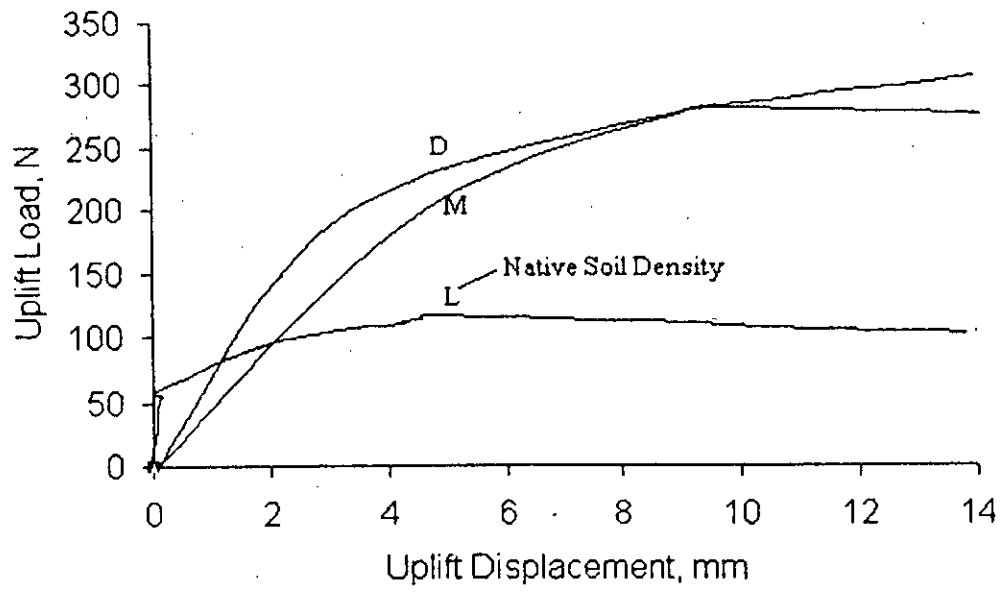
a) Loose Native soil $D/B = 3$ Square anchor

Fig. 2.21(a) Variation of uplift load due to backfill density in loose native soil. (after Kulhawy, 1987)



b) Dense native soil, $D/B = 3$, square anchor

Fig. 2.21(b) Variation of uplift load due to backfill density in dense native soil. (after Kulhawy, 1987)



b) Loose Backfill, D/B = 2, Square Anchor

Fig. 2.22 Variation of uplift load due to native soil density (after Kulhawy, 1987)

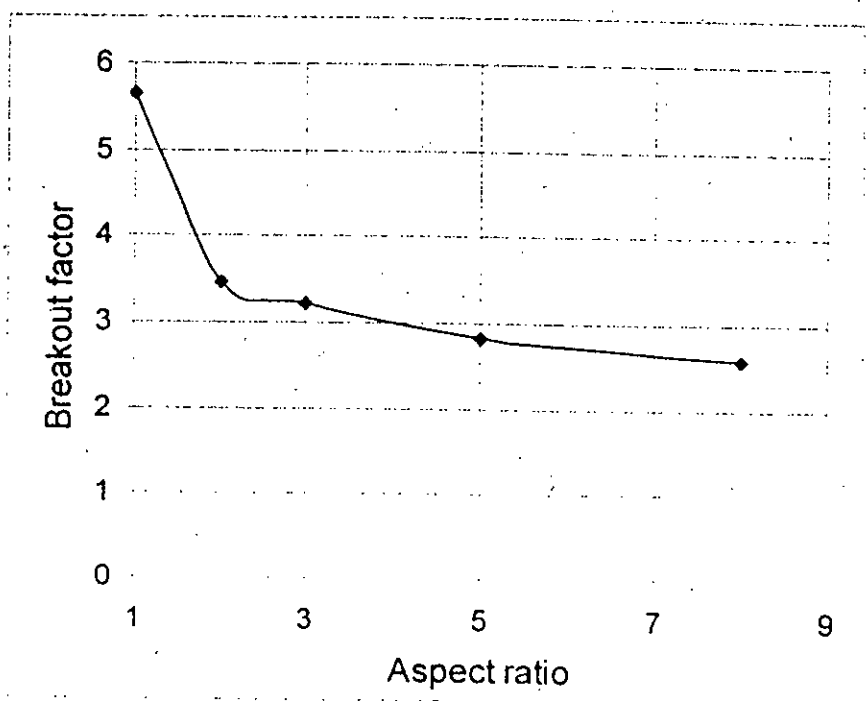


Fig. 2.23 Variation of breakout factor with aspect ratio (after Rowe & Davis, 1982)

2.5 BEHAVIOR OF HORIZONTAL ANCHOR PLATES IN LAYERED SOIL

Some experimental investigations have been conducted in recent years to observe plate anchor behaviour in layered soil. Some of those observations are interesting and worthy of practical application. In this part of the chapter, summary of such experimental investigations are presented. It covers layering in both cohesive and cohesionless soil.

2.5.1 Effect of layering on the uplift capacity of anchors in clay

For deep anchors in clay, the uplift capacity remains almost constant when D/B increases above about 4.5. The uplift capacity of anchors in cohesionless soil increases as D/B increases and the increase is greater with increased density of cohesionless soil. Then, given that an anchor is embedded in clay, it may be possible to increase the uplift capacity of the anchor by placing a cohesionless overlay on the clay layer (Stewart, 1985). Below, the experiments performed by Stewart and the results are given Table 2.2 and Table 2.3

Table 2.2 Layering effect on the uplift capacity of anchors in clay (experiments)

Test no.	Depth of Clay layer (D_g) (mm)	Depth of Clay layer (D_s) (mm)	D/B $D=D_g+D_s$ B =diameter of anchor=50mm	Cohesion C (kpa)	Density* (Kg/m^3)
1	75	--	1.5	9.5	1530
2	75	75	3.0	8.9	1744/1530
3	75	--	1.5	8.8	1530
4	75	225	6.0	8.9	1744/1530
5	75	--	1.5	8.8	1530
6	75	375	9.0	8.7	1744/1530
7	75	375	9.0	8.8	1598/1530 [#]

* For overlay tests, sand density is given first.

Loose-sand overlay is used, in other tests, dense-sand overlay is used.

Table 2.3 Results of uplift capacity of anchors in clay tests (after experiments)

Test no.	Ultimate uplift capacity per area of the anchor, ρ_u (kpa)	Ultimate uplift capacity of anchor, P_u (N)
1	38.2	71
2	47.4	88
3	36.2	66
4	127.8	253
5	34.1	62
6	481.4	945
7	202.8	394

The load-displacement curves for the seven tests in Fig 2.24 shows that the uplift

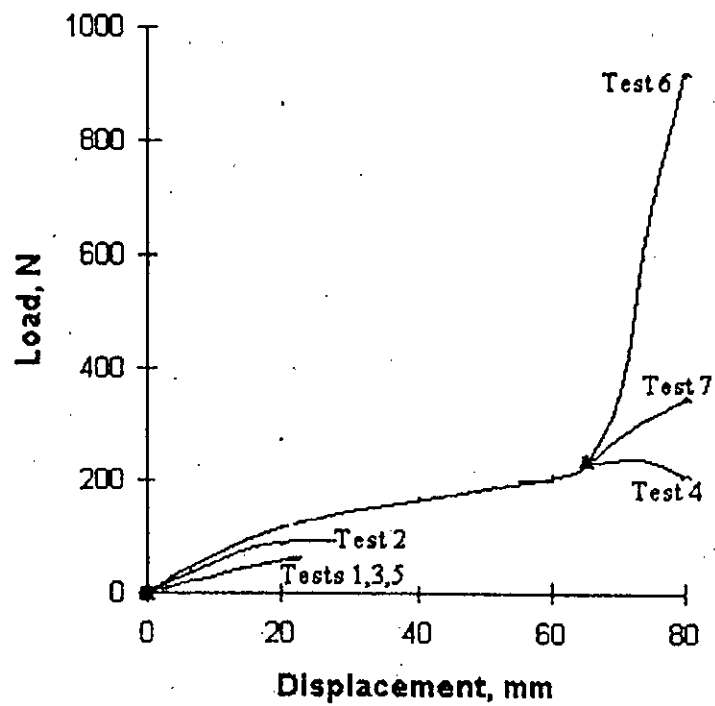


Fig. 2.24 Load-displacement curve of anchors in clay with various kinds of layering (after Stewart, 1985)

capacity is significantly increased by the sand overlay. The increase appears to be composed of two parts, (i) an increase in uplift capacity caused by the additional overburden pressure of the anchor, due to the weight of the sand layer, and (ii) an additional increase in the uplift capacity caused by the mobilization of the frictional resistance of the sand.

Dealing initially with (i), a significant increase in the overburden pressure will increase the uplift capacity of a shallow anchor buried in any soil. The overburden pressures for tests 4, 6 and 7 were 3.8, 6.4 and 5.9 kPa respectively. The load-displacement curves for these tests, as shown in Fig. 2.24, followed the same path over the first 65 mm of anchor displacement and then diverged as the displacement increased beyond 65 mm. In test 2 the overburden pressure was 1.3 kPa and the load-displacement curve in this case was similar to that of tests 1, 3 and 5 in which no overburden pressure was applied to the clay layer.

Recalling the approximate limits on D/B for shallow and deep anchors in purely cohesive soils, tests 4, 6 and 7 all have values of $D/B > 4.5$, i.e., deep anchors. Test 2 has a D/B ratio of 3.0, which lies in the indeterminate range between shallow and deep anchors. However, the test results indicated a predominantly shallow-type failure for test 2. It would appear, therefore, that a shallow type anchor buried in clay layer can be transformed into a deep anchor by placing cohesionless material on top of the layer. When deep anchor conditions are established, any further increase in D, E ratio has little effect on the uplift capacity, until the anchor approaches the sand/clay interface. Its independence of the D/B ratio is identical to the behaviour of deep anchors in purely cohesive soil.

Considering the second part of the increase, it is useful to define a dimensionless parameter called the displacement ratio. This is the ratio of anchor displacement to anchor diameter, Z/B . Thus for a 60 mm displacement in model tests 4, 6 and 7, just before the frictional resistance of the sand is mobilised, $Z/B = 1.2$. Presuming dimensional similarity between prototype and model for this particular parameter, The prototype must

also have $Z/B=1.2$. With a prototype anchor of say 1m diameter, it would require a displacement of 1.2 m to begin to mobilise the frictional resistance of the sand overlay. For conventional foundation design, displacements of this magnitude would be unacceptable.

Sutherland (1988), pointed out that in practice little real benefit would be achieved on uplift capacity by placing a cohesionless material overlay on an anchor embedded in clay, as a large displacement is required to mobilize the shear strength of the overlays. A more sensible solution would be to place the anchor on the surface of the clay.

2.5.2 Effect of layering on the uplift capacity of anchors in sand

Some tests were performed by Bouzza and Finlay in 1990 to observe anchor plate behavior in layered sand. The two layered soils for test series conducted by Bouzza and Finlay (1990) consisted of a layer of loose or medium sand overlying a dense stratum. The sand used was a coarse uniform Leighton Buzzard sand with the following properties: uniformity coefficient = 1.8, specific gravity = 2.65, grain shape = sub rounded, porosity limits: minimum = 33.2%, maximum = 44.2%. The researchers had the following findings:

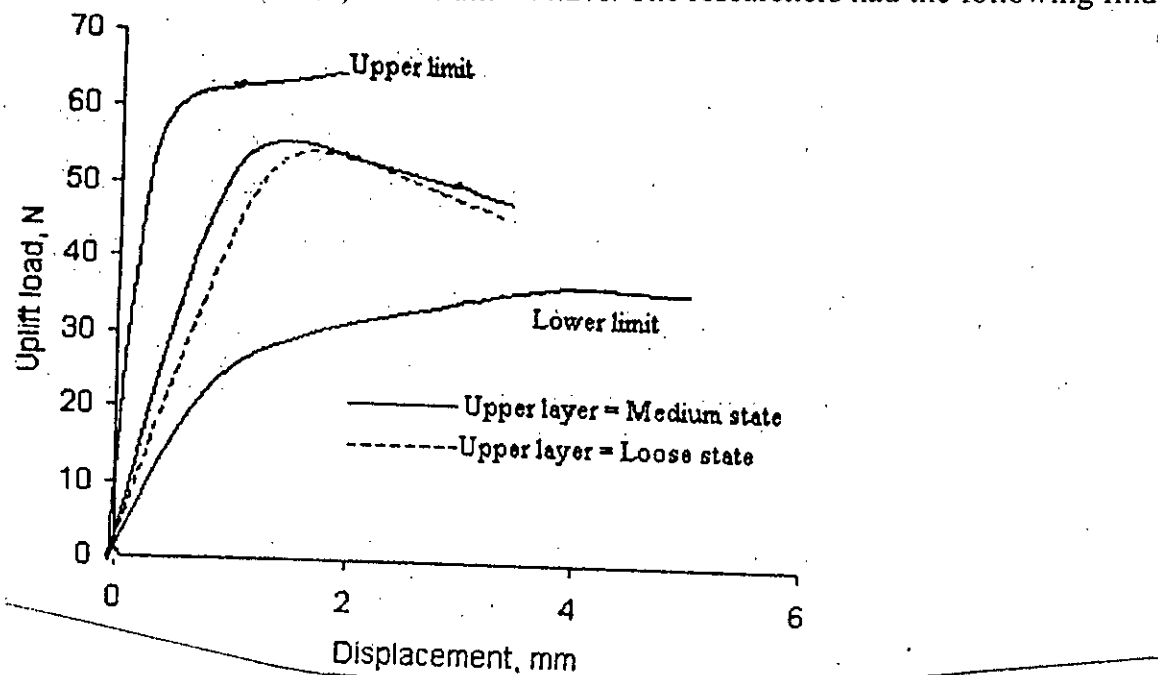


Fig 2.25: Load-displacement relationship of plate anchor embedded in a two layered sand, $\lambda=1$ (after Bouazza et al, 1990)

A dimensionless parameter called the upper thickness ratio λ was introduced. This is the ratio of the upper layer thickness H to anchor diameter B . Fig. 2.25 shows the load-displacement relationship for an anchor embedded in a sand bed where $\lambda = 1$. The ultimate pullout load remained the same whether the upper layer is loose or medium. This suggested that for this particular case ($\lambda = 1$) the pullout load is independent of the state of the weak layer as it would appear that the dense layer was providing most of the strength. However, when the thickness of the upper layer (loose or medium) was increased ($2 < \lambda < 4$) a different phenomenon occurred as the load displacement relationship was, as expected found to be dependent on the type of upper layer. In Fig. 2.26, for the particular case of $\lambda = 2$ and $D/B = 4$, it can be seen that two distinct curves representing a loose upper layer and a medium upper layer lay between the homogeneous upper and lower layer soils. This observation suggests that the density of the upper layer govern the load-displacement relationship: the weaker the upper layer, the lower is the ultimate uplift load.

Another important conclusion of the tests is that the non-layered soil shows a typical load-displacement curve (lower and upper limits in Fig. 2.25) while the layered soil shows a distinct peak point in the load displacement curve (Fig. 2.25). This behavior could be explained by the fact that the load transferred from the anchor to the sand started at the beginning to break out the dense layers of the sand and, once the weaker layers (medium or loose) had been reached, less force was required to break out the soil and, consequently, a drop in the pullout load occurred.

Typical test results of the variation of the ultimate capacity with increasing thickness of the loose or medium layer above the dense stratum are shown in Fig. 2.25 for different depth / diameter ratios D/B . The ultimate uplift load decreases with the increase in the upper layer thickness ratio), to a minimum value which is close to that obtained for the same D/B ratio in a homogenous soil deposit at the same density as the upper layer. As expected, the results show that the ultimate uplift capacity increased with increasing depth of embedment to anchor diameter ratio D/B .

2.6 BEHAVIOR OF HORIZONTAL ANCHOR PLATES UNDER CYCLIC LOADING

As ocean operations and construction have expanded and moved into deeper waters, the need for development of high capacity and reliable anchor systems for long time moorings has emerged. Embedment anchor systems which may be used to moor vessels of buoys, as well as semi submersible structures, are subjected to a combination of sustained and repeated loads that will vary with the tautness of the mooring system and the nature of the ocean wave action. Experiences show that the response of soils due to repeated loading or to sustained-repeated loading combinations may be more critical than that due to sustained loads of the same magnitude.

Andreadis, Harvey and Burley performed some tests in 1978 to predict the behaviour of anchor plate under repeated loading. The tests were performed in a medium, uniform saturated sand with the following characteristics (Table 2.4).

Table 2.4 Andreadis, Harvey and Burley (1978) test results

Specific gravity	Uniformity coefficient	Maximum dry density, lb/ft ³	Minimum dry density, lb/ft ³	Relative density, %	Permeability, cm/sec	Angle of friction Degree	Coefficient of lateral stress at rest
2.68	2	112.3	87.5	75	0.022	43.6 at e=.6	.65-.85

Typical sets of data are presented in Fig. 2.26 and Fig. 2.27 in terms of number of sinusoidal 10-sec duration cycles N , relative anchor movement $\Delta\lambda = \Delta/B$, and relative cyclic load Q_c/Q_{ult} , as a percentage. Where Δ = deformation of anchor, B = diameter of anchor plate, Q_c = given load and Q_{ult} = ultimate load. Data of sustained repeated load

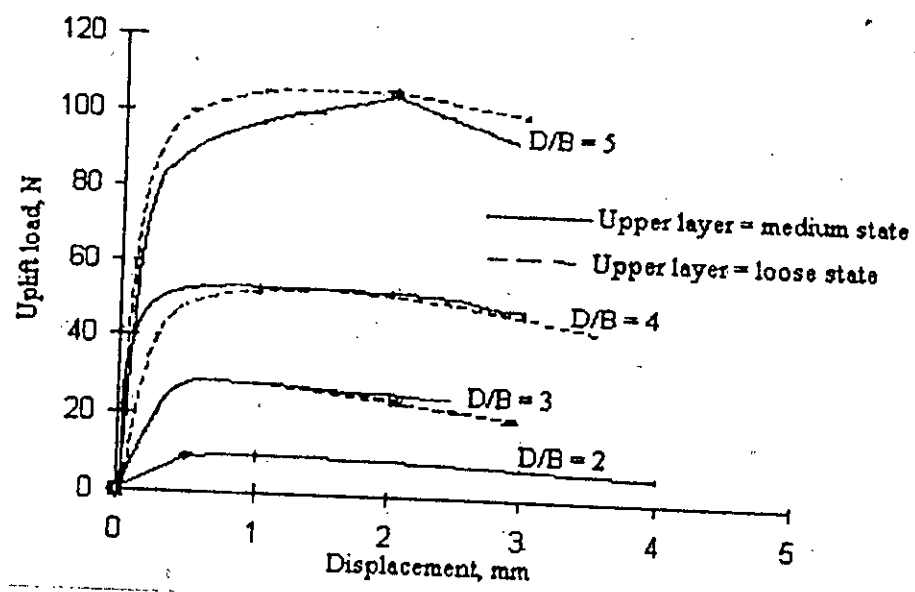


Fig. 2.26 Load-displacement relationship of plate anchor embedded in a two layered sand, $\lambda=2$ (after Bouazza et al,1990)

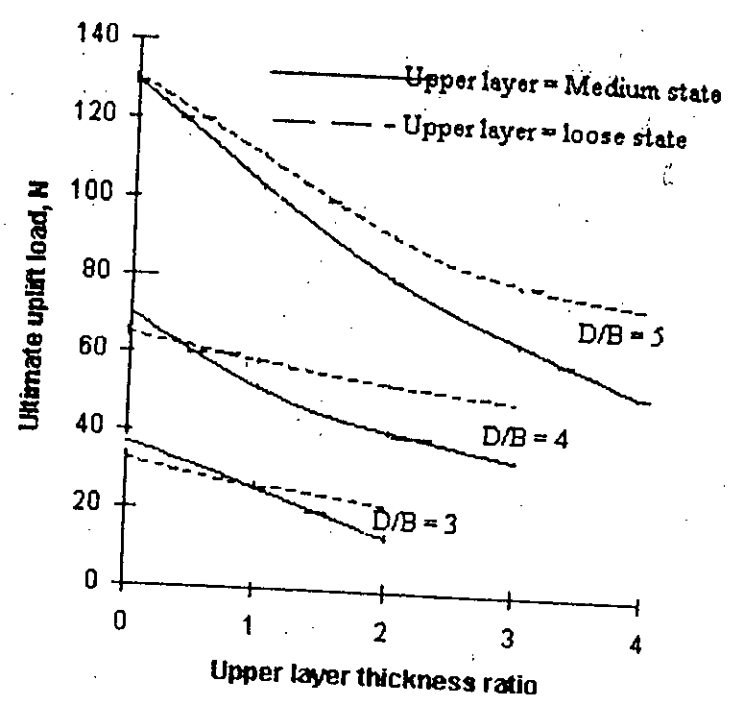


Fig. 2.27 Load-displacement relationship of plate anchor embedded in a two layered sand, $\lambda=1$ (after Bouazza et al,1990)

combinations also quote the additional relative permanent static load $Q_s Q_{ult}$ as a percentage.

The deterioration of the cyclic loading-relative movement properties of an embedment anchor appeared due to the accumulated amount of cyclic relative movement, whether developed by a few strong or many small stress pulses. Fig. 2.28 & 2.29 give a clear picture of the progressive accumulative cyclic relative movement of the anchor as it will develop after three consecutive 2-day storms with equivalent uniform relative cyclic loads of 20%, 30% and 40%, respectively (path A-B-C-D-E-F-G, Fig. 2.28 & 2.29).

The few permanent static-cyclic loading combination curves presented in Fig. 2.28, however, emphasizes that care must be taken when the using simple cyclic loading tests to predict the behaviour of anchor systems subjected to long-term sustained repeated loading conditions.

Tests performed at different stress levels for deep anchors suggest that when the cyclic relative movement of the anchor is kept below about half the relative movement to failure in a static pull-out test, there is essentially no reduction in strength due to cyclic loading. If this criterion is adopted, cyclic loading failure could be defined as a cyclic strain of 50% of the static stress to failure. In Fig. 2.29, the $\Delta\lambda = 0.10$ "critical" curve, which corresponds to the preceding criterion, is used to represent failure of the anchor. A reliable design procedure should ensure that the progressive accumulative cyclic strain storm path A-B-C-D-E-F-G would be kept under the failure curve during the life span of the anchor.

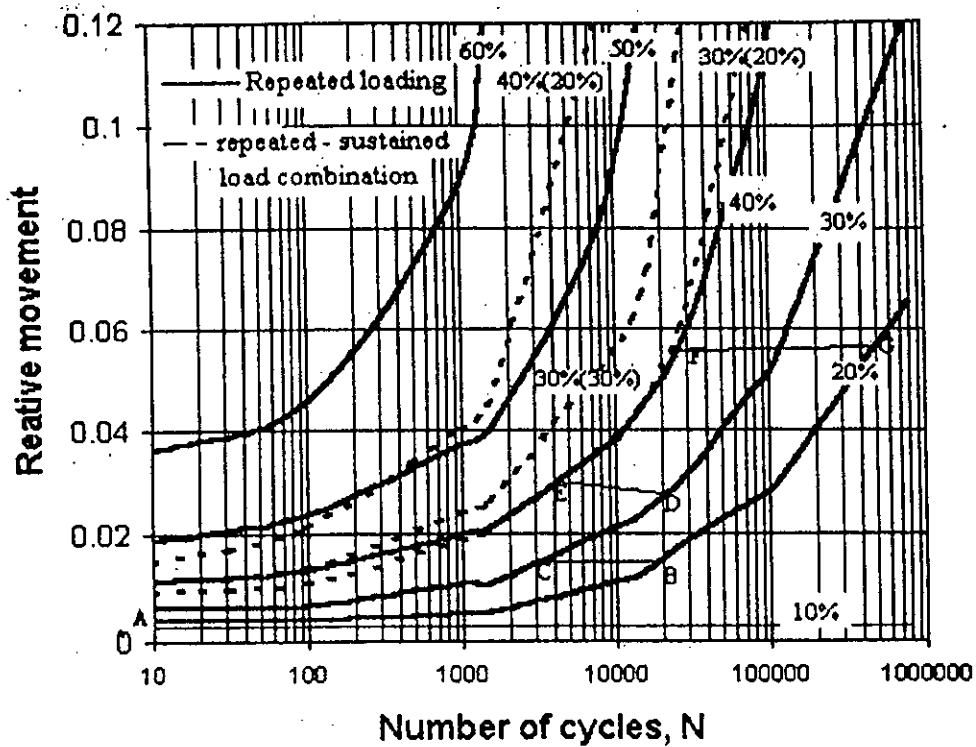


Fig. 2.28 Number of cycles Vs relative anchor movement for dense sand at $\lambda=12$ (after Harvey et al,1978)

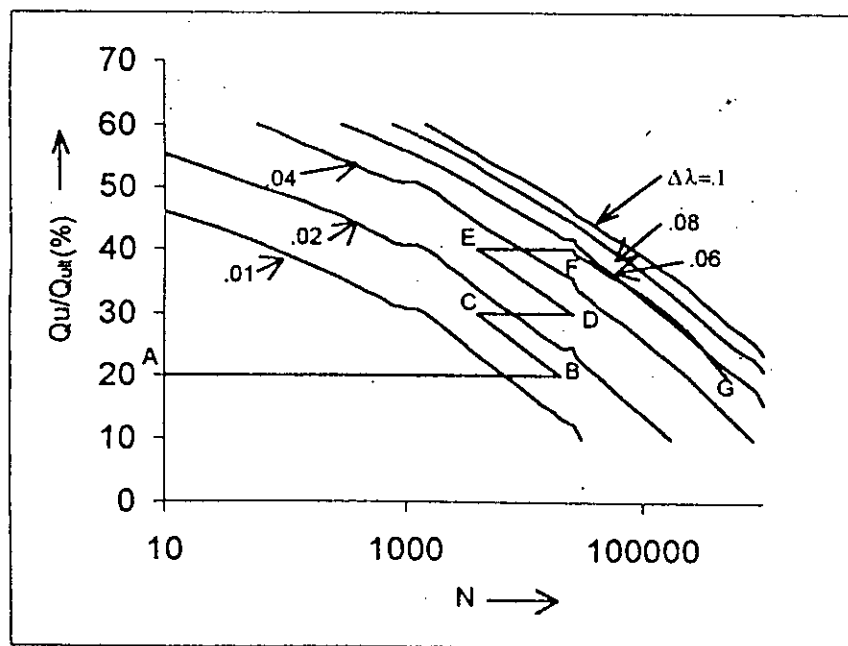


Fig. 2.29 Number of cycles Vs relative cyclic load for dense sand at $\lambda=12$ (after Harvey et al,1978)

2.7 SUMMARY OF LITERATURE REVIEW

From the discussions of this chapter, following remarks can be made:

1. Considerable amounts of theoretical works have been performed concerning uplift behaviour of shallow anchors in both sand and clay. But behavior of deep anchors is still not understood well. Moreover, theories are more concerned about ultimate uplift capacity of anchors rather than their displacement characteristics.
2. Density of backfill and native soil can play a vital role in determining uplift capacity of backfilled anchors. This is a very important feature of anchor behavior as a large portion of the anchor plates is installed in backfilled manner.
3. Anchors are subjected to large displacements before failure (relative displacement upto 100%) when they are installed in clay. Displacement in sand is considerably less (<5%).
4. Suction resistance can considerably increase anchor capacity when they are installed in clay.
5. Long-term loading can lead to considerable reduction of uplift capacity of anchors in clay.
6. Increase of uplift capacity of anchors in clay by insertion of sand overlay is practically not feasible.

CHAPTER 3

EXPERIMENTAL SET UP, TEST PROCEDURE AND RESULTS

3.1 GENERAL

An experimental program was designed to observe uplift behaviour of horizontal anchor plate in Sylhet, Local and Filling sand. Although the current study covers uplift behaviour of anchor plates in sands, lack of laboratory facilities and time constraints led the researcher to confine their laboratory investigation for three types of sands only. The material and sample properties, test set-up and tests procedures are described below.

3.2 CHARACTERIZATION OF SAND SAMPLES

Three types of sands, such as Sylhet, Local (Gazaria) and Fills (Vethi sands) will be collected locally. These were characterised in the laboratory. This characterisation included determination of specific gravity, grain size distribution, relative density and strength parameters. Specific gravity and angle of internal friction of Sylhet, Local (Gazaria) and Fills (Vethi sands) are 2.75, 37⁰; 2.72, 36⁰ and 2.71, 34⁰ respectively. The salient properties are given below in Table 3.1

Table 3.1: Soil properties during carrying out test

Name of sample	Density in loose compaction, ton/m ³	Density in dense compaction, ton/m ³	Density at test condition, ton/m ³	Relative Density, D _r	Type of sand
Sylhet sand	1.54	1.89	1.73	0.59	Medium
Local sand	1.31	1.41	1.37	0.62	Medium
Fills sand	1.19	1.29	1.26	0.72	Dense

3.3 THE TEST SET UP

The details of test bin anchor plates and loading arrangement are described below:

3.3.1 The test tank

The dimensions of the test tank are given in the Fig. 3.1. The test tank walls were made of thick glass sheets to prevent buckling effect. Framing of steel angles strengthened Glass walls. The base of the tank was made of steel. The tank was wheeled and placed on a rail to facilitate experimental requirements.

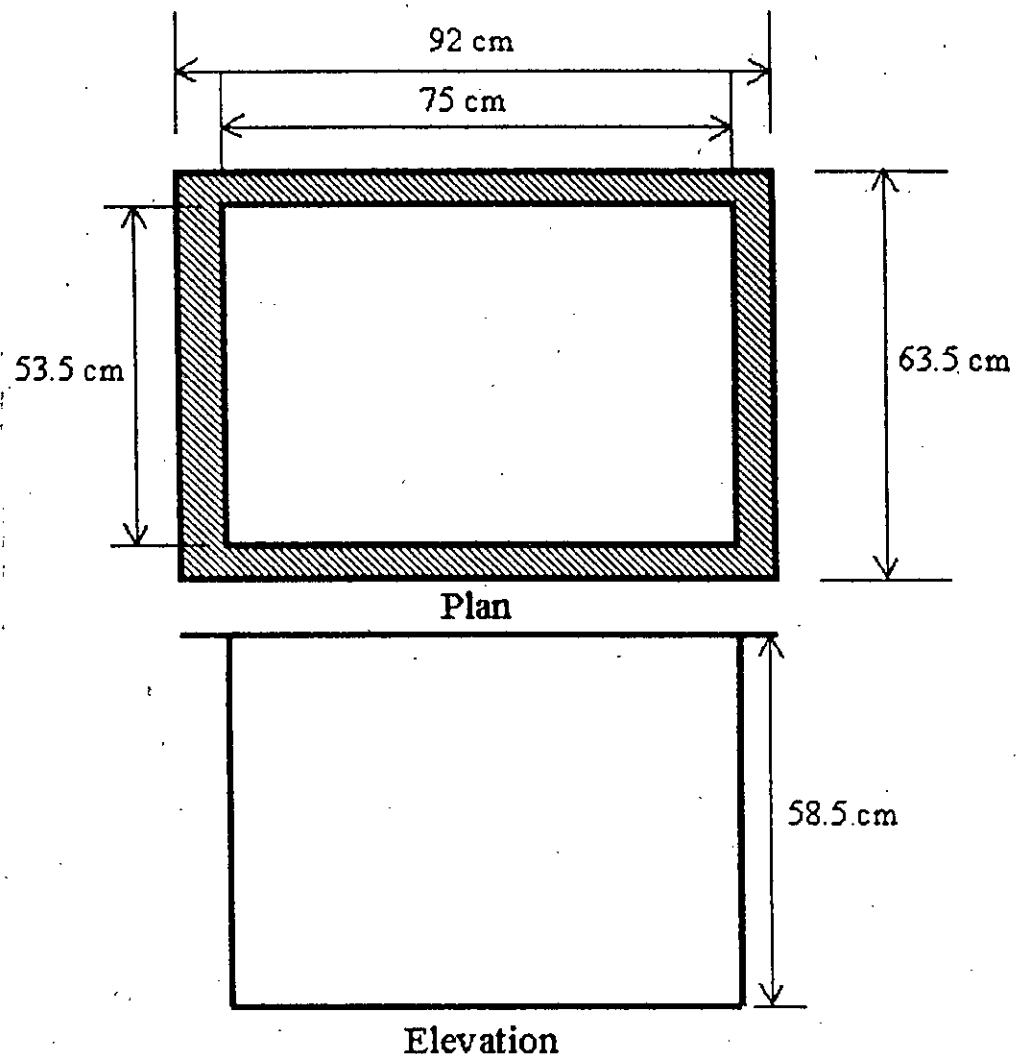


Fig. 3.1 Plan and elevation of the test tank (Scale=1:12.5)

3.3.2 The anchor plate

Cast iron anchor plates and rod were used for the tests. The anchor rod diameter, mass and height are 12.7 mm, 1109 gm and 10.03 cm respectively. The dimensions and mass of the anchor plates are given in Table 3.2.

Table 3.2 Description of Anchor Plates

Anchor plates	Diameter/ Width (cm)	Area (cm ²)	Mass (gm)	Ratio with least tank dimension	Thickness of anchor plates (mm)
Circular	11.43	103	753.5	4.68	9.53
Circular	19.1	285	1037	2.81	4.83
Square	19.5	379	1196	2.75	3.18

3.3.3 Other equipment

The test set up is shown in Fig. 3.3. The loading hanger was used for load increment. A deformation gauge was used to measure vertical deformation of the anchor plate. Cable through which load was transmitted was greased to minimize friction. A #4 sieve was used as sand-rain to ensure proper placement of sand (Fig. 3.2). Two steel trusses with smooth pulleys were used for proper uplift loading. The whole set-up was installed in a frame that facilitated placement of sand-rain at different heights.

3.4 THE TEST PROCEDURE

3.4.1 Preparation of sand bed

A # 4 sieve was used as to deposit the sand in layer (Fig.3.2). Air-dry sand sample was poured in the test tank by raining through the # 4 sieve. The falling height of was kept constant to gain a constant sand density. Sand density at test condition was measured by

placing small pots at different layers of sand. The pots were collected after the test and average density was evaluated by measuring the mass and volume of the pots. Constant falling height was kept by increasing the height of the sand-rain with the help of threaded frame after placing every layer of sand. No compaction process was performed on sand layers. So the prepared sand bed can be considered as loosely compacted.

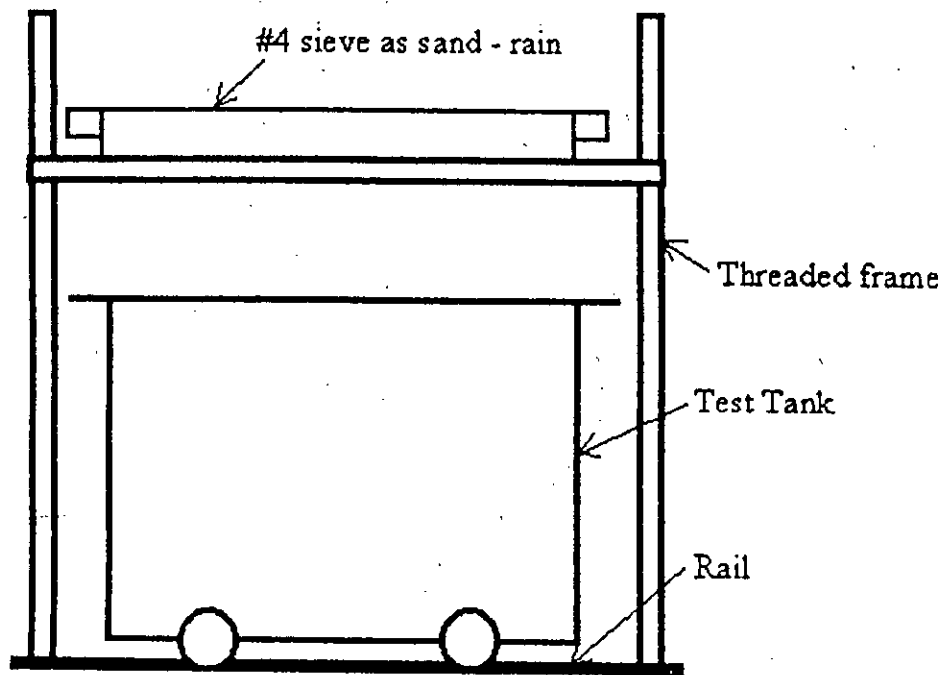


Fig. 3.2 Schematic of the test tank and #4 sieve as sand-rain

3.4.2 Pullout of anchor plate

Pullout load was applied on the anchor plate by placing weights of different magnitudes in the loading hanger. The load was transmitted through a smooth cable (Fig. 3.3).

Adding weights to the loading hanger did load increment. No uniform load increment was kept. Unloading was avoided as it simulates cyclic load condition². Vertical deformation of the anchor plate after each load increment was measured with a deformation gauge attached to the anchor rod as shown in Fig. 3.3. Load increment was continued upto complete failure or up to that degree where small increment of load caused excessive deformation.

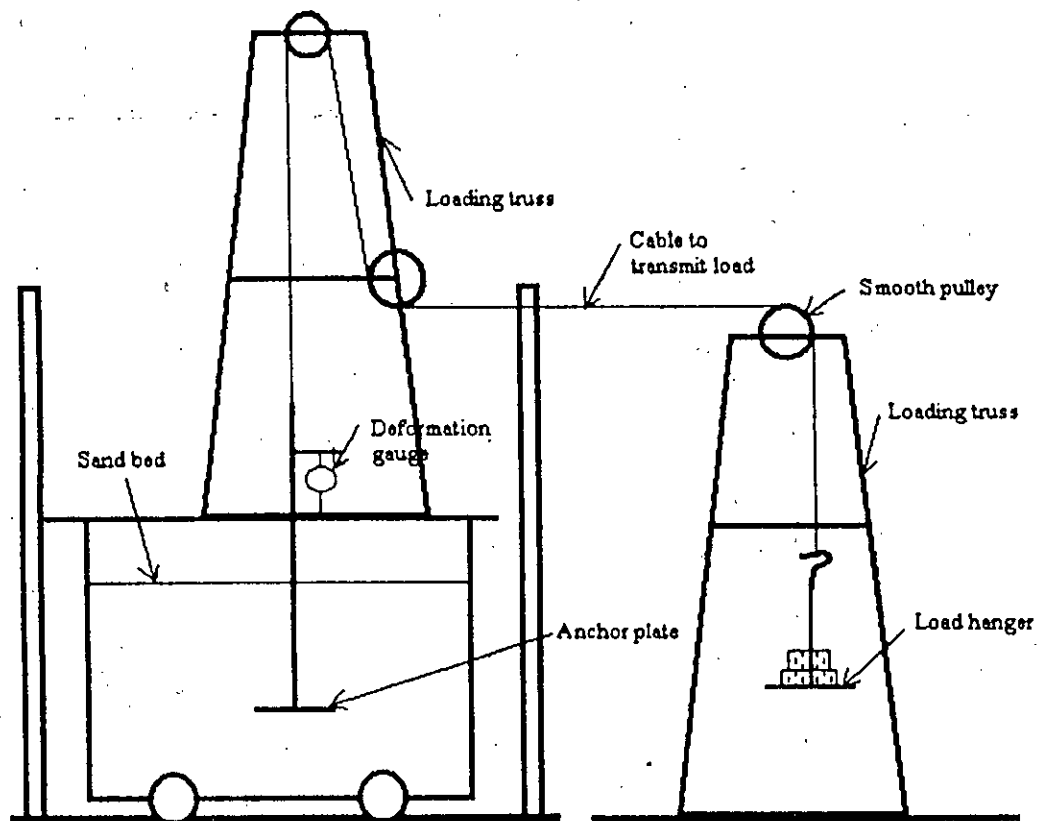


Fig. 3.3 Schematic of the experimental set-up



Fig. 3.4 Experimental set-up at laboratory (ready for test)

3.5 DESCRIPTION OF PULLOUT TESTS

In total, 30 pullout tests were performed with variation of anchor size, shape and embedment ratio. Table 3.3 has the summary of those.

Table 3.3 Description of pullout tests

Shape of anchor	Diameter/width, cm, B	Sand sample	Embedment, cm, D	Embedment ratio (D/B)
Circular	11.43	Sylhet	11.43	1.0
Circular	11.43	Sylhet	22.86	2.0
Circular	11.43	Sylhet	37.26	3.0
Circular	11.43	Sylhet	45.72	4.0
Circular	11.43	Local	11.43	1.0
Circular	11.43	Local	22.86	2.0
Circular	11.43	Local	37.26	3.0
Circular	11.43	Local	45.72	4.0
Circular	11.43	Fills	11.43	1.0
Circular	11.43	Fills	22.86	2.0
Circular	11.43	Fills	37.26	3.0
Circular	11.43	Fills	45.72	4.0
Circular	19.1	Sylhet	19.1	1.0
Circular	19.1	Sylhet	38.2	2.0
Circular	19.1	Sylhet	57.3	3.0
Circular	19.1	Local	19.1	1.0
Circular	19.1	Local	38.2	2.0
Circular	19.1	Local	57.3	3.0
Circular	19.1	Fills	19.1	1.0
Circular	19.1	Fills	38.2	2.0
Circular	19.1	Fills	57.3	3.0
Square	19.5	Sylhet	19.5	1.0

Shape of anchor	Diameter/width, cm, B	Sand sample	Embedment, cm, D	Embedment ratio (D/B)
Square	19.5	Sylhet	39.0	2.0
Square	19.5	Sylhet	58.5	3.0
Square	19.5	Local	19.5	1.0
Square	19.5	Local	39.0	2.0
Square	19.5	Local	58.5	3.0
Square	19.5	Fills	19.5	1.0
Square	19.5	Fills	39.0	2.0
Square	19.5	Fills	58.5	3.0

3.6 THE TEST RESULTS

A series of anchor pull tests were performed in the laboratory by varying anchor size, its shape, and embedment depth and embedment ratio. Loads were applied in incremental manner until failures were observed. Here failure condition is defined as the conditions at which a small increment of load causes a substantial displacement.

Table 3.4 Laboratory test results

Shape of anchor (sample)	Dia/width, cm, B	Embedment, cm, D	Embedment ratio, D/B	Ultimate load, Q_u N	$Q_u/2$, N	Deformation at ultimate load, Z_f , mm	Deformation at $Q_u/2$, Z_{50} , mm
Cir(Sylhet)	11.43	11.43	1.0	88.3	44.15	4.00	2.50
Cir(Sylhet)	11.43	22.86	2.0	215.8	107.9	1.50	1.00
Cir(Sylhet)	11.43	34.29	3.0	529.7	264.85	3.75	0.50
Cir(Sylhet)	11.43	45.72	4.0	725.2	362.6	4.5	1.5
Cir(Local)	11.43	11.43	1.0	58.86	29.43	1.00	0.25
Cir(Local)	11.43	22.86	2.0	147.15	73.58	3.00	0.80
Cir(Local)	11.43	34.29	3.0	333.54	166.77	6.75	1.75
Cir(Local)	11.43	45.72	4.0	490.5	245.25	6.75	0.75

Shape of anchor (sample)	Dia/width, cm, B	Embedment, cm, D	Embedment ratio, D/B	Ultimate load, Q_u , N	$Q_u/2$, N	Deformation at ultimate load, Z_f , mm	Deformation at $Q_u/2$, Z_{50} , mm
Cir(Fills)	11.43	11.43	1.0	49.05	24.53	1.95	1.00
Cir(Fills)	11.43	22.86	2.0	127.53	63.77	4.25	0.75
Cir(Fills)	11.43	34.29	3.0	235.49	117.75	5.25	0.80
Cir(Fills)	11.43	45.72	4.0	412.02	206.01	8.75	0.30
Cir(Sylhet)	19.1	19.1	1.0	137.34	68.67	3.80	2.20
Cir(Sylhet)	19.1	38.2	2.0	412.02	206.01	3.00	0.75
Cir(Sylhet)	19.1	57.3	3.0	588.6	294.30	8.50	3.75
Cir(Local)	19.1	19.1	1.0	127.53	63.77	1.75	0.80
Cir(Local)	19.1	38.2	2.0	264.87	132.44	4.75	1.60
Cir(Local)	19.1	57.3	3.0	490.5	245.25	5.50	1.70
Cir(Fills)	19.1	19.1	1.0	117.72	58.86	4.50	3.00
Cir(Fills)	19.1	38.2	2.0	255.06	127.53	5.50	1.60
Cir(Fills)	19.1	57.3	3.0	480.06	240.03	4.75	1.80
Sq(Sylhet)	19.5	19.5	1.0	166.77	83.39	4.25	1.50
Sq(Sylhet)	19.5	39.0	2.0	441.45	220.71	5.25	1.75
Sq(Sylhet)	19.5	58.5	3.0	657.27	328.64	6.25	2.75
Sq.(Local)	19.5	19.5	1.0	156.96	78.48	3.50	1.25
Sq.(Local)	19.5	39.0	2.0	392.4	196.20	5.10	0.25
Sq.(Local)	19.5	58.5	3.0	588.6	294.30	12.50	3.75
Sq. (Fills)	19.5	19.5	1.0	147.15	73.58	4.50	1.20
Sq. (Fills)	19.5	39.0	2.0	323.73	161.87	5.10	3.00
Sq. (Fills)	19.5	58.5	3.0	519.93	259.97	6.75	1.10

3.7 LIMITATIONS OF THE MODEL TESTS

The model tests performed by the present investigators had the following limitations:

1. Now-a-days, model pullout tests are usually done in centrifugal condition (Dickin, 1988) to simulate field conditions. Significant scale effect had been observed by several investigators comparing results of model tests with large-scale field tests (Harvey et al, 1981). Small-scale model tests show significant increase of breakout factor in comparison with large-scale tests. In this project, the laboratory studies were made in small-scale experiment model. So, scale error associated with conventional modelling is common.
2. Boundary effect offered by rigid test tank walls was not eliminated. Extent of stressed sand could be 16 times the anchor diameter during anchor pullout in sand (Harvey et al, 1981). In the present research, the largest ratio of least dimension of test tank to the anchor plate diameter was 4.68.
3. Static loads were applied manually. Adding weights to the loading hanger manually did load increment, which is not a standard procedure. So, a constant rate of loading cannot be maintained. A mechanical loading device could provide such facility.
4. No proving ring dial or load cell was installed to measure actual pullout load.
5. Various connections were used throughout the system from the beginning of the anchor plates to the end of the loading. The threaded anchor rod could offer significant friction resulting increased pullout capacity. So, various losses resulting from connections, frictions are likely to occur. But this could not be quantified by the simple mechanical arrangement used.
6. To be closer with the field condition it would be justified regarding the sand to be saturated up to certain degree. But the sand used throughout was dry because wet

sand could cause some additional problem in connection with the spreading of sand by raining up.

96745

CHAPTER 4

ANALYSIS AND INTERPRETATION OF TEST RESULTS

4.1 GENERAL

Results of the model tests performed in the laboratory research are analysed and interpreted in this chapter. Test results are also compared with other published test results along with predictions of different theoretical analyses.

4.2 INTERPRETATION OF TEST RESULTS

A series of anchor pullout tests were performed in the laboratory by varying anchor size, its shape, embedment depth and embedment ratio. Loads were applied in incremental manner until failures were observed. Here failure condition is defined as the conditions at which a small increment of load causes a substantial magnitude of displacement.

4.2.1 Load-Displacement Behaviour

1. Load-displacement behaviour with circular anchor area ($D=11.43$ cm) for $D/B=1.0$; 2.0; 3.0 and 4.0 of Sylhet, Gazaria and Fills sand are shown in Fig: 4.1, 4.2 and 4.3 respectively. These figures 4.1 and 4.2 show uplift ultimate resistance increased not linearly with anchor displacement but figure 4.3 shows uplift ultimate resistance increased linearly with anchor displacement. In all cases it is observed that the load displacement behaviour at the initial range of loading is linear. This is because soil remains essentially in elastic stage in that range of loading.

Load-displacement behaviour with circular anchor area ($D=19.1$ cm) for $D/B=1.0$; 2.0 and 3.0 of Sylhet, Gazaria and Fills sand are shown in fig: 4.4, 4.5 and 4.6 respectively. In fig. 4.4 represents uplift resistance increased not linearly with

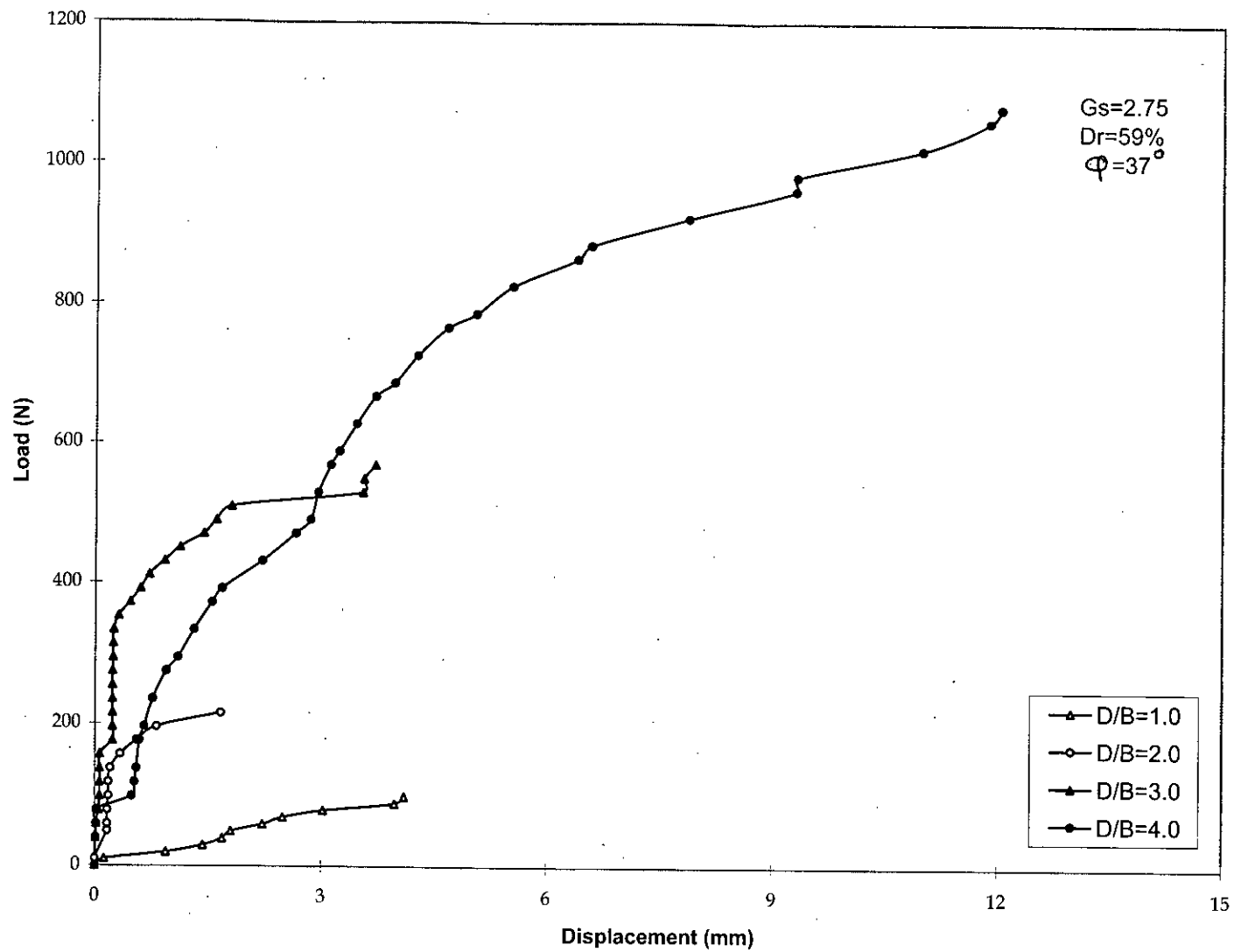


Fig. 4.1 Load-displacement curve of circular anchor (D=11.43cm, Sylhet sand)

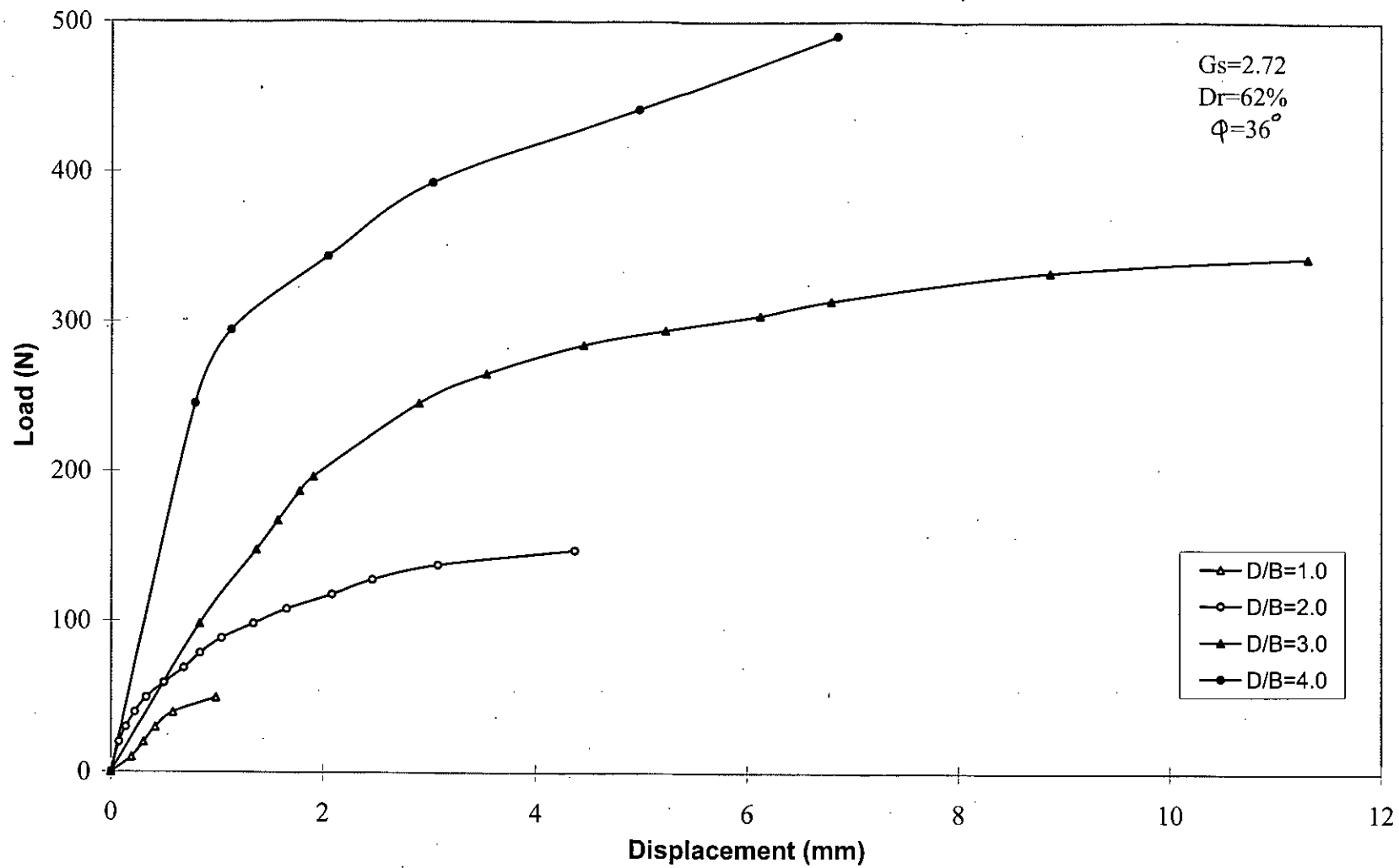


Fig. 4.2 Load-displacement curve of circular anchor (D=11.43 cm, Gazaria sand)

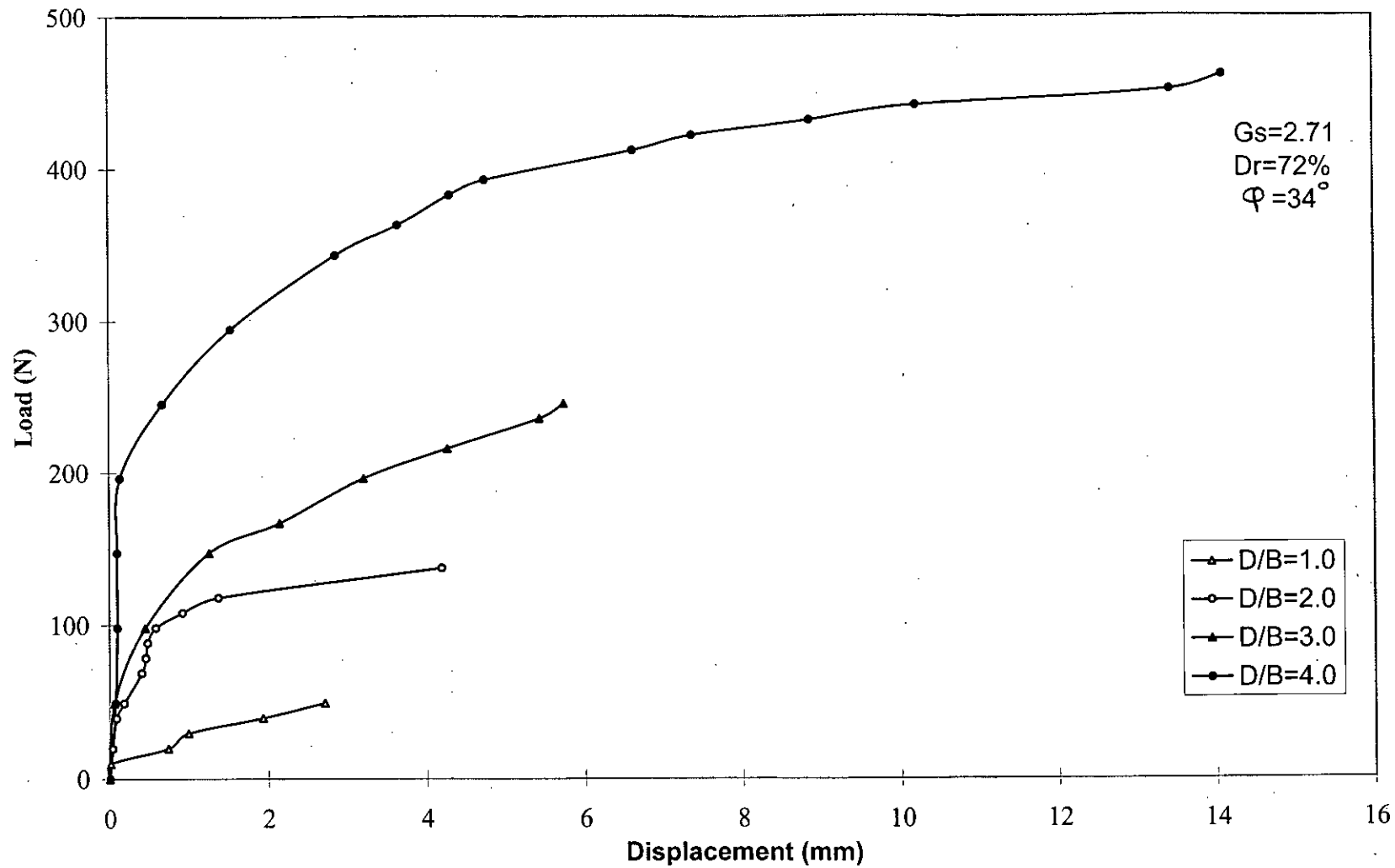


Fig. 4.3 Load-displacement curve of circular anchor ($D=11.43$ cm, Fills sand)

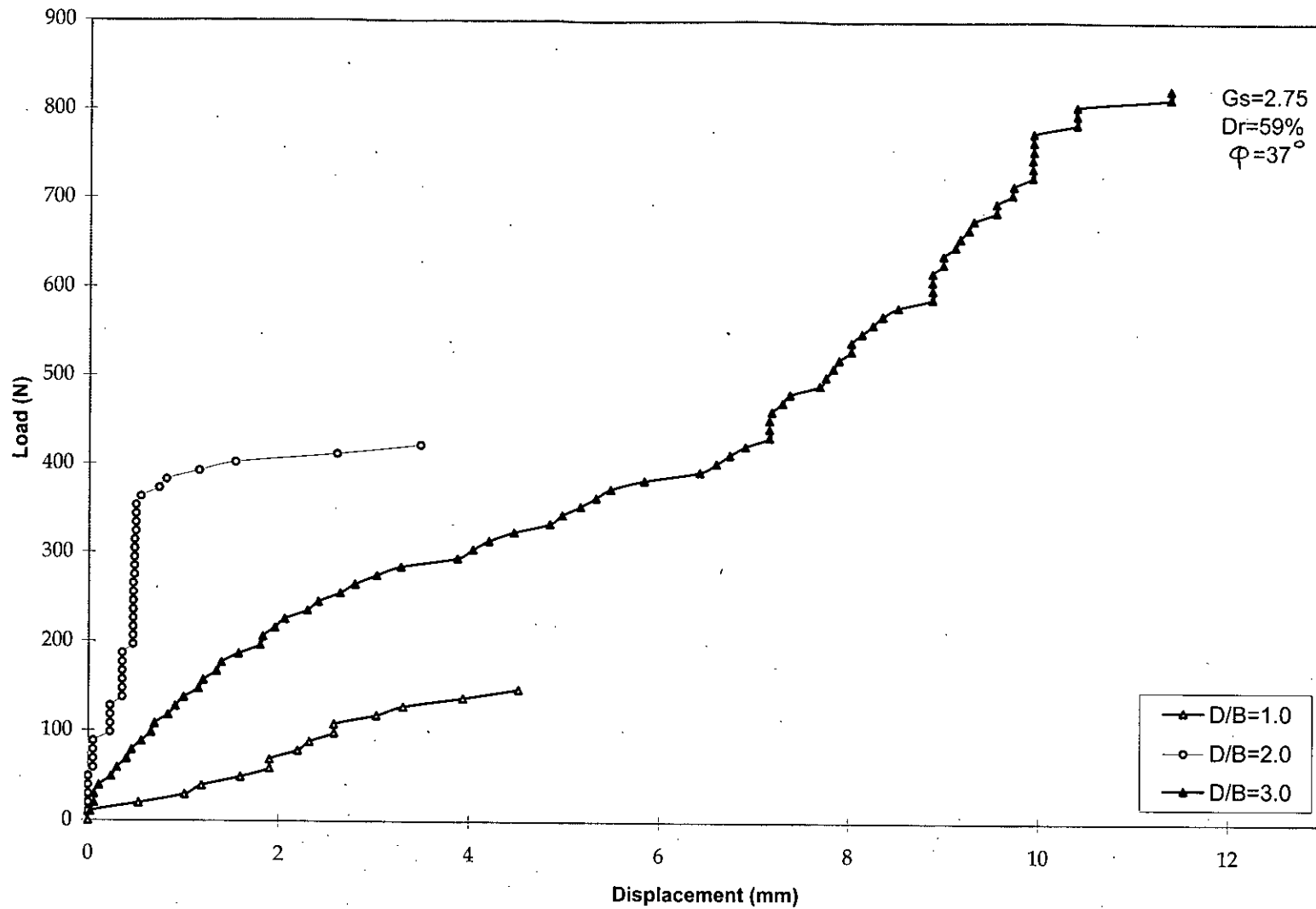


Fig. 4.4 Load-displacement curve of circular anchor (D=19.1cm, Sylhet sand)

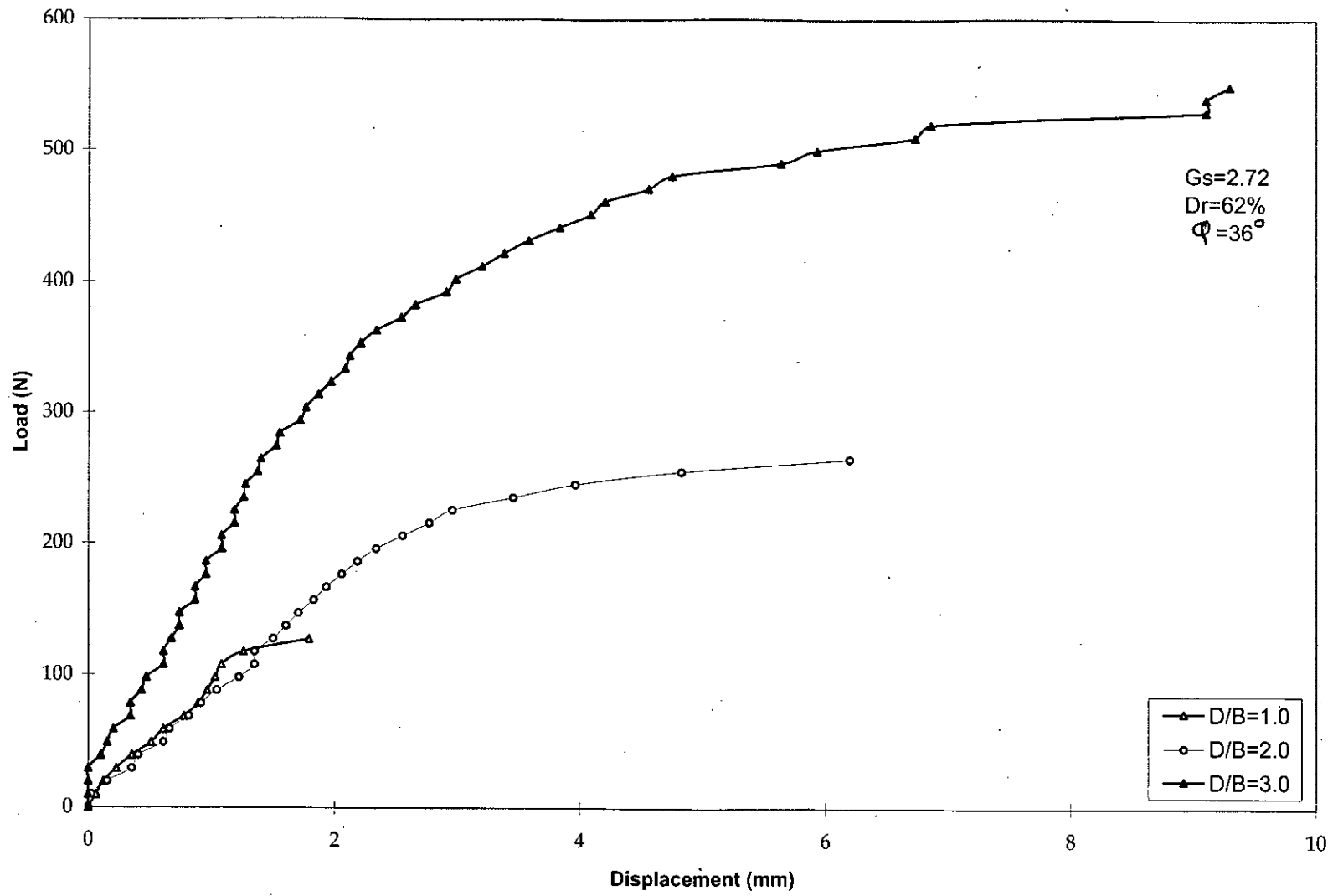


Fig. 4.5 Load-displacement curve of circular anchor (D=19.1cm, Gazaria sand)

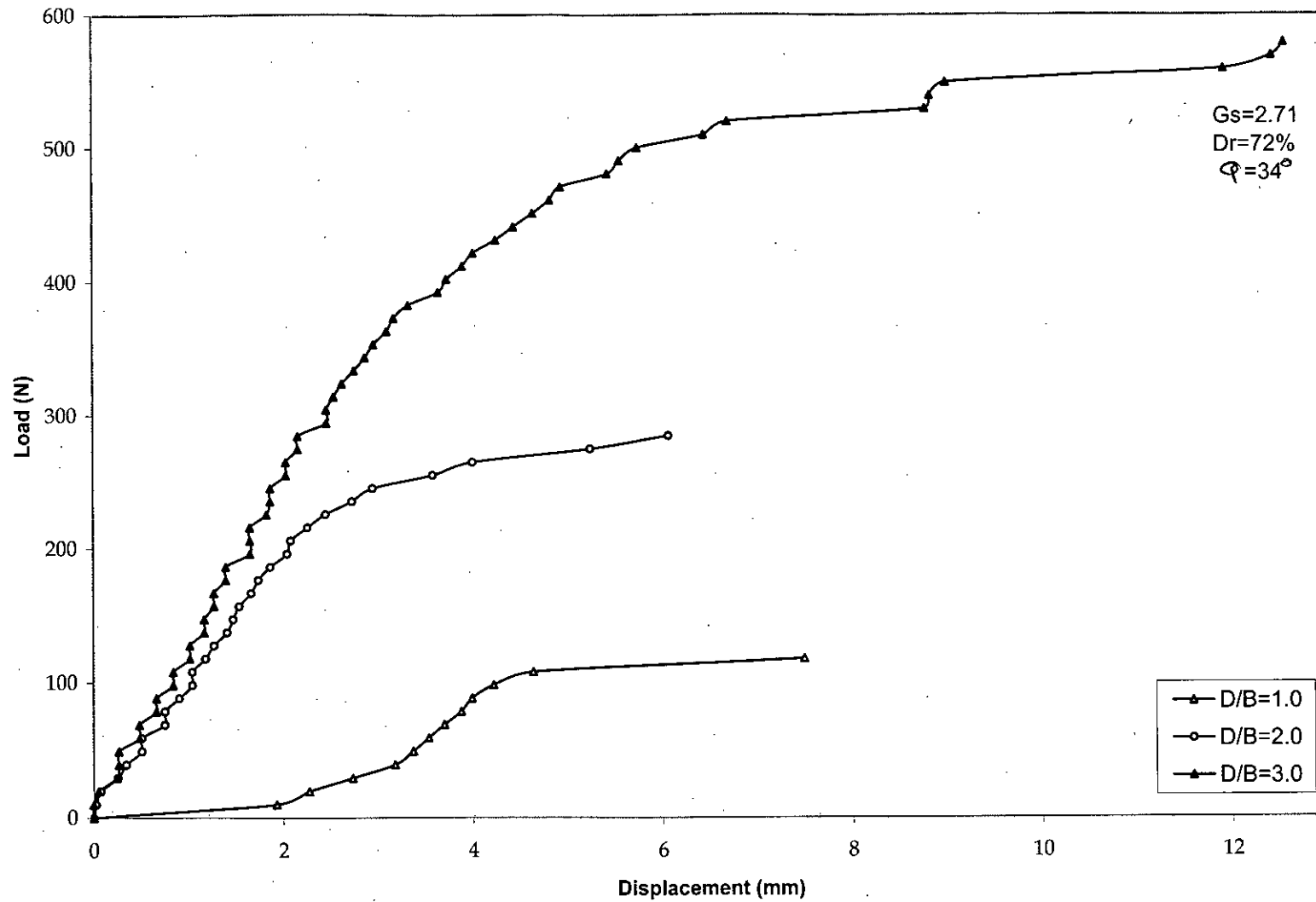


Fig. 4.6 Load-displacement curve of circular anchor (D=19.1cm, Fills sand)

anchor displacement. Similar graphical representations are observed in fig. 4.5 and 4.6.

3. Load-displacement behaviour with square anchor area ($D=19.5$ cm) for $D/B=1.0$; 2.0 and 3.0 of Sylhet, Gazaria and Fills sand are showing in fig: 4.7, 4.8 and 4.9 respectively. In fig. 4.7 represents uplift resistance increased linearly with anchor displacement. Similar graphical representations are not observed in fig. 4.8 and 4.9.

According to this graph, both the geometry of, square and circular, plates exhibits a substantial increase in ultimate load with embedment ratio, as seen from Fig. 4.1 to 4.9 the increase is not linear in nature. So, it is clear that *the ultimate capacity increases not linearly with the increasing depth.*

But the effect of shape is not that much evident. As seen from Fig. 4.1 to 4.9 that the *soil characterised such as relative density, specific gravity and frictional angle depend on plate yields. Better characterisation (except relative density) gives better performance.*

Almost all the anchors show typical load-displacement behaviour. As the circular anchors were embedded in loose sand, initial portions of their load-displacement curves are of flat nature. But square anchors show steeper load-displacement curve, due to the denser bed in which they were embedded. Square anchor shows unconventional load-displacement behaviour, the cause may be explained by of experimental error of unloading weights from the loading hanger during the tests. Distinct peaks and oscillations were not observed in the load-displacement curves. Displacements of anchors at failure were less than 3% (if presented in dimensionless form $Z_f/B\%$, where Z_f , deformation at ultimate load).

Anchors up to embedment ratio 3.0 showed catastrophic failure mode (general shear failure). Extent of heavy increased with the increase of embedment ratio. Little surface

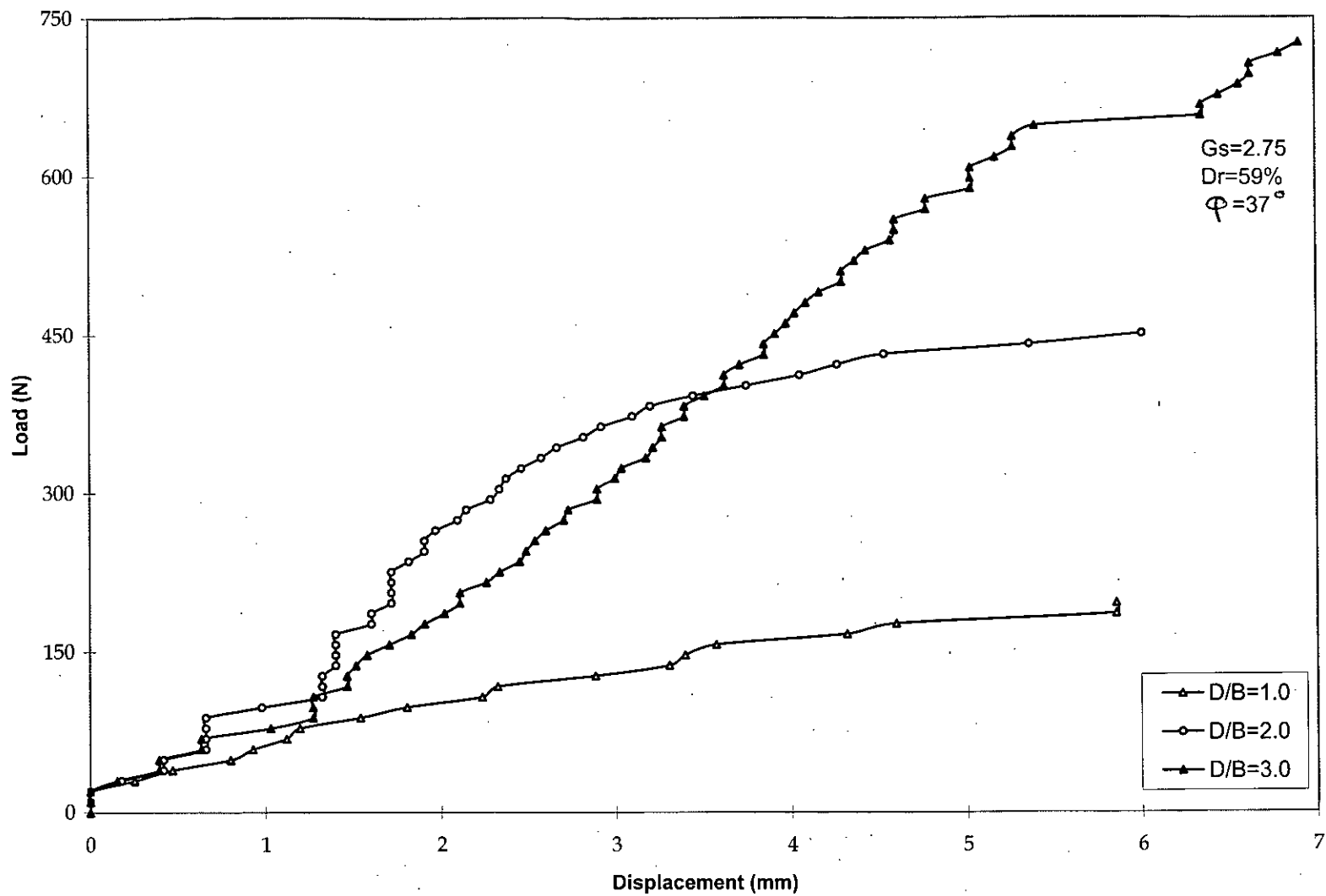


Fig. 4.7: Load-displacement curve of square anchor (D=19.5cm, Sylhet sand)

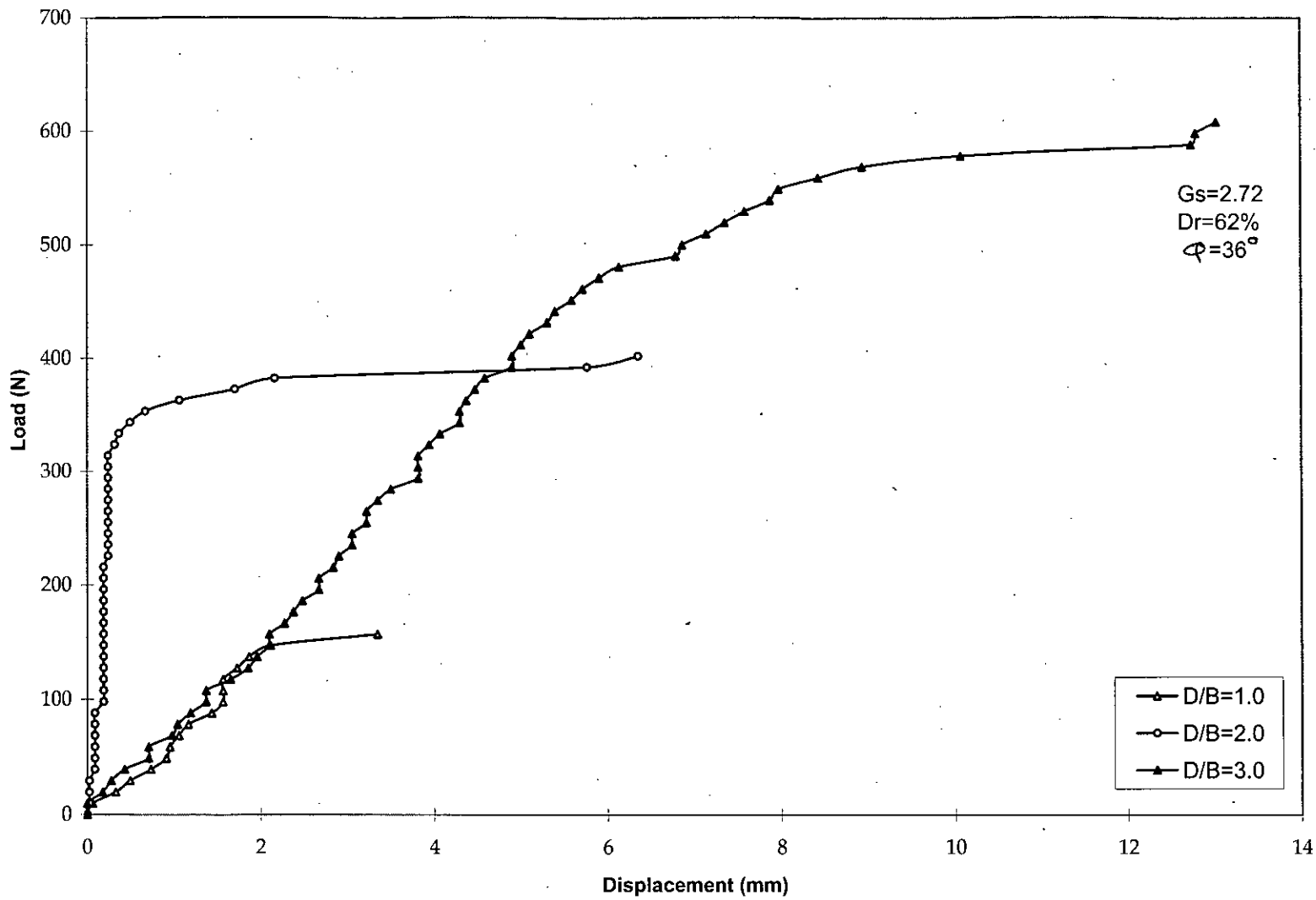


Fig. 4.8 Load-displacement curve of square anchor (width=19.5 cm, Gazaria sand)

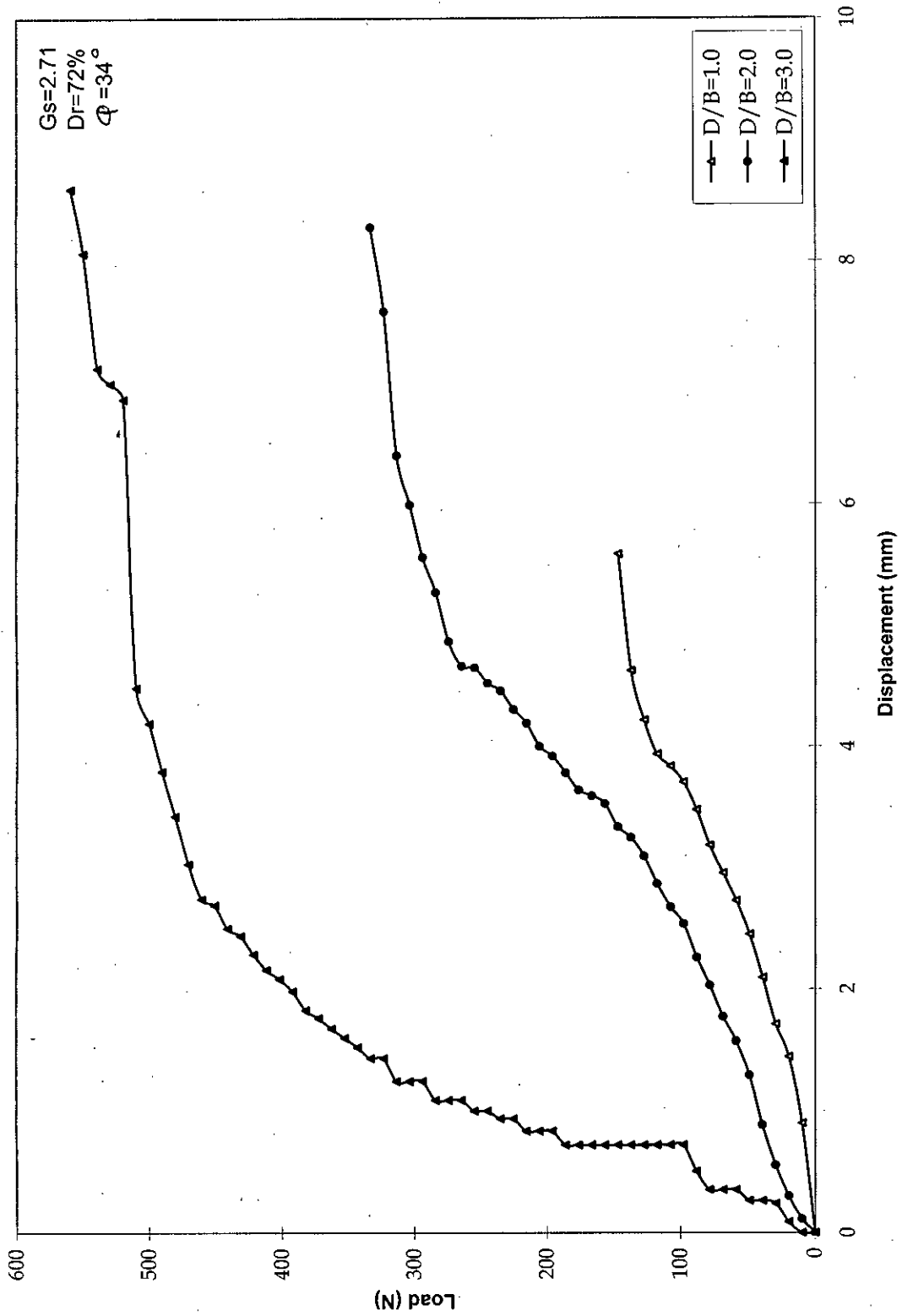


Fig. 4.9 Load-displacement curve of square anchor (width=19.5 cm, Fills sand)

heavy was observed for anchors having embedment ratio of 3.0 and 4.0. So in these cases, failures were predominantly of punching nature. No exact measure of zone of heavy was performed. According to the definition of Sutherland et al. (1982), anchors embedded in Sylhet sand with relative density of 0.45 (loose density) can be termed as deep anchor when the embedment ratio is greater than 3.0.

4.2.2 Variation of breakout factor with embedment ratio

Variation of breakout factor with embedment ratio of Sylhet, Gazaria and Fills sand are showing in fig: 4.10, 4.11 and 4.12 respectively. Semi-log plot of breakout factor and embedment ratio (breakout out factor is plotted in log scale) (Fig: 4.10) shows that the breakout factor increases in exponential order with the increase of embedment ratio up to $D/B = 3.0$ and then becomes almost constant. So according to the definition of Das (1975), anchors embedded in Sylhet sand with relative density of 0.45 (loose density) can be termed as deep anchor when the embedment ratio is greater than 3.5. Embedment ratio 3.5 can be called as critical depth, $(D/B)_{cr}$. Similar type trends are observed in Fig. 4.11 and 4.12.

4.2.3 Variation in relative displacement with embedment ratio

Variation in relative displacement (Z_f/B , where Z_f , deformation at ultimate load) with embedment ratio in anchor area ($D=11.43$ cm & 19.1 cm and width= 19.5 cm) Sylhet, Gazaria and Fills sand are showing in Fig: 4.13, 4.14 and 4.15 respectively. Normal plot of dimensionless failure displacement ($Z_f/B\%$) with embedment ratio (Fig. 4.13) shows that the failure displacement increases with embedment ratio up to 3, beyond which it does decrease. So there is a limiting failure displacement close to $(D/B)_{cr}$.

4.2.4 Variation of breakout capacity with anchor area

Variation of breakout capacity with anchor area in embedment ratio ($D/B=2.0$) Sylhet sand is showing in fig. 4.16. For the same embedment ratio, normal plot of ultimate uplift

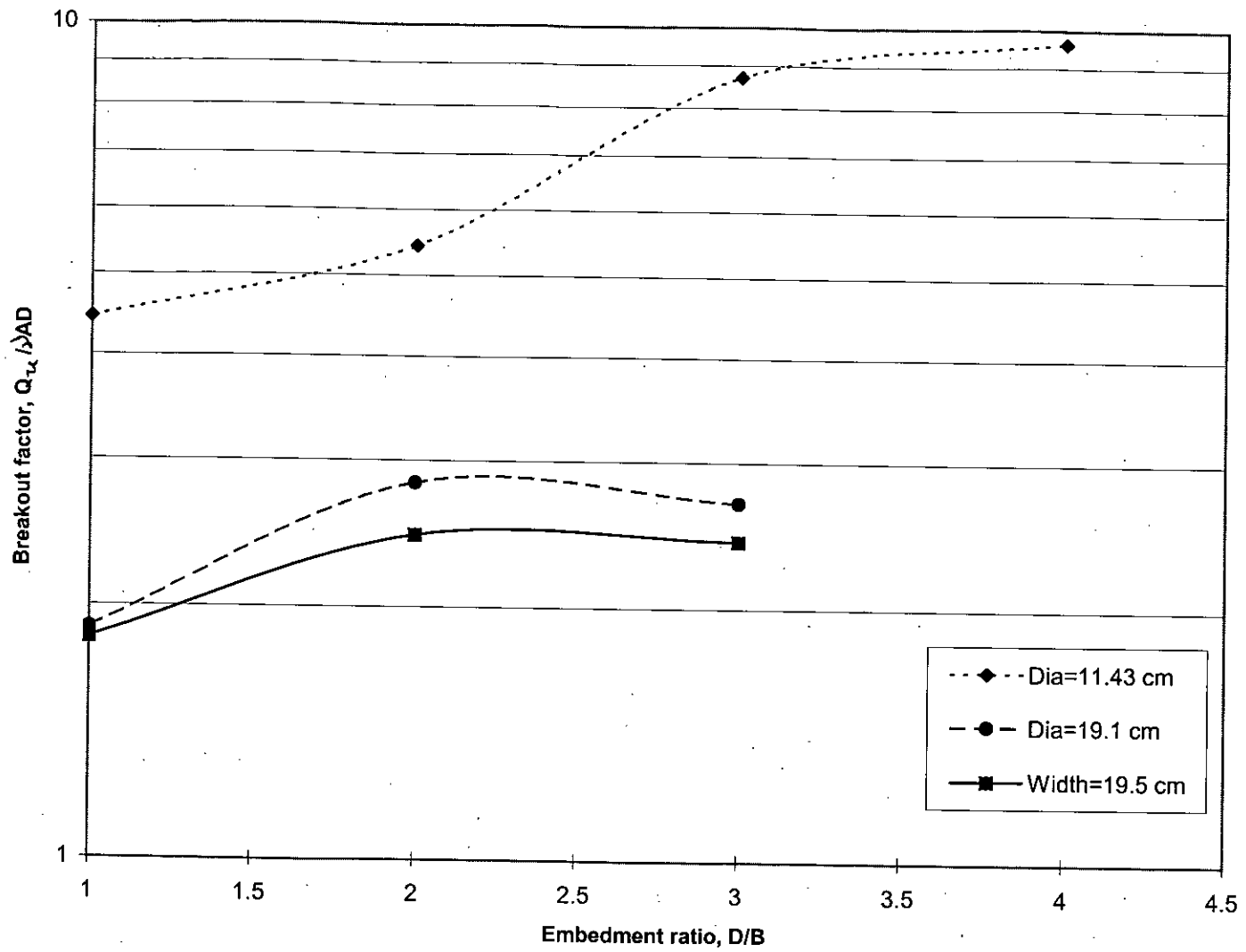


Fig 4.10 Variation of breakout factor with embedment ratio (Sylhet sand)

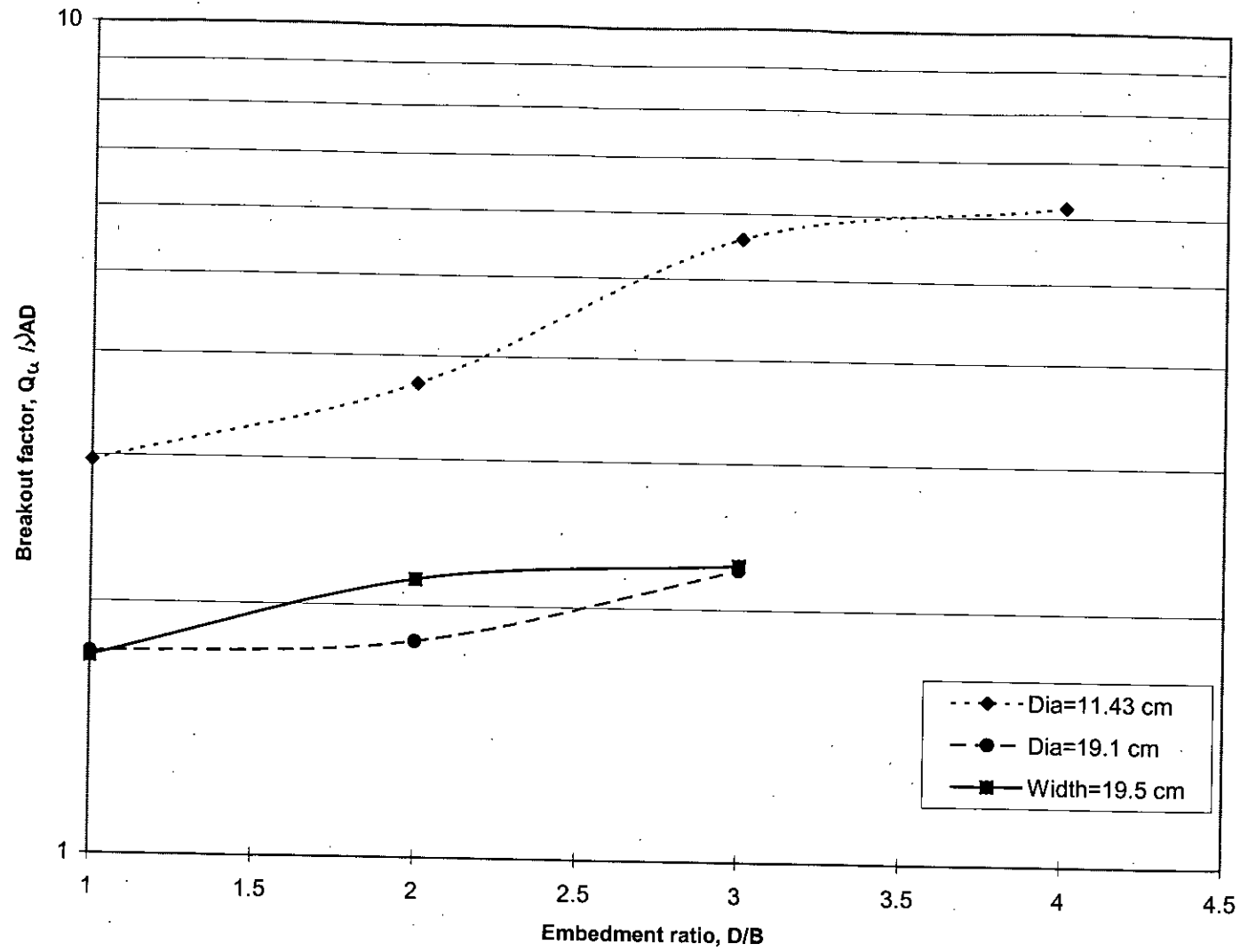


Fig 4.11 Variation of breakout factor with embedment ratio (Gazaria sand)

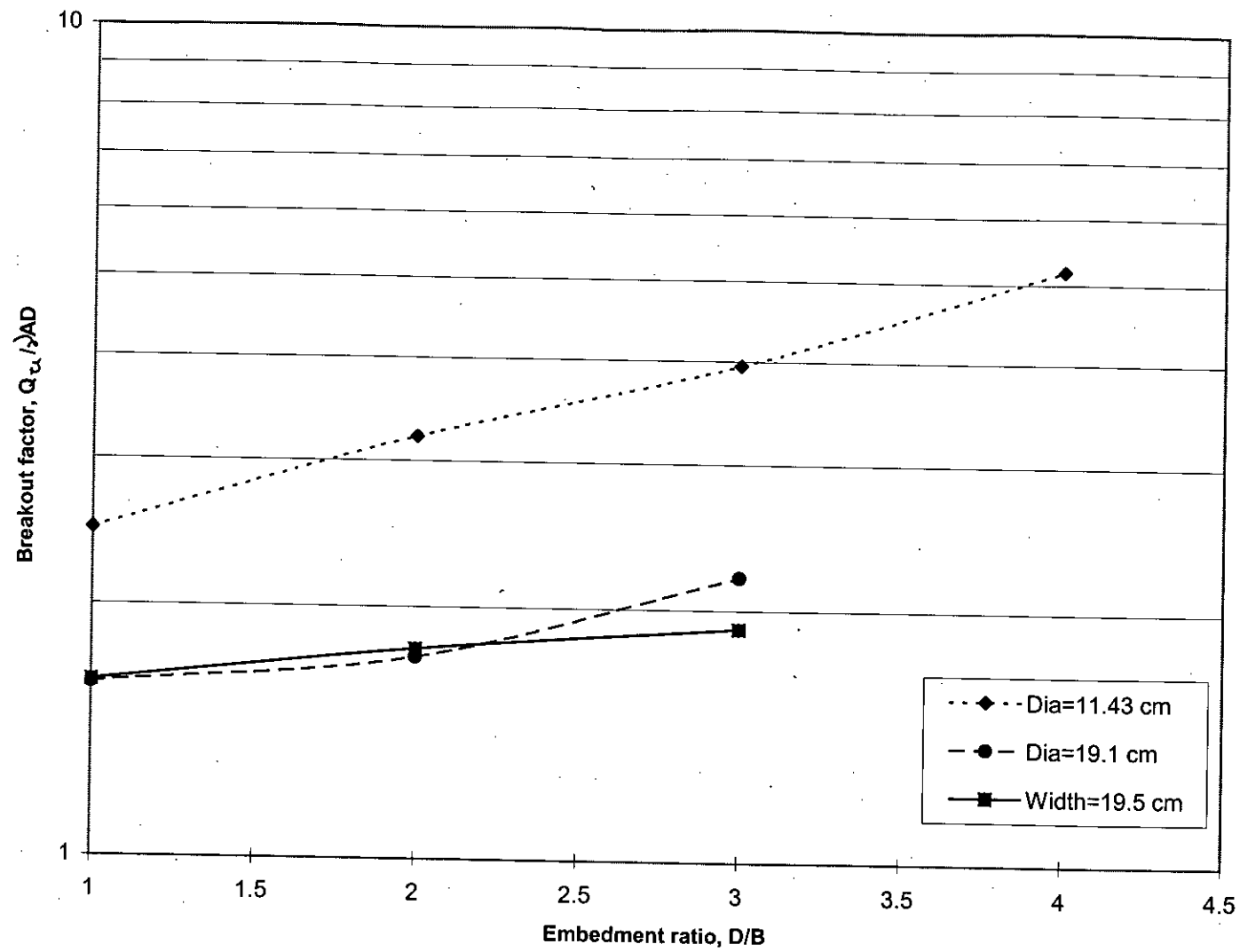


Fig 4.12 Variation of breakout factor with embedment ratio (Fills sand)

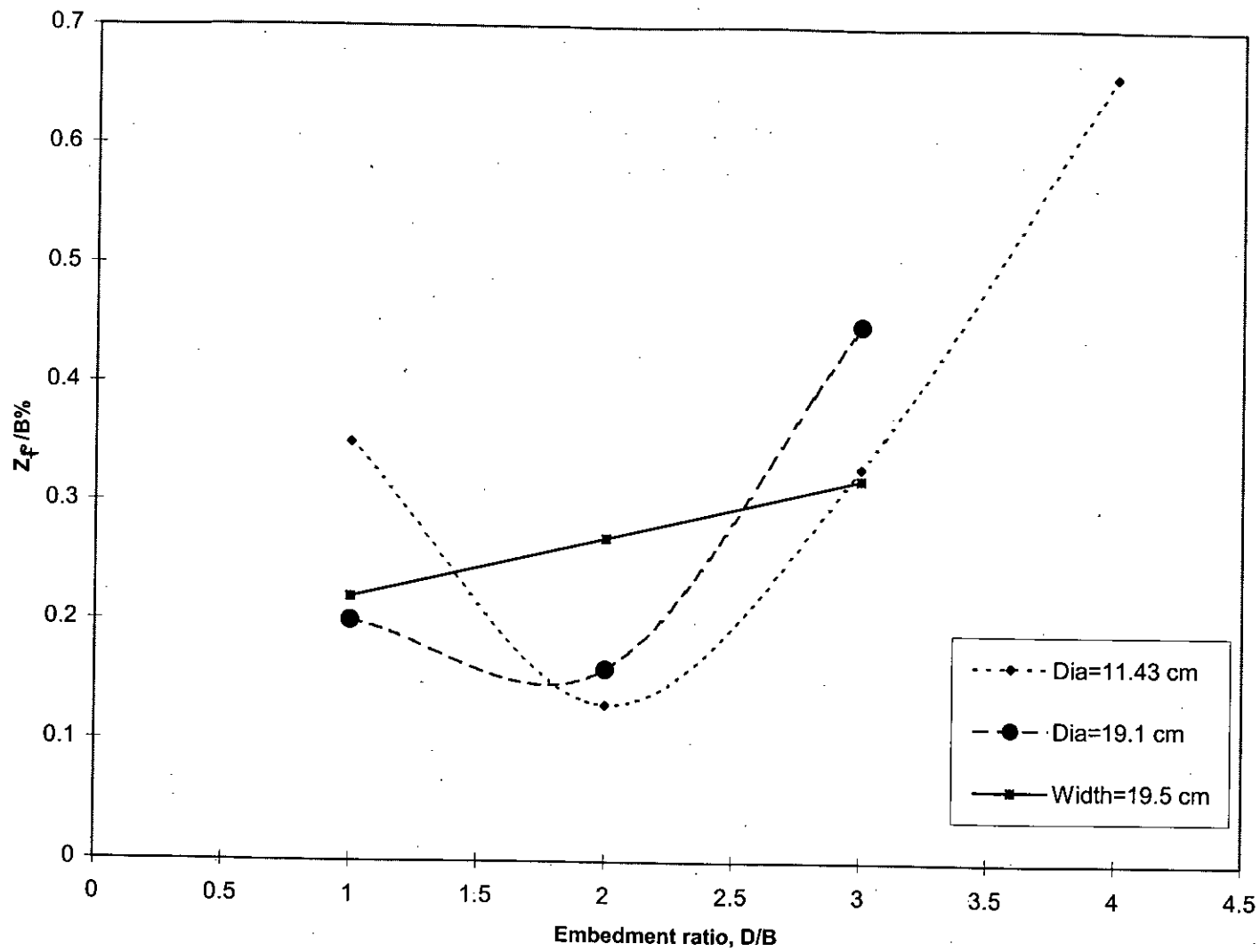


Fig.4.13 Variation in relative displacement with embedment ratio (Sylhet sand)

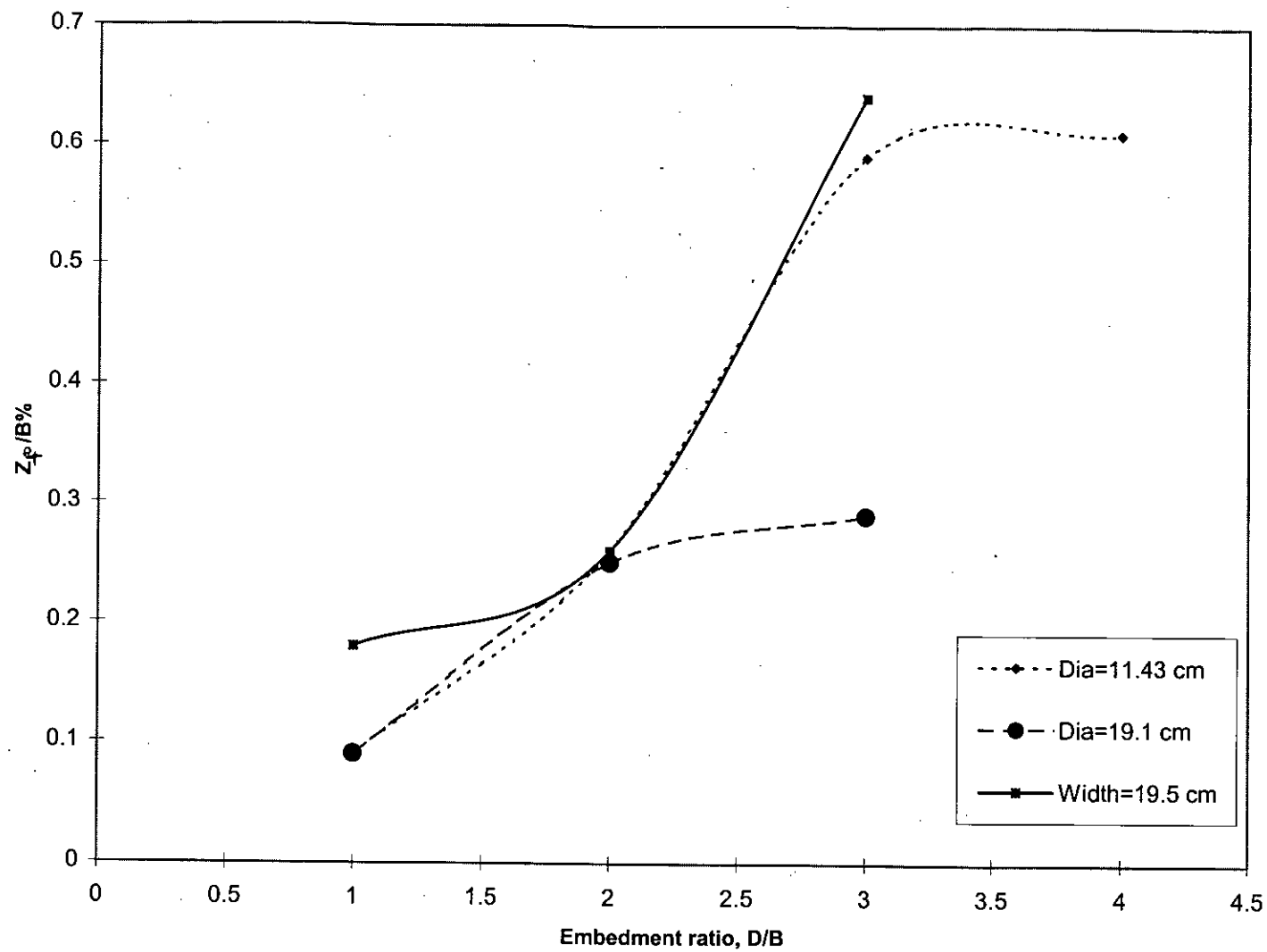


Fig.4.14 Variation in relative displacement with embedment ratio (Gazaria sand)

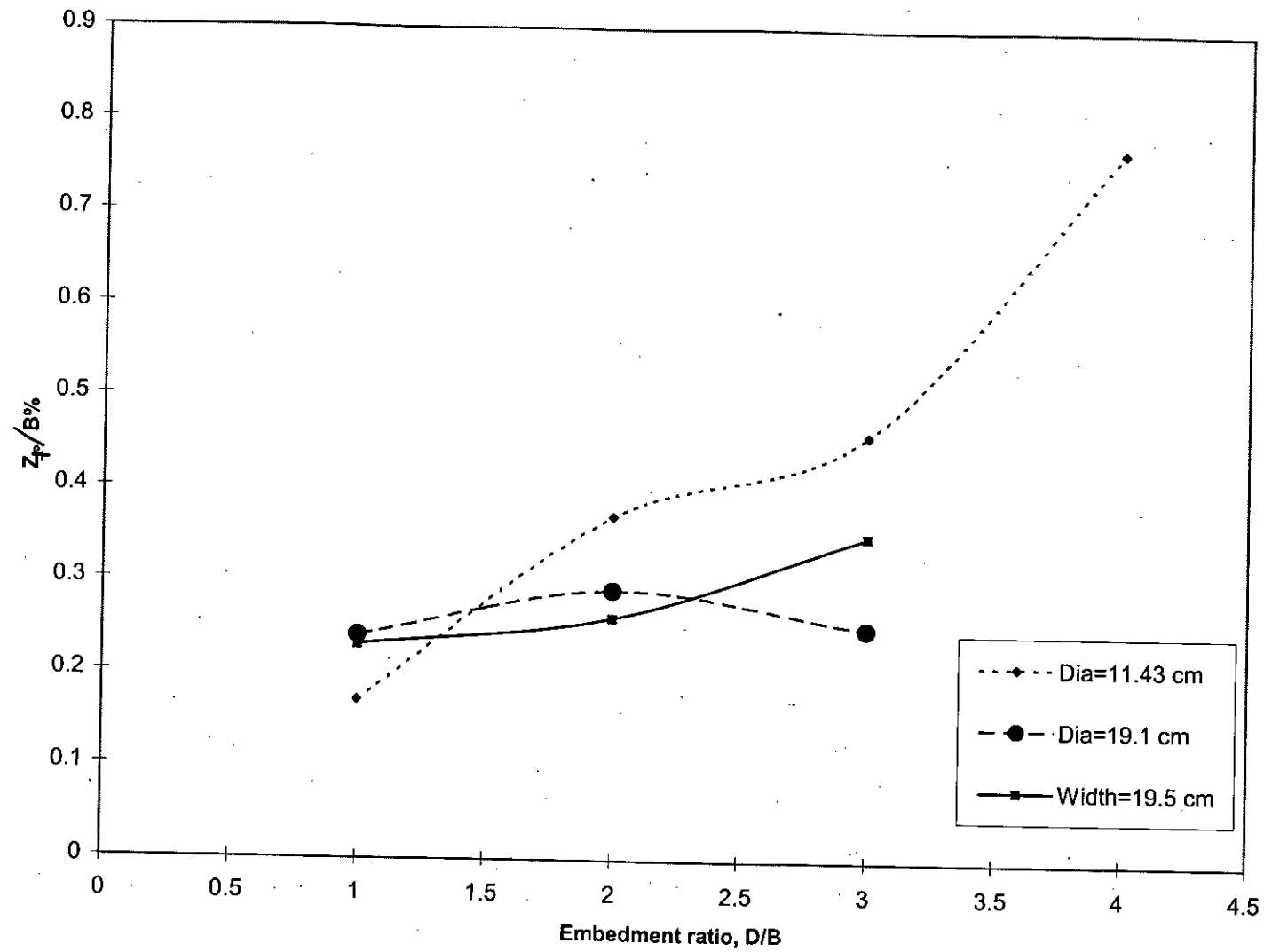


Fig. 4.15 Variation in relative displacement with embedment ratio
(Fills sand)

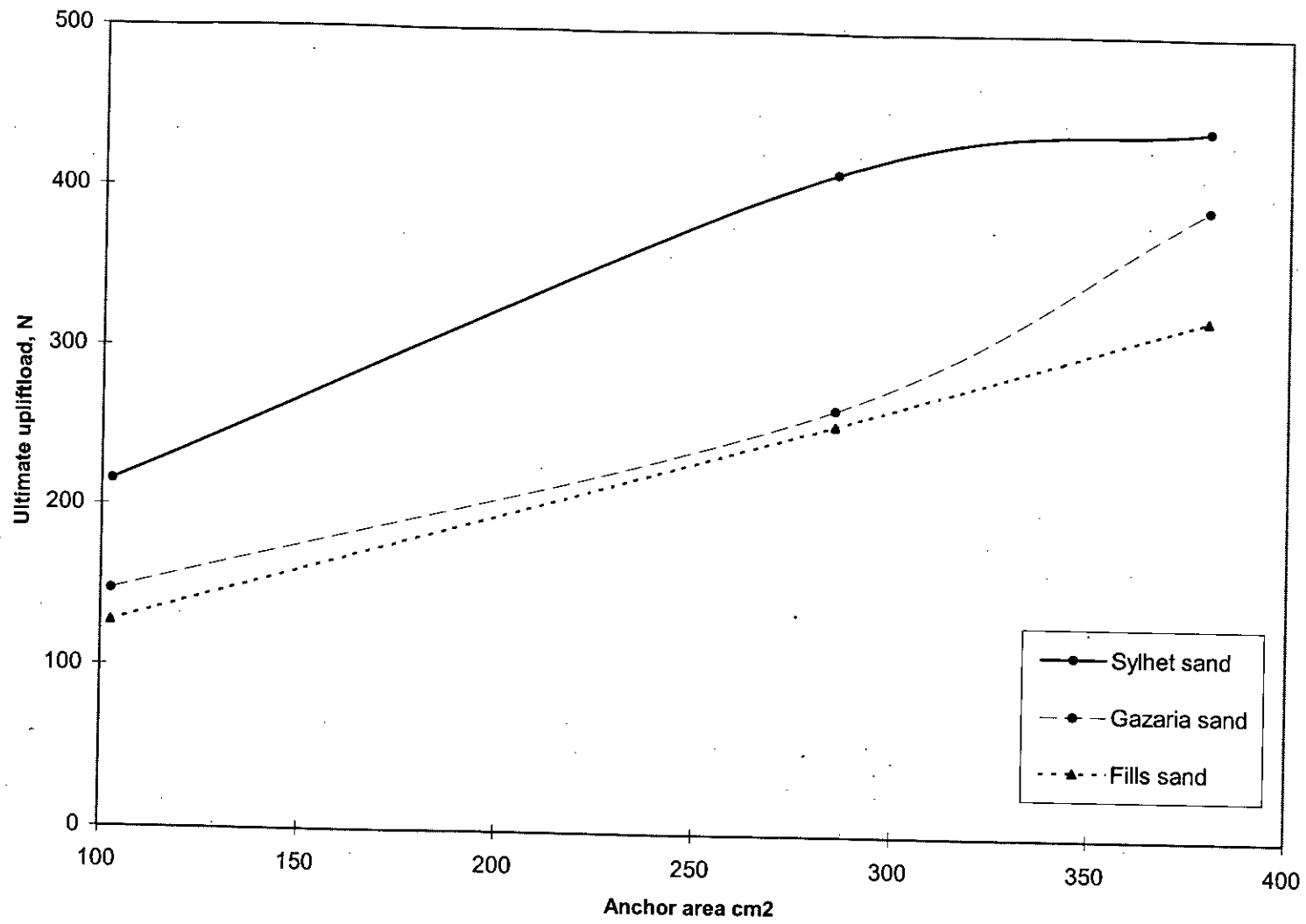


Fig. 4.16 Variation of ultimate Uplift load with anchor area ($D/B=2.0$)

capacity with anchor plate area shows ultimate uplift capacity (in Newton) increases with anchor plate area (in cm^2) in almost linear variation.

4.2.5 Variation of breakout capacity with anchor area

Variation of breakout capacity with anchor area in embedment ratio ($D/B=2.0$) Sylhet sand is showing in fig. 4.17. Here the breakout factor increases with the decreasing to anchor area. For the same embedment ratio, normal plot of breakout factor with anchor plates area shows that the breakout factor decreases with the increase of anchor plate area (in cm^2) in almost linear variation. So, it is clear that, the anchor area increases with the decrease breakout capacity.

4.2.6 Variation of the pattern of failure surface

The present test results show that for a particular embedment ratio, with the variation of anchor plate area, breakout factor decreases. This phenomena is supported by Harvey et al, 1981, who suggested that smaller sized anchor show significant increase of breakout factor in comparison with larger sized anchors having the same embedment ratio. However, the authors have their own explanation. Fig. 4.18 shows schematic of a small and a larger anchor having the same embedment ratio in a test tank. When uplift load is applied, the extent of slip surface does not reach the test tank wall. So, full mobilisation of shearing resistance along the slip surface is possible in the range of the test tank. But in case of larger anchor, the extent of slip surface reaches the test tank wall. So, full mobilization of the shearing resistance along the slip surface is not possible. The shearing resistance provided by the smooth test tank wall reduces the actual uplift capacity (uplift capacity when the slip surface is allowed to be fully developed in the extent of the test tank). So, it is clear that slip surface for larger anchor area needed larger width test tank.

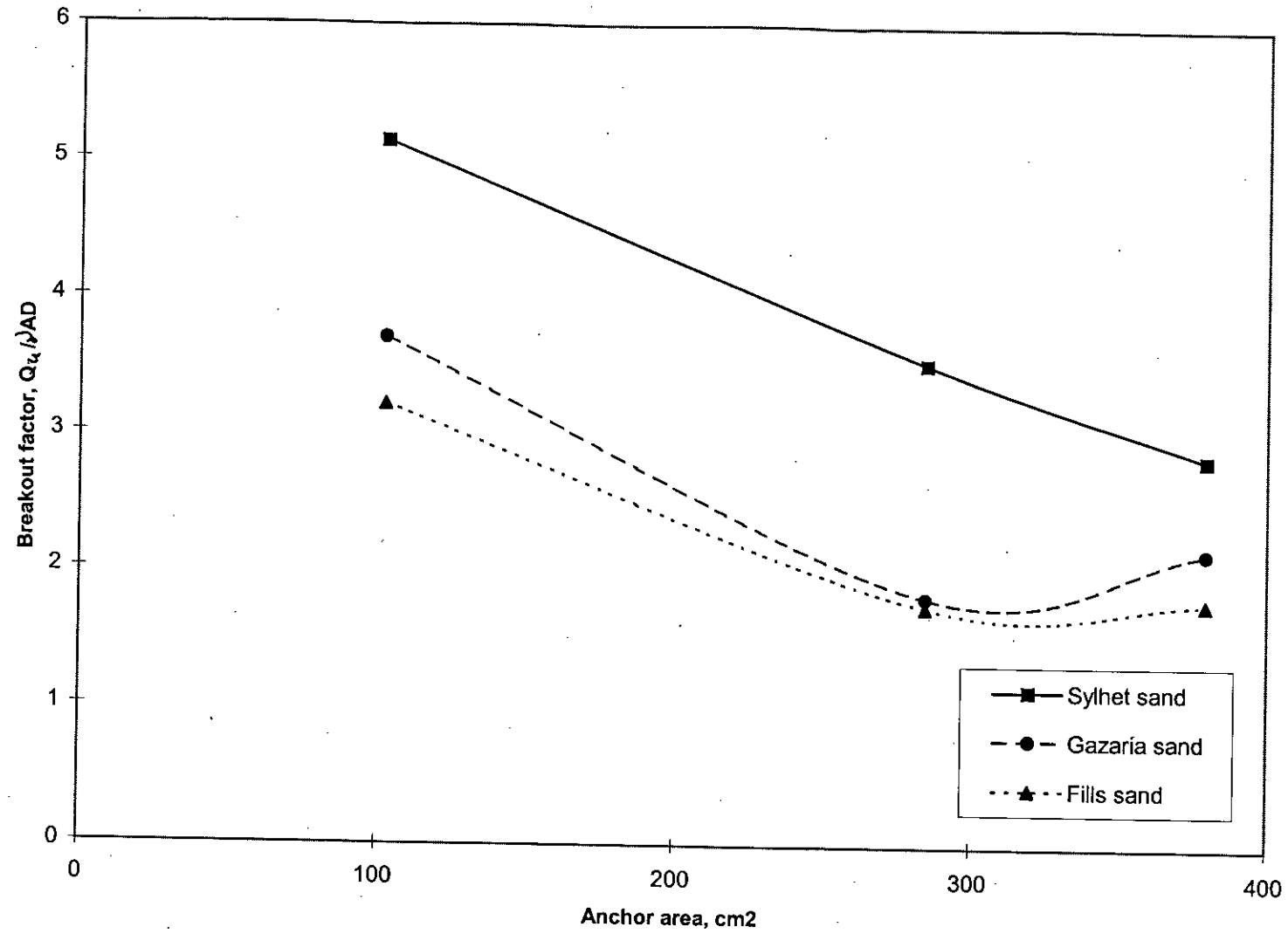


Fig. 4.17 Variation of Breakout capacity with anchor area ($D/B=2.0$)

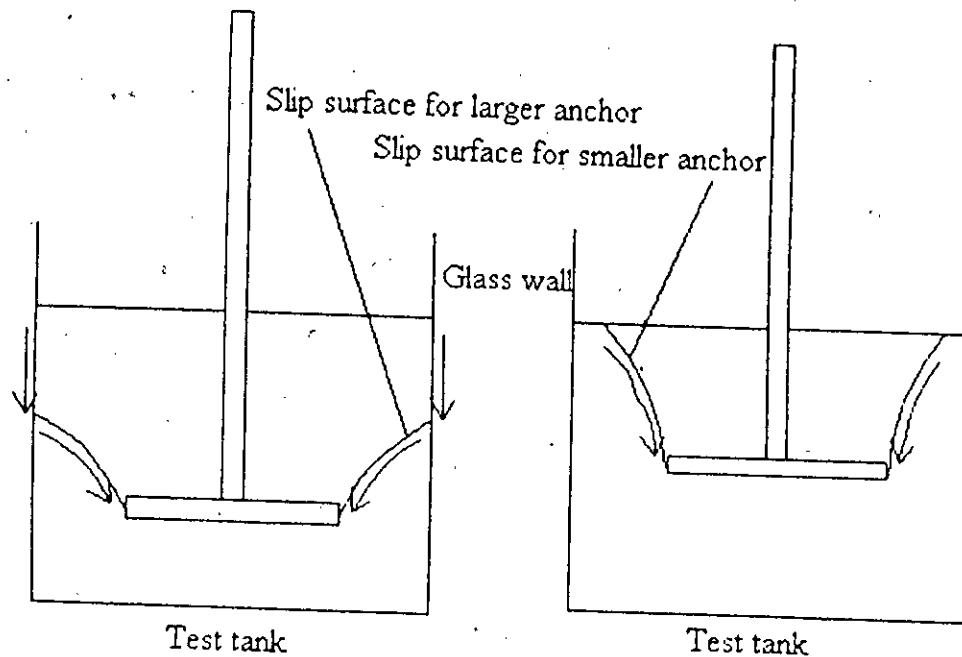


Fig. 4.18 Schematic of the failure surfaces of large & small anchor plates in test tank.

4.2.7 Variation of load with embedment ratio in different plate size at Sylhet sand

Variation of load with embedment ratio in different plate size at Sylhet sand is showing in Fig. 4.19. Here, the ultimate capacity of anchor plates increases with the increasing depth and this variation is not linear. It is apparent from Fig. 4.19 that for larger plate sizes (285 cm^2 and 379 cm^2) the variation is almost linear. However, for smaller size (102 cm^2) the variation is not linear. This is because slip surface reaches the test tank wall.

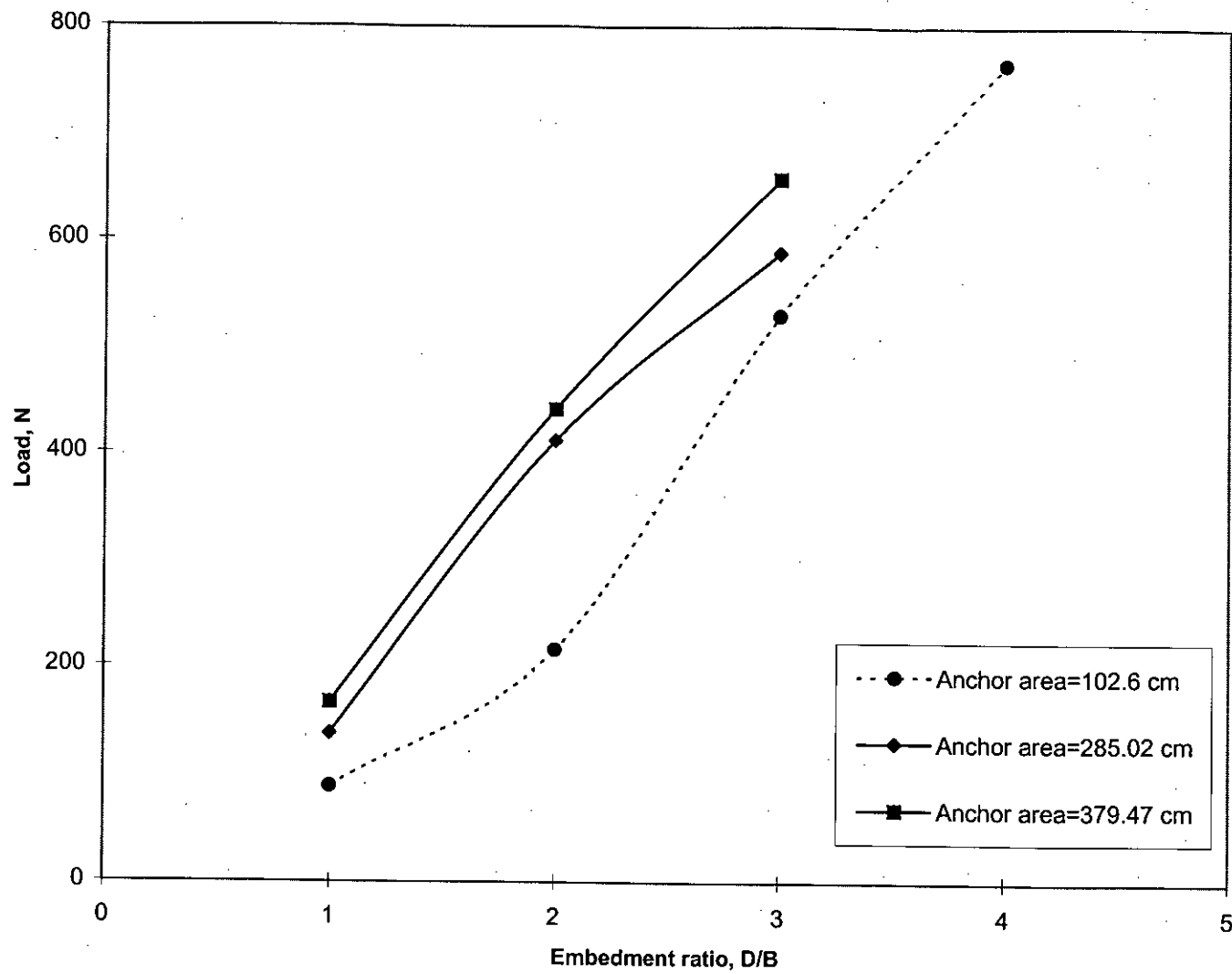


Fig: 4.19 Variation of Load with embedment ratio in different plate size at Sylhet sand

4.2.8 Variation of breakout capacity with relative density

Variation of breakout capacity with relative density in embedment ratio ($D/B=1.0, 2.0, 3.0$ & 4.0) Sylhet sand, Local (Gazaria) sand and Fills (Vethi sand) sand at anchor plate dia =11.43 cm are showing in Fig. 4.20. Here, the breakout capacity of anchor plates increases with the decreasing of relative density in sands and this variation is not linear.

4.2.9 Variation of breakout capacity with angle of friction

Variation of breakout capacity with angle of friction in embedment ratio ($D/B=1.0, 2.0, 3.0$ & 4.0) Sylhet sand, Gazaria sand and Fills (Vethi sand) sand at anchor plate dia =11.43 cm are showing in Fig. 4.21. Here, the breakout capacity of anchor plates increases with the increasing of angle of friction in sands and this variation is not linear.

4.3 COMPARISON OF MODEL TEST RESULTS WITH SIMILAR TESTS AND THEORETICAL ANALYSES BY DIFFERENT RESEARCHERS.

1. The shapes of the load-displacement curves have similarity with all the similar (available to present researchers) tests performed by other researchers (Dickin, 1988; Kulhawy et al., 1987; Rowe and Davies, 1982). Tests performed by Kulhawy et al (1987) showed that the load-displacement curve for anchor plate in loose sand is of flat nature, which is completely consistent with the findings of the present researchers. However, those mentioned researchers had observed distinct peaks and oscillations in the load-displacement curves for some anchors. This phenomenon were not observed by the present researcher as no proving ring dial or load cells were installed in his experimental set-up. The degree of relative displacement of anchor plates ($< 3\%$) are consistent with the findings of Kulhawy (1987) and Rowe and Davies (1982) (for both, the relative displacement is $< 5\%$). But wide variation in relative displacement can be observed with the findings of Dickin (1988) where degree of relative displacement ranged between 5% to 30% , According to the explanation of Dickin himself, small sized model anchors show significantly smaller displacements in comparison with large sized anchors or prototype anchors. This may

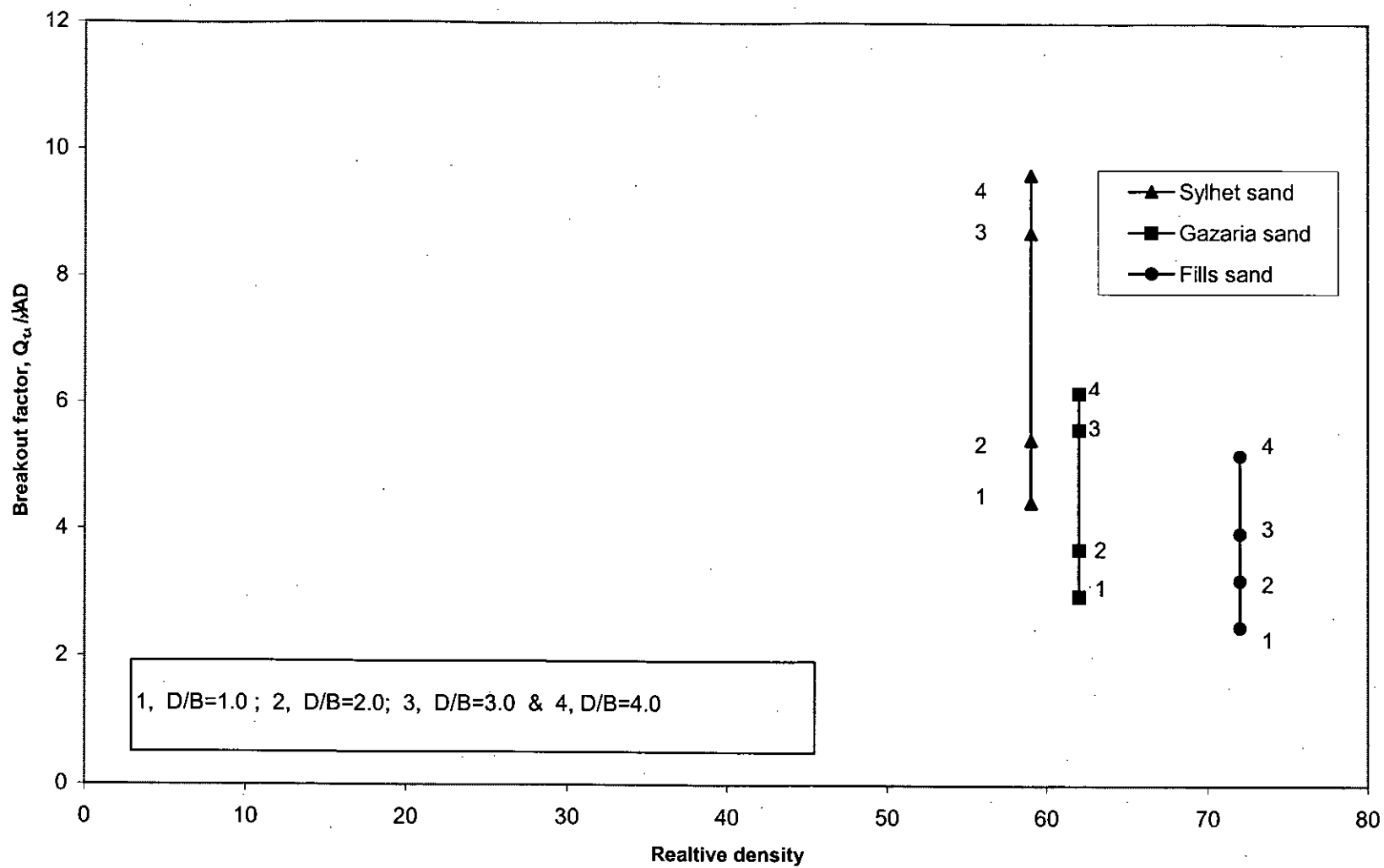


Fig. 4.20 Variation of Breakout capacity with relative density (dia. 11.43 cm)

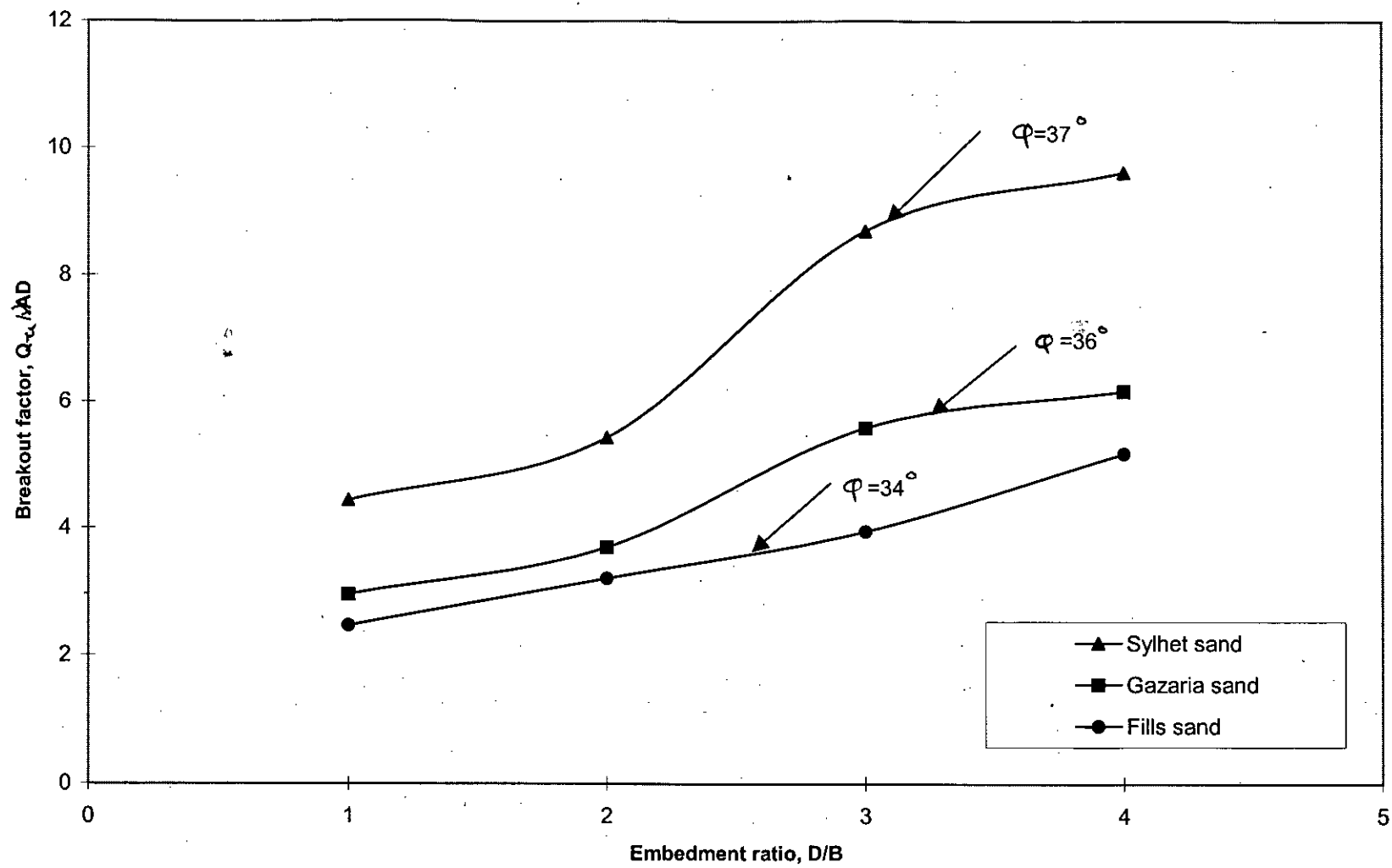


Fig. 4.21 Variation of Breakout capacity with angle of friction (dia. 11.43 cm)

be the reason of such a wide variation in displacements of model anchors used in the present research in comparison with Dickin's prototype anchors.

2. The failure modes of the anchors observed in the present research are fully consistent with almost all the available similar tests (Dickin, 1988; Rowe and Davies, 1982, Kulhawy, 1987, Ghaly and Hanna, 1994). However, the critical-embedment ratio (according to Sutherland, 1982) differed from test to test as sand samples with differing density were used in those tests.

3. The variation of breakout factor with embedment ratio is also compared with several existing plate anchor theories. Experimental results of present researcher shows the graphical line in Sylhet sands (anchor dia., $D=11.43$ cm). This comparison is shown in Fig. 4.22. The comparison shows that all the theories except one (Ghaly and Hanna, 1994) are conservative. Predictions of all the theories except that of Ghaly and Hanna have been calculated from design equations. This is the reason of the conservative nature of those theories (as design equations have some conservative assumptions). Experimental results of present researcher shows the graphical line in Sylhet sand is an over estimate than Clemence et al (1977) and under estimate than Ghaly and Hanna(1993). Therefore, the average line (shown as dotted in Fig. 4.22) of Clemence et al (1977) and Ghaly and Hanna (1993) is the experimental result of this present study.

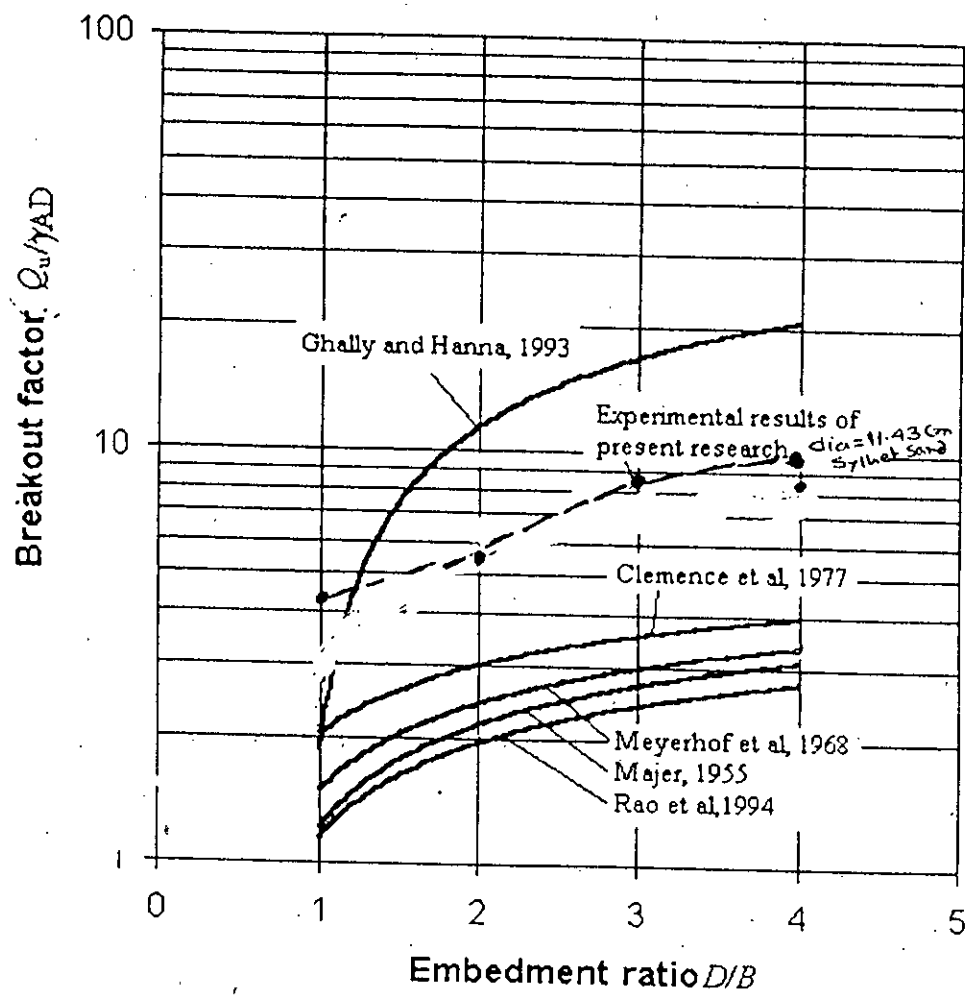


Fig. 4.22 Comparison of present test results with some theoretical analysis

CHAPTER 5

CONCLUSIONS AND RECOMMENDATIONS

5.1 CONCLUSIONS

This research aimed to investigate the variation of uplift capacity of a horizontal anchor plate for different sizes, shapes and depths of embedment. In this model test three anchor plates of sizes 11.43 cm (dia.), 19.1 cm (dia.) and 19.5 cm (square) were used. Here uplift capacities of the three anchor plates were found at depth of embedment to width ratio (D/B) of 1.0, 2.0, 3.0 and 4.0. Anchor test program was carried out on Fills, Local and Sylhet sands. In the current study, load-displacement behaviour, variation of breakout factor with embedment ratio, variation in relative displacement with embedment ratio, variation of uplift load with anchor area and variation of the pattern of failure surface were analysed. Based on the forgoing discussion the following conclusions can be drawn:

1. The ultimate capacity of anchor plates increases with the increasing depth and this variation is not linear. It is found that the uplift capacities for Sylhet sand with anchor plate area 103 cm^2 and embedment ratio $D/B=1.0, 2.0, 3.0$ and 4.0 are 88 N, 216 N, 520 N and 765 N respectively. For the same embedment ratio (D/B) such as 1.0, 2.0 and 3.0 with anchor plate area 285 cm^2 and 379 cm^2 the uplift capacity for local and fills sands are 137 N, 412 N, 589 N, 167 N, 441 N and 657 N respectively. Therefore, uplift capacity increases with the increasing of anchor plates area. It is also apparent that the variation of load different with embedment ratio in different plate size at Sylhet sand that for larger plate sizes (285 cm^2 and 379 cm^2) the variation is almost linear. However, for smaller size (103 cm^2) the variation is not linear. This is because slip surface reaches the test tank wall for larger plates sizes.
2. The variation of breakout factor with embedment ratio is also compared with several existing plate anchor theories. The comparison shows that all the theories except one (Ghaly and Hanna, 1994) are too conservative. Predictions of all the theories except

that of Ghaly and Hanna have been calculated from design equations and the derivations (of these design equations have some conservative assumptions). Result of the experiment carried out by the present researcher reveals that the break out factor for Sylhet sand with anchor dia.=11.43 cm was over estimated by Clemence et al (1977) while under estimated Ghaly and Hanna(1993). However, the average value of break out factor of Clemence et al (1977) and Ghaly and Hanna (1993) satisfactory matches with experimental value.

3. For smaller anchor area and with larger D/B ratio, the extent of slip surface does not reach the test tank wall. So, full mobilisation of shearing resistance along the slip surface is possible in the range of the test tank. But in case of larger anchor, the extent of slip surface reaches the test tank wall. So, full mobilisation of the shearing resistance along the slip surface is not possible. The shearing resistance provided by the smooth test tank wall reduces the actual uplift capacity (uplift capacity when the slip surface is allowed to be fully developed in the extent of the test tank).

5.2 RECOMMENDATIONS FOR FUTURE STUDY

In these current research covered only three different parameters like size, shape and depth in a model test to investigate the uplift behaviour in response to the variation of those parameters. It is clear that there is a wide scope for future research and much more detailed study regarding the behaviour of horizontal anchor plates in sands subjected to uplift pressure is required. Form the experience of the present researcher propose the following recommendations:

1. It has been observed that density of soil has a marked influence of uplift capacity of anchor plates. So extensive literature and experimental studies should be done concerning this particular feature of anchor plates.
2. So far, research on anchor plate has been concentrated mostly on ultimate uplift capacity. But often design of foundations is governed by displacement of foundation

rather than its ultimate capacity. So, displacement characteristics of anchors should be stressed by the researcher bearing in mind its practical applications.

3. Angle of inclination is an important factor of the uplift capacity of anchor plates, which also deserves consideration.
4. Group behaviour of anchor plates could be an interesting topic of research (Murray and Geddes, 1996). Anchors installed in-groups can be more efficient than single anchors. So concerning economy of foundation design, group behaviour of anchor plates should be studied comprehensively.
5. Static loads were applied manually. Adding weights to the loading hanger manually did load increment, which is not a standard procedure. So, a constant rate of loading cannot be maintained. For getting accurate results, a mechanical loading device could provide such facility.
6. Lastly, study should be extended to analyse uplift behaviour of other types of anchors (e.g. screw anchors, helical anchors, grouted anchors etc.) to get a generalised picture of anchor behaviour irrespective of shape.

REFERENCES

Andreadis A., Harvey R.C. and Burley E. (1981), "Embedded anchor response to uplift loading", Journal of the Geotechnical Division, Proceedings of ASCE, Vol. 107, No. GT 1, January, pp 59-78.

Andreadis A., Harvey R.C. and Burley E. (1982), "Embedment anchors subjected to repeated loading", Journal of the Geotechnical Division, Proceedings of ASCE, Vol. 108, No. GT, 7, July.

Ashraf M. Ghaly, " Load-displacement prediction for horizontally loaded vertical plates" Journal of the Geotechnical Division, Proceedings of ASCE, January (1997), pp 74-84

Bashar Md. Zafry Md. (1992), "Uplift behaviour of horizontal anchor plates" In partial fulfillment of the B.Sc. Engg. Thesis.

Bouzza A. and Finlay T.W. (1990), " Uplift capacity of plate anchors buried in two layered soil" Journal of the Geotechnical Division, Proceedings of ASCE, Vol. 115, No. GT, 09, September, pp 293-297.

Das B. M. and Kaun Y. J. (1987), "Uplift behaviour of model group Anchors in sand", Special publication of ASCE on tower foundations.

Das B. M. (1975), "Pullout resistance of vertical anchors" Journal of the Geotechnical Division, Proceedings of ASCE, Vol. 101, No. GT, 1, pp 87-91. .

Davie J. R. and Sutherland B.(1977), " Uplift resistance of cohesive soils", Journal of the Geotechnical Division, Proceedings of ASCE, Vol. 103, No. GT9, September, pp 935-952

- Dickin E.A. (1988), "Uplift behaviour of horizontal anchor plates in sand", Journal of the Geotechnical Division, Proceeds of ASCE, Vol.114, No. GT 11, November, pp1300-1317.
- Frydman S. and Shaham I. (1989), " Pullout capacity of slab anchors in sand", Can. Geotech.
- Geddes J.D. and Marray E.J. (1996), " Plates anchor groups pulled vertically in sand", Journal of the Geotechnical Division, Proceedings of ASCE, Vol. 122, No. GT07, July
- Ghaly A., Hanna A. and Hanna M. (1991), "Uplift behaviour of screw anchors in dry sand", Journal of the Geotechnical Division, Proceedings of ASCE, Vol. 116, No. GT05, May
- Hanna T. H. (1982), "Foundations in tension-ground anchors", McGraw-Hill publications.
- Hanna A. and Ghaly A.(1993), " Effects of K_0 and Overconsolidation on uplift capacity", Journal of the Geotechnical Division, Proceedings of ASCE, Vol. 109, No. GT 9, September, pp1449-1467.
- Kulhawy F.H. (1987), "Uplift behaviour of shallow soil anchor-An overview", Special publication of ASCE on tower foundations, New York, N.Y., pp1-5.
- Kyle M. Rollins, Kris T. Peterson and Thomas J. Weaver(1998), " Lateral load behaviour of full-scale pile group in clay", Journal of the Geotechnical Division, Proceedings of ASCE, pp 468-478.
- Matyas E. L. and Davis J.B. (1983), "Prediction of vertical earth loads on rigid pipes", Journal of the Geotechnical Division, Proceedings of ASCE, Vol. 109, No. GT 1, January.

Meyerhof G.G. & Adams, J.I.(1968), "The ultimate uplift capacity of foundations", Canadian Geotechnical, Journal vol-5, No-4, November, pp 225-244.

Nene A.S., Saran S. and Ranjan G. (1985), " Model study of shallow plate anchors", Indian Geotechnical Conference Vol.1.

Rao K.S.S. and Kumar J. (1994), "Vertical uplift capacity of horizontal anchors" Journal of the Geotechnical Engineering, ASCE, Vol. 119, No. GT 09, September.

Rowe R.K. and Davies E.H. (1982), "The behaviour of anchor plates in sand", Geotechnique Vol. 32, No. 1, pp 25-39.

Trautmann C.H. and Kulhawy F.H. (1988), "Uplift load-displacement behaviour of spread foundations", Journal of the Geotechnical Division, Proceedings of ASCE, Vol. 114, No. GT 2, February, pp 168-184.

Xenthakas P.P. (1991), "Ground anchors and anchored structures", McGrawHill Publication.

